PREDICTIVE MODELING OF CUTTING TEMPERATURE AND CUTTING FORCE IN HIGH-PRESSURE COOLANT JET MACHINING

By

Prianka Binte Zaman

A Thesis
Submitted to the
Department of Industrial & Production Engineering
in Partial Fulfilment of the
Requirements for the Degree
of
M.Sc. in Industrial and Production Engineering

DEPARTMENT OF INDUSTRIAL & PRODUCTION ENGINEERING
BANGLADESH UNIVERSITY OF ENGINEERING & TECHNOLOGY
DHAKA, BANGLADESH

March 2011

The thesis entitled as **Predictive Modeling of Cutting Temperature and Cutting Force in High-Pressure Coolant Jet Machining** submitted by Prianka Binte Zaman, Student No. 040808004P, Session- April 2008, has been accepted as satisfactory in partial fulfillment of the requirement for the degree of M. Sc. in Industrial and Production Engineering on March 20, 2011.

BOARD OF EXAMINERS

1.	Dr. Nikhil Ranjan Dhar Professor Department of Industrial & Production Engineering BUET, Dhaka	Chairman
2.	Head Department of Industrial & Production Engineering BUET, Dhaka.	Member (Ex-officio)
3.	Dr. Nafis Ahmad Associate Professor Department of Industrial & Production Engineering BUET, Dhaka.	Member
4.	Dr. A.B.M. Zohrul Kabir Professor Department of Mechanical & Chemical Engineering Islamic University of Technology (IUT)) Board Bazar, Gazipur	Member (External)

Declaration

It is hereby declared that this thesis or any part of it has not been submitted elsewhere for the award of any degree or diploma.

Prianka Binte Zaman

This work is dedicated to my
Loving Parents

Md. Anisuzzaman
and
Begum Shireen Zaman

Table of Contents

List of Tables..... viii

List of Figures..... ix

List of Symbols..... xii

Acknowledgements..... xvii

Abstract..... xviii

Chapter 1 Introduction..... 1

1.1 High Speed Machining……..…….. 2

1.2 Effects and Control of Cutting Temperature…….. 5

1.3 High-Pressure Coolant (HPC) Jet Machining……. 15

1.4 Literature Review…… 19

1.4.1 Modeling of Cutting Temperature ……..……..…….. 19

1.4.1.1 Numerical Evaluation of Cutting Temperature…… 20

1.4.1.2 Analytical Modelling of Cutting Temperature……. 28

1.4.1.3 Other Approaches of Modelling Temperature…….. 35

1.4.2 Modeling of Cutting Force …….. 36

1.4.2.1 Numerical Evaluation of Cutting Forces……... 36

1.4.2.2 Analytical Modelling of Cutting Forces……... 39

1.4.2.3 Other Approaches of Modelling Cutting Forces…….. 44

1.5 Summary of the Review…….……..…….. 48

1.6 Scope of the Thesis……. 50

Chapter 2 Objectives of the Present Work..... 53

2.1 Objectives of the Present Work..... 53

2.2 Methodology..... 54

Chapter 3 Experimental Investigations..... 56

3.1 Introduction..... 56

3.2 Experimental Procedure and Conditions..... 57

3.3 Experimental Results..... 60

3.3.1 Chip Formation……..... 60

3.3.2 Chip Reduction Coefficient..... 61
3.3.3 Cutting Temperature..... 64
3.3.4 Cutting Force…… 67

Chapter 4 Modeling of Cutting Temperature ……..…..……. 70
4.1 Introduction…….…… 70
4.2 Mechanics of Machining…..…… 72
4.3 Heat Generation in Machining.…….……..…….. 84
4.4 Temperature Rise due to Heat Source (Stationary and Moving)…. 86
4.5 Predictive Modeling of Cutting Temperature……..... 89
4.5.1 Shear Plane Temperature……..…… 92
4.5.2 Chip-tool Interface Temperature……..…… 96
4.6 Model Validation of Cutting Temperature……..……..….. 100

Chapter 5 Modeling of Cutting Force…… ……..…..……..…. 102
5.1 Introduction…….…… 102
5.2 Predictive Model of Cutting Force Correlating with Cutting Speed, Feed Rate and Depth of cut …… 106
5.3 Model Validation of Cutting Force……. 111

Chapter 6 Finite Element Modeling (FEM) of Cutting Zone Temperature.. 114
6.1 Introduction……. 114
6.2 Modeling Procedures…….. 117
6.2.1 Creating Parts…… 117
6.2.2 Defining the Assembly……..……... 118
6.2.3 Defining Materials……. 119
6.2.4 Defining and Assigning Section Properties…..…… 120
6.2.5 Meshing the Model…… 121
6.2.6 Configuring Analysis……..……. 122
6.2.7 Applying Boundary Conditions and Loads to the Model…… 126
6.2.8 Creating an Analysis Job & Running the Analysis……... 131
6.2.9 Postprocessing with Abaqus/CAE…… 131
6.3 Finite Element Modeling Results……..…….…… 132

Chapter 7 Discussion on Results…… 135

7.1 Cutting Temperature…..... 135

7.2 Cutting Force.……..……... 139

Chapter 8 Conclusions and Recommendations..... 143

8.1 Conclusions…….... 143

8.2 Recommendations……..…. 145

References..... 147

List of Tables

Table 3.1	Experimental conditions	59
Table 4.1	Test conditions for temperature validation	100
Table 5.1	Regression table for the second order mathematical model	108
Table 5.2	Analysis of variance for the second order mathematical model	109
Table 5.3	Regression table for the non-linear model	110
Table 5.4	Analysis of variance for the non-linear model	110
Table 5.5	Test conditions for force validation	112
Table 6.1	Defining the assembly	118
Table 6.2	Thermal-mechanical properties of materials	120
Table 6.3	Defining and asigning section properties	121
Table 7.1	% error for the cutting temperature prediction	137
Table 7.2	% error for the cutting force prediction	142

List of Figures

Fig. 3.1	Photographic view of high-pressure coolant delivery nozzle injecting coolant during machining	58
Fig. 3.2	Photographic view of experimental set-up	58
Fig. 3.3	Shape and color of chip during turning of AISI 1060 steel by SNMM insert under Dry and HPC conditions	60
Fig. 3.4	Schematic view of the chip formation mechanism	62
Fig. 3.5	Variation of chip reduction coefficient with that of cutting speeds and feed rates under dry and HPC conditions at depth of cut 1.0 mm	62
Fig. 3.6	Variation of chip reduction coefficient with that of cutting speeds and feed rates under dry and HPC conditions at depth of cut 1.5 mm	63
Fig. 3.7	Variation of average chip tool interface temperature with that of cutting speeds and feed rates under dry and HPC conditions at depth of cut 1.0 mm	65
Fig. 3.8	Variation of average chip tool interface temperature with that of cutting speeds and feed rates under dry and HPC conditions at depth of cut 1.5 mm	66
Fig. 3.9	Variation of average chip tool interface temperature with machining time at different V_c-S_o combination under HPC condition	66
Fig. 3.10	Variation of main cutting force with that of cutting speeds and feed rates under dry and HPC conditions at depth of cut 1.0 mm	68
Fig. 3.11	Variation of main cutting force with that of cutting speeds and feed rates under dry and HPC conditions at depth of cut 1.5 mm	68
Fig. 4.1	Type of machining process	72
Fig. 4.2	Orthogonal machining	73

Fig. 4.3	Schematic view of the chip formation mechanism	74
Fig. 4.4	Velocity of the cutting process	78
Fig. 4.5	Forces in machining	79
Fig. 4.6	Merchant Circle Diagram (MCD)	80
Fig. 4.7	Stationary heat source	87
Fig. 4.8	Scemetic diagram of moving heat source	88
Fig. 4.9	Heat sources in metal cutting process	90
Fig. 4.10	Flow chart for calculating the average shear plane temperature	95
Fig. 4.11	Stationary heat source at chip tool interface	97
Fig. 4.12	Flow chart for calculating the average chip-tool interface temperature	99
Fig. 4.13	Comparison of the measured and the predicted cutting temperature for different tests when turning AISI 1060 steel by SNMM insert under HPC condition.	101
Fig. 5.1	(a) Main effect plot and (b) interaction plot for cutting force	107
Fig. 5.2	Surface plot for cutting force	107
Fig. 5.3	Second order mathematical model (a)Normal probability plot for residuals (b) Residual VS fitted value plot	109
Fig. 5.4	Non-linear model(a) Normal probability plot for residuals (b) Residual VS fitted value plot	111
Fig. 5.5	Comparison of the measured and the predicted cutting force from the second order mathematical model for different tests when turning AISI 1060 steel by SNMM insert under HPC condition.	113

Fig.5.6	Comparison of the measured and the predicted cutting force from non-linear equation model for different tests when turning AISI 1060 steel by SNMM insert under HPC condition	113
Fig. 6.1	Flow chart for the analysis by ABAQUS	115
Fig. 6.2	Schematic view of chip formation mechanism	116
Fig. 6.3	Workpiece-chip-tool for FEM	118
Fig. 6.4	Assembly model of workpiece-chip-tool	119
Fig. 6.5	Section assignment to the assembly model (three sections)	120
Fig. 6.6	Materials on the assembly model (two materials)	121
Fig. 6.7	Mesh generation on the workpiece-chip-tool	122
Fig. 6.8	Boundary conditions of the model	126
Fig. 6.9	Mechanical loads in metal cutting	127
Fig. 6.10	Thermal loads in metal cutting	129
Fig. 6.11	Mechanical and thermal loads applied in the model	131
Fig. 6.12	Pattern of temperature distribution in work piece, chip and tool for turning AISI 1060 steel by SNMM insert under HPC condition	132
Fig. 6.13	Temperature distribution in work piece, chip and tool for turning AISI 1060 steel by SNMM insert under HPC condition at different cutting conditions	133
Fig. 6.14	Comparison of the measured and predicted average chip-tool interface temperature for different tests when turning AISI 1060 steel by SNMM insert under HPC condition.	134

List of Symbols

a_1 : Uncut chip thickness

a_2 : Chip thickness

A_s : Area of the shear plane

b : Width of cut

B' : Quantity specified in Eq. 4.57

BHN : Hardness

a, b, c : Exponents of the non-linear equation (only in Chapter 5)

C : Constant of the non-linear equation

c : Specific heat

C_N : Natural chip-tool contact length

C' : Quantity specified in Eq. 4.57

e : Error in the response surface equation

E : Young's modulus

F : Frictional force working on the rake surface

f : Response function

HPC : High-pressure coolant

J : Mechanical equivalent of heat

k_w : Thermal conductivity of the workpiece

k_{ch} : Thermal conductivity of the chip

k_t : Thermal conductivity of the tool

K : Thermal diffusivity

K_w : Diffusivity of the work piece material at temperature θ_s

K_{ch} : Diffusivity of the chip at its final temperature

L_{sh} : Length of shear plane

L : Dimensionless velocity parameter

L_1 : Dimensionless velocity parameter for shear plane

L_2 : Dimensionless velocity parameter chip-tool interface

l : Half of the length of rectangular heat source

m : Half of the width of rectangular heat source

N : Normal force working on the rake surface

P_s : Component of force directed along the shear plane

P_n : Component of force perpendicular the shear plane

P_x : Thrust force

P_x : Feed force

P_{xy} : Resultant force of P_x and P_y

P_z : Main cutting force

Q : Strength of an instantaneous point heat source

q : Heat flux in W/m^2

q_f : Heat intensity of the secondary shear zone (Friction heat source)

q_s : Heat intensity of the primary shear zone (Shear heat source)

q_r : Heat intensity of the tertiary shear zone (Rubbing heat source)

R_1 : fraction of energy of the shear plane going to the chip

R_2 : fraction of energy at chip-tool interface going to the chip

R : Distance between points

S_o : Feed rate

t : Depth of cut

T, t : Time

u : Total energy per unit volume of chip formed

u_s : shear energy per unit volume on the shear plane

u_f : friction energy per unit volume on the rake face

u_a : surface energy per unit volume as a result of the formation of new surface areas

u_m : momentum energy per unit volume

U : total energy consumed per unit time

U_s : rate of shear energy expended along the shear plane

U_s' : rate of energy expended per unit area on the shear plane

u_{cs} : energy per unit volume going to the chip on the shear plane

u_{cf} : energy per unit volume going to the chip at chip-tool interface

V_c : Cutting velocity

V_f : Chip flow velocity

V_s : Shear velocity

V : Velocity of moving heat source

Y : Dependent variable of the response surface equation

θ : Cutting temperature

α : Clearance angle

β : Shear angle

γ : Rake angle

ε : Shear strain

ξ : Chip reduction co-efficient

η : Mean angle of friction at the rake surface

θ : Temperature at any location x, y, z

θ_o : Ambient workpiece temperature

θ'_o : Ambient temperature of the tool

$\overline{\theta}_s$: Mean temperature of the shear plane

$\overline{\theta}_{s\,(est)}$: Estimated average temperature of the shear plane

$\overline{\theta}_{s\,(calc)}$: Calculated average temperature of the shear plane

$\overline{\theta}_T$: Mean temperature of the chip-tool interface

$\overline{\theta}_{T\,(est)}$: Estimated mean temperature of the chip-tool interface

$\overline{\theta}_{T\,(calc)}$: Calculated mean temperature of the chip-tool interface

$\Delta\overline{\theta}$: Mean surface temperature rise over the area of the source

$\Delta\theta$: Rise of temperature due to a uniform heat source

$\Delta\bar{\theta}_f$: Mean temperature rise due to friction

μ : Frictional co-efficient

ν : Poisson's ratio

ρ : Density

$\rho_w c_w$: volume specific heat of the workpiece

$\rho_{ch} c_{ch}$: Volume specific heat of chip

σ_u : Ultimate tensile strength of the work material at normal condition

τ_s : Dynamic yield shear strength

φ : Principal cutting edge angle

Δ : Percentage elongation of the work material

Acknowledgement

I would like to acknowledge my respected supervisor, Dr. Nikhil Ranjan Dhar, Professor of the Department of Industrial and Production Engineering (IPE) for his guidance and support during my post-graduate career at Bangladesh University of Engineering and Technology (BUET) which cannot be expressed through words only. I consider it to be a great honor to work under him. I am grateful and indebted to him forever for his constant encouragement and supports for becoming a competitive engineer, a strong researcher and obviously a good human being.

I would also like to thank all teachers and employees of the Department of Industrial & Production Engineering, BUET. I am also grateful to Dr. A. K. M. Masud, Dr. Nafis Ahmad and Dr. A.B.M Zohrul Kabir for being on my M.Sc. thesis committee and providing valuable suggestions to improve the content of this thesis.

I am deeply obliged to Nusrat Tarin Chowdhury, and Abdullah Al Mamun and Sanjana Shahnewaz, for their availability during experimental work and A special thanks goes to Dr. Kamruzzaman, Assistant Professor, DUET and Ireen Sultana, Lecturer, Department of Industrial & Production Engineering, BUET for giving a huge support in solving technical problems.

I also acknowledge the help rendered by the Director, DAERS, BUET who provided machine shop and welding & foundry shop facilities whenever required. I would like to express my heartfelt gratitude to all the staff members of Central Machine Shop and Machine Tools Lab who have helped a lot whenever required, especially M. A. Wahab, M. A. Razzak, Tony G. Gomes and Shankar Chandra Das for their helps in conducting the experimental work. I would also like to acknowledge the staff members of welding & foundry shop.

Abstract

The energy dissipated in machining operation is converted into heat which raises the temperature in the cutting zone. With the increase of cutting temperature; tool wear, surface roughness, dimensional inaccuracy increases significantly. Cutting force is also increased with tool wear which results the increase of power and specific energy consumption. Various researchers worked on various techniques to effectively control the increased cutting temperature as well as cutting force, tool wear rates, surface integrity. The cutting temperature, which is the cause of several problems restraining productivity, quality and hence machining economy, can be controlled by the application of high-pressure coolant (HPC) jet. High-pressure coolant (HPC) jet cooling is a promising technology in high speed machining, which economically addresses the current processes, environmental and health concerns.

Based on cutting condition, cutting environment and work/tool material the physical behavior during metal cutting has been changed. From an economic viewpoint, it is evident that having knowledge about the machining responses such as tool life, cutting forces, cutting temperature and work piece surface integrity at different cutting conditions would be highly desirable as a means of realizing cost savings, increased productivity, efficiency and for preventing any hazard occurring to the machine, cutting tool or the deterioration of the product quality. Optimization of process parameters for improving product quality, shortening processing time and reducing production cost is very important and for this purpose modeling of process parameters is necessary.

By laborious and costly experimental investigation, machining responses like cutting temperature, cutting force, tool wear and surface roughness can be measured. Engineers and researchers have been realizing that efficient quantitative and predictive

models that establish the relationship between a big group of input independent parameters and resultant performance are required for the wide spectrum of manufacturing processes, cutting tools and engineering materials currently used in the industry could contribute in industrial applications along with theoretical understanding.

The aim of the present work is to investigate the role of high-pressure coolant jet in respects of chip formation, cutting temperature and force experimentally and then develop predictive models for cutting temperature and force in turning medium carbon steel (AISI 1060 steel) by uncoated carbide insert at industrial speed feed conbinations under high pressure coolant condition.

The experimental results indicate that the performance of the machining under HPC condition is quite good and more effective compared to machining under dry condition. With the help of the experimental results, predictive models of cutting temperature and force have been developed to understand the basic phenomenon in metal machining. Prediction of cutting temperature has been conducted from analytical studies, where empirical correlations have been used to determine heat generation and temperature. Analytical calculations have been done under simplified assumptions. Using statistical analysis, predictive models of force has been developed. Finally, finite element model has been developed to evaluate temperature distribution by ABAQUS/CAE. The developed models satisfactorily validate its accuracy by comparing predicted values with experimental values.

Chapter-1

Introduction

The most emerging trend of the modern metal cutting operations is to increase the material removal rate with good surface roughness and high machining accuracies. As in all metalworking processes (when machining metals and alloys) where plastic deformation is involved to form the chips, the energy dissipated in cutting is converted into heat which in turn, raises the temperature in the cutting zone. This factor is of a major importance to the performance of the cutting tool and quality of the workpiece [**Gökkaya et al. 2001]**. Temperatures in cutting zone depend on contact length between tool and chip, cutting forces and friction between tool and workpiece material. A considerable amount of heat generated during machining is transferred into the cutting tool and workpiece. The remaining heat is removed with the chips. The highest temperature is genarated in the flow zone. Therefore, contact length between the tool and the chip affects cutting conditions and performance of the tool and tool life [**Bever et al. 1953**].

Currently generous research and investigations have been done world wide on the machinability of different materials mainly in respect of chip-tool interface temperature, chip morphology, chip-tool interaction, cutting forces, wear and life of cutting tool, dimensional accuracy and surface integrity along with surface finish under different cutting environments with or without using cutting fluids. During machining the application of conventional cutting fluids arise severe alarm on environmental pollution

and health hazard on workers. Research has also been initiated on control of such pollution by completely dry cutting using high heat and wear resistant cutting tools, Cryogenic machining, high-pressure coolant (HPC) jet assisted machining and minimum quantity lubricant (MQL) machining and their technological effects particularly in temperature intensive machining and grinding.

A brief review of some of the attractive and significant contributions in the closely related areas is presented in this section. This chapter also provides the background information relevant to this research. The ecological and economical dry machining and the problems of high temperature rises in dry machining, machining with conventional cutting fluids and the effects of cutting fluids on finish products and environment, other alternative lubrication system and the high-pressure coolant (HPC) jet system and its positive effects on the finished products with researchers remarks are described thoroughly in this chapter. Literature about the necessity of modeling of different process parameters, different work done by different researchers about temperature and cutting force modeling are also described.

1.1 High Speed Machining

Machinability is the term used to describe how easily a material can be cut to the desired shape with respect to the tooling and machining processes involved. In a machining operation tool life, metal removal rate (MRR), cutting forces and power consumption, surface finish generated and surface integrity of the machined component as well as the shape of the chips can all be used to measure machinability. The machinability index can be significantly affected by the properties of the material being machined,

properties and geometry of the cutting tool, cutting conditions employed and cutting environment, etc. Machining productivity can be significantly improved by employing the right combination of cutting tools, cutting conditions, machine tool and cutting environment that will promote high speed machining without compromising the integrity and tolerance of the machined components.

High-speed machining is one of advanced production technologies with great future potential. The most obvious rationale for pursuing a study of high-speed machining (HSM) is the promise of increased metal removal rate (MRR), which is the product of surface speed, depth of cut, and feed rate. While HSM generally means high surface speed, most practical applications also require some minimum chip load and this means a feed rate above a minimum value.

The term high-speed machining (HSM) is a relative one from a materials viewpoint because of the vastly different speeds at which different materials can be machined with acceptable tool life. One way of defining HSM is to consider it as that speed beyond which chip morphology is markedly different from the conventional continuous chip. In the case of very difficult-to-machine alloys, it is preferable to use the term high-throughput machining (HTM) rather than high-speed machining in order to keep a proper focus on realistic goals in machining.

High-speed machining for a given material can be defined as that speed above which shear-localization develops completely in the primary shear zone. Due to shear localization, a huge amount of heat generates at the chip tool interface, which leads a very high cutting temperature [**Kitagawa et al. 1997**]. Such high cutting temperature not only

reduces dimensional accuracy and tool life but also impairs the surface integrity of the product [**Chattopadhyay and Chattopadhyay 1982**]. The rapid wear rate of cutting tools due to high cutting temperature is a critical problem to be solved in high-speed machining (HSM) of hardened steels. In recent years, high-speed machining (HSM) technology is becoming matured owing to the advance of machine tool and control system. In comparison with the conventional methods, HSM not only exhibits a higher metal removal ate but also results in lower cutting force, better surface finish, no critical heat of the workpiece, etc.

High speed machining (HSM) of hard alloy steels (up to hardness of 62 HRC) offers several advantages such as reduction of finishing operations, elimination of part distortion, achievement of high metal removal rates and lower machining costs as well as improved surface integrity. However, HSM results in high temperatures and stresses at the tool-workpiece interface. Consequently, cost effective application of this technology requires a fundamental understanding of the relationships between process variables. Thus, it is necessary to understand how temperatures and stresses, developed during HSM, influence tool wear and premature tool failure (chipping of cutting edge) as well as residual stresses on machined surfaces. Time savings on manual work up to 80% and cost reductions up to 30% are quite realistic in high speed machining.

In applications where higher speed is limited by rapid tool wear, higher metal removal rates can be achieved by increasing depth of cut instead of speed. This can be accomplished only with a high-power, adequately rigid machine tool. The part should also be stiff enough to yield the required accuracy and finish under these cutting conditions.

However, today there is no longer any doubt concerning the economic efficiency of high-speed machining. Also conventional machine tool engineering already benefits from this trend. However, tool life decreases with increasing cutting speed, and so there is still today a substantial demand for further developments to minimise this shortcoming life will contribute substantially to growing application of the HSC technology.

1.2 Effects and Control of Cutting Temperature

Excessive temperature adversely affects the strength, hardness, stiffness and wear-resistance of the cutting tool; tools also may soften and undergo plastic deformation, thus tool shape is altered which eventually leads to tool failure, particularly the rate of wear is greatly dependent on the tool–chip interface temperature [**Usui et al. 1978**]. High temperatures at the tool–chip interface result in an increase of diffusion and chemical wear [**Endrino et al. 2006**]. Tool wear is a major consideration in all machining operations. The high specific energy required in machining under high cutting velocity and unfavorable condition of machining results in very high temperature [**Chattopadhyay and Chattopadhyay 1982, Singh et al. 1997**]. At elevated temperature and pressure the cutting edge deforms plastically and wears rapidly, which lead to dimensional inaccuracy, increased cutting forces and premature tool failure [**List et al. 2005**]. Increasing cutting forces result the increase of power consumption. Tool wear and increased heat can induce thermal damage and metallurgical changes in the machined surface**.** The experimental results show that tool wear is a dominant factor affecting the values of induced residual stress, strain, subsurface energy, and the quality of the machined surface. The increase of tool wear caused an increase of residual stress and strain beneath the machined surface. It

was also found that the overall energy stored in the machined subsurface increases as the tool wear increases and as the tool surface gets rougher. When the cutting tool is severely worn, the machined surface not only becomes very rough, but also contains many partially fractured laps or cracks. This makes tool wear a key factor in controlling the quality of the machined surface**.**

Rapid increase in notching occurs on carbide tools at higher cutting speed. This usually leads to the premature fracture of the entire insert edge [**Ezugwu and Bonney 2004**]. Flank wear generally causes an increase in the cutting force and the interfacial temperature, leading normally to dimensional inaccuracy in the work pieces machined and to vibration which makes the cutting operation less efficient [**Bouzid et al. 2004**].

High production (high speed-feed rate) machining is inherently generated high cutting zone temperature. Uncoated carbide insert creates more cutting temperature than coated insert when turning different steels [**Sultana et al. 2009**].Turning difficult to cut (DTC) materials (stainless steel, titanium, Inconel etc.) using existing conventional techniques is an un-economical as the turning process results in high tool wear, takes longer time [**Khan and Ahmed 2008**] and require high cutting force. The generation of heat was very high while turning these materials due to strong adhesion between the tool and work material resulting from their low thermal conductivity, high work hardening rate, high viscosity, high reactivity, tendency to form built-up-edge (BUE) at tool edge compared to other alloy steels.

Vleugels [**1995**] observed that the contact length between the tool and chip has a direct influence on the cutting temperatures and the amount of heat energy that is

dissipated in the tool which enhances thermally activated chemical wear. Strafford and Audy [**1997**] investigated the relationship between hardness and machining forces during turning of AISI 4340 steel with mixed alumina tools. The results suggest that an increase in hardness leads to an increase in the machining forces. Liu et al. [**2002**] observed that the cutting temperature is optimum when the work piece material hardness is HRC 50. With further increase in the work piece hardness, the cutting temperature shows a descending tendency. Liu et al. [**2002**] also suggests that, under different cutting parameters, the role of cutting force changes with work piece hardness. The main cutting force features an increasing tendency with the increase of the work piece hardness.

Reed and Clark [**1983**] reported that the hardness, plastic modulus and the fracture toughness of the tool decline with increase in cutting temperature, which accelerates tool wear rate. Moreover, thermal stresses in the tool increase with the temperature resulting in more cracks in the tool and premature failure of the tool. The amount of energy dissipated through the rake face of the tool raises the temperature at the flanks of the tool [**Wu and Matsumoto 1990**]. The cutting temperature and force are tried to be controlled or reduced to some extent by (i) appropriate selection of process parameters, (ii) appropriate selection of cutting tool geometry, (iii) proper selection of cutting tools and (iv) proper selection and application of cutting fluids.

Proper selection of the levels of the process parameters (V_c, S_o and t) can provide better machinability characteristics of a given work – tool pair even without sacrificing productivity or MRR. Amongst the process parameters, depth of cut, plays least significant role and is almost invariable compared to feed (S_o) variation of cutting velocity (V_c) governs machinability more predominantly. Increase in V_c, in general, reduces tool life but

it also reduces cutting forces or specific energy requirement and improves surface finish through favorable chip-tool interaction. Some cutting tools, specially ceramic tools perform better and last longer at higher V_c within limits. Increase in feed raises cutting forces proportionally but reduces specific energy requirement to some extent. Cutting temperature is also lesser susceptible to increase in S_o than V_c. But increase in S_o, unlike V_C raises surface roughness. Therefore, proper increase in V_c, even at the expense of S_o often can improve machinability quite significantly [**Sun et al. 2005**]. Hasçalık and Çaydaş [**2008**] showed that feed rate and cutting speed were the most influential factors on the surface roughness and tool life, respectively. The surface roughness was chiefly related to the cutting speed, whereas the axial depth of cut had the greatest effect on tool lif**e.**

The geometrical parameters such as; tool rake angles, clearance angle, cutting angles, nose radius, inclination angle and depth, width, form of integrated chip breaker of cutting tools significantly affect the machinability of a given work material under given machining conditions. Increase in tool rake angles reduces main cutting force through reduction in cutting strain, chip reduction coefficient. Presence of inclination angle enhances effective rake angle and thus helps in further reduction of the cutting forces. The variation in the principal cutting edge angle influences feed force and the cutting temperature quite significantly. Feed force, if large, may impair the product quality by dimensional deviation and roughening the surface due to vibration. Inadequate clearance angle reduces tool life and surface finish by tool - work rubbing, and again too large clearance reduces the tool strength and hence tool life. Proper tool nose radiusing improves machinability to some extent through increase in tool life by increasing mechanical strength and reducing temperature at the tool tip and also reduce of surface roughness.

Proper edge radiusing also often enhances strength and life of the cutting edge without much increase in cutting forces.

The cutting tool geometry plays a significant role on the performance of conventional machining operations, irrespectively of the work material. For instance, alterations in the cutting edge preparation will result in changes in tool wear rate, cutting forces, temperature, and machined surface finish. The results indicated that, in general, the turning force components are reduced with the tool nose radius and the specific cutting force decreased as feed rate is elevated, presenting values comparable to metallic alloys. Finally, the surface roughness increased as feed rate is elevated and tool nose radius is reduced [**Leonardo and Davim 2009**].

Tool geometry is another important factor affecting machining forces, especially the feed (axial) and thrust (radial) force components [**Thiele and Melkote 1999**]. The use of large nose radius together with low depths of cut leads to low true side cutting edge angle values, thus resulting in high thrust forces [**Muller and Blumke 2001**].

Rahman et al. [**1997**] investigated the machinability index of Inconel 718 subjected to various machining parameters including tool geometry, cutting speed and feed rate on flank wear, surface roughness and cutting force as the performance indicators for tool life. They observed that tool life increases with the increase in side cutting edge angle for the inserts and the heat generated during the cutting process is distributed over a greater length of cutting edge. This improves the heat removal from the cutting edge, distributes the cutting forces over a larger portion of the cutting edge, reduces tool notching and substantially improves tool life.

Most of the major parameters including the choice of tool and coating materials, tool geometry, machining method, cutting speed, feed rate, depth of cut, lubrication, must be controlled in order to achieve adequate tool lives and surface integrity of the machined surface [**Ezugwu and Tang 1995**]. In machining a given material, the tool life is governed mainly by the tool material which also influences cutting forces and temperature as well as accuracy and finish of the machined surface. The composition, microstructure, strength, hardness, toughness, wear resistance, chemical stability and thermal conductivity of the tool material play significant roles on the machinability characteristics though in different degree depending upon the properties of the work material. High wear resistance and chemical stability of the cutting tools like coated carbides, ceramics, cubic Boron nitride (CBN) etc also help in providing better surface integrity of the product by reducing friction, cutting temperature and BUE formation in high speed machining of steels. Very soft, sticky and chemically reactive material like pure aluminium attains highest machinability when machined by diamond tools.

Cubic boron nitrate (CBN) and polycrystalline diamonds (PCD) cutting tools have been found important place in machining processes. Cubic Boron Nitride (CBN) can maintain its hardness and resistance to wear at elevated temperatures and has a low chemical reactivity to the chip/tool interface [**Narutaki and Yamane 1979**]. The CBN tool, if properly manufactured, provides less cutting forces, temperature and less tensile residual stresses [**Davies et al. 1996**]. Polycrystalline Cubic Boron Nitride (PCBN) also displays a unique combination of hardness, toughness and thermo-chemical stability, properties which are increasingly important in a cutting tool material to meet the demands of machining hard materials. But these tools are so much expensive and recommended to

use in that case where other tool materials are not effective. However, these cutting tools are expensive and they can protect their characteristics in high temperature machining conditions. They are generally used in finish machining operation to obtain high dimensional accuracy and excellent surface finish quality.

In metal cutting processes, the basic purpose of employing cutting fluid is to improve machinability characteristics of any work-tool pair through improving tool life by cooling and lubrication, reducing cutting forces and specific energy consumption and improving surface integrity, size accuracy by cooling, lubricating and cleaning at the cutting zone. Cutting fluids also make chip-breaking and chip-transport easier. For reducing the cutting zone temperature through cooling and lubricating action a copious amount of fluid is flushed into the cutting zone to facilitate heat transfer from the cutting zone. Lubricants reduce friction and coolants effectively reduce high cutting temperature of tools/work pieces. It can flush chips away from the cutting zone, protect the machined surface from environmental corrosion and these factors improve tool life and help make a better more efficient cut [**Beaubien and Cattaneo 1964**]. On the other hand, using a cutting fluid may cause the material to become 'curly', which concentrates the heat closer to the tip. This is detrimental because it decreases the tool's life. Some conditions like machining steels by carbide tools, the use of coolant may increase tool wear [**Paul et al. 2001**] though it can reduce temperature. In case of high speed-feed machining, which inherently generated high cutting zone temperature, cutting fluid can't reduce the temperature because fluid can't reach to the chip-tool interface [**Dhar et al. 2002**]. The favorable roles of cutting fluid application depend not only on its proper selection based on the work and tool materials and the type of the machining process but also on its rate of

flow, direction and location of application. Proper selection and application of cutting fluid generally improves tool life. At low cutting speed almost four times longer tool life was obtained by such cutting fluid [**Satoshi et al. 1997**]. But surface finish did not improve significantly.

Application of conventional cutting fluids creates several other techno-environmental problems. Additional cutting fluid systems are needed in industry to deliver fluid to the cutting process, re-circulate fluid, separate chips and collect fluid mist. Moreover, for using cutting fluid environment becomes polluted. Because, for improving the lubricating performance Sulfur(S), Phosphorus(P), Chlorine(Cl) or other pressure additives are mixed with cutting fluid (Peter et al., 1996). If the cutting fluids are not handled appropriately, it may damage soil and water resource, which can cause serious environment pollution. Additionally in the factory cutting fluid may cause skin and breathing problem of the operator [**Sokovic and Mijanovic 2001**].

Cutting fluid systems are used in industry to deliver fluid to the cutting process, re-circulate fluid, separate chips and collect fluid mist. In flood cooling method, fluid is used in very large amount (6-10 l/hr). The cost associated with the use of cutting fluid is estimated to be about 16% to 20% of the total manufacturing costs [**Byrne and Scholta 1993, Brockhoff and Walter 1998**], where only 4% of the total manufacturing cost is associated with cutting tools [**Aronson 1995**]. So, in respect of costs, it is very important to reduce the amount of cutting fluid. Some conditions like machining steels by carbide tools, the use of coolant may increase tool wear [**Paul et al. 2001**].

Furthermore, the permissible exposure level (PEL) for metal working fluid aerosol concentration is 5 mg/m^3 as per the U.S. Occupational Safety and Health Administration [**Aronson 1995**] and is 0.5 mg/m^3 according to U.S. National Institute for Occupational Safety and Health [**Thornberg and Leith 2000**]. The oil mist level in U.S. automotive parts manufacturing facilities has been estimated to be generally on the order of 20-90 mg/m^3 with the use of traditional flood cooling and lubrication [**Bennett and Bennett 1985**]. This suggests an opportunity for improvement of several orders of magnitude.

Also coolants and lubricants incur a significant part of the manufacturing cost. For instance in the production of camshafts in European automotive industry, the cost of coolants/lubricants constituted 16.9% of the total manufacturing cost, while the cost of tools was 7.5%. That is, the cost of purchase, storage, care and disposal of coolants are two times higher than the cost of tool.

So, from the viewpoint of cost, ecological and human health issues, manufacturing industries are now being forced to implement strategies to reduce the amount of cutting fluids used in their production lines [**Klocke 1997**]. New approaches for elimination of cutting fluids application in machining processes have been examined and "dry machining" was presented as an important solution [**Sreejith and Ngoi 2000, Popke et al. 1999**]. But some times dry machining cannot show better performance if higher machining efficiency, better surface finish and other special cutting conditions are required. For these reasons many special techniques can be used as alternative of the traditional flood cooling method. Such as, Mist lubrication system by water based fluids, Cryogenic Machining where nitrogen and carbon dioxide are used as a coolant, Near-dry

cooling/ minimum quantity lubrication (MQL) system with the application of a mist of a mixture of water and cutting fluid, High-pressure coolant (HPC) system, Coolant through the cutting tool system which allows a direct route for the coolant to the hot area. All these methods are proved as good for tool life, good for the environment.

Cryogenic machining with liquid nitrogen has improved machinability of steel to a certain extent in case of turning, grinding, milling, drilling operations. In high production machining, where conventional cutting fluids are ineffective in controlling the high cutting temperature, force, tool wear, dimensional accuracy and surface finish; cryogenic machining where the cutting tool is chilled by liquid nitrogen jets enhances tool hardness shows better effectiveness [**Paul and Chattopadhyay 1995**]. Favorable chip-tool and work-tool interactions can be achieved by this technique. Cooling the chip makes it brittle and aids removal. Moreover, by cryogenic cooling environmental pollution is reduced and it also helps in getting rid of recycling and disposal of conventional fluids [**Paul et al. 2000, Paul et al. 2001, Dhar et al. 2002, Dhar and Kamruzzaman 2007**]. But cryogenic machining is costly due to high cost of liquid nitrogen. It also accelerated notch wear on the principal flank of the carbide insert was observed at nitrogen rich atmosphere of cryogenic machining.

Minimum quantity lubrication (MQL) is a established alternative of the traditional flood cooling method but it over come the negative side of flood cooling as MQL is a near dry lubrication process. So, cost for coolant and environment pollution may be reduced [**Weinert et al. 2004**]. With the application of MQL cutting and feed force, variation of cutting force, cutting zone temperature, tool wear, dimensional inaccuracy, chip-tool contact length are reduced and surface finish, tool life are increased [**Dhar[a] et al., 2006**

and Dhar[b] et al., 2006]. Here the manner of lubricant supply is more important than the total amount of lubricant supplied. That means the amount which actually reaches in the chip-tool interface to reduce temperature. Dimensional accuracy also substantially improved mainly due to significant reduction of wear and damage at the tool tip by the application of MQL.

If the coolant is applied at the cutting zone through a high speed nozzle, it could reduce the contact length and co-efficient of friction at chip-tool interface then cutting force and temperature may be reduced and tool life can be increased [**Mazurkiewicz et al. 1998, Kumar et al. 2002**]. High-pressure is often the solution to get the coolant to the target so it can cool, lubricate, and sometimes perform its third function-breaking chips that do not break neatly with ordinary machining processes [**Lo´pez de Lacalle et al. 2000**]. Concern for the environment, health and safety of the operators, as well as the requirements to enforce the environmental protection laws and occupational safety and health regulations are compelling the industry to consider a high-pressure coolant (HPC) machining process as one of the viable alternative instead of using conventional cutting fluids.

1.3 High Pressure Coolant (HPC) Jet Machining

The life of a cutting tool, and the efficiency in metal cutting, is mainly dependent on the heat that is generated in the contact zone between the tool rake and the machined material. Conventional or low-pressure cooling methods are not sufficiently efficient to penetrate the zone and change the thermal, frictional and mechanical conditions in the cutting zone. Kaminski and Alvelid [**2000**] investigate the effects of a high- and ultra-high-

pressure water jet directed into the tool-chip interface on tool temperature, cutting forces, chip shape and surface roughness in regular turning operations. The results show that a significant reduction of edge temperature, by 40-45%, is possible.

High pressure coolant systems generate high velocity coolant streams moving at several hundred mph. This high speed coolant easily penetrates the vapor barrier to effectively lubricate and cool the tool. This system not only provides adequate cooling at the tool–workpiece interface but also provides an effective removal (flushing) of chips from the cutting area. The temperature generally reduced by approximately 50% when high-pressure cooling was applied compared with conventional cooling [**Dahlman 2002**].

Excellent chip breakability has been reported when machining difficult-to-cut materials with high-pressure coolant supply [**Crafoord et al. 1999, Nabhani 2001**]. This is attributed to a coolant wedge, which forms between the chip and tool forcing the chip to bend upwards giving it a desirable up curl required for segmentation. It can reduce the contact length and coefficient of friction. There is a drastic reduction in the cutting forces required to remove material from the work piece and increase tool life to some extent with the application of high-pressure coolant jet. The application the cutting fluid at high pressures in the form of a narrow jet, leads to a reduction in the quantity of the cutting fluid being used, reducing the amount of disposal which is a primary concern of Environmental Protection Authorities.

The use of a high-pressure coolant supply when machining nickel-based (Inconel 901) super alloy with cemented carbide tools gives higher tool lives compared to machining with conventional coolant technique [**Ezugwu et al. 1990**]. Cutting tools

operate within a safety temperature zone with minimal tool wear when machining at the critical coolant pressure as thermal stresses are kept to a minimum, thereby prolonging tool life [**Ezugwu and Bonney 2003**].

Ezugwu and Bonney [**2004**] reported that machining Inconel-718 with coated carbide inserts under high-pressure coolant supplies improve tool life by up to 7 folds, especially at high speed conditions. Tool life tends to improve with increasing coolant pressure. There is also evidence that once a critical pressure has been reached any further increase, in coolant pressure may only result to a marginal increase in tool life. Lower cutting forces where generated when machining Inconel 718 with whisker reinforced ceramic tool at higher coolant supply pressures due to improved cooling and lubrication (low frictional forces) at the cutting interface and also as a result of chip segmentation caused by the high-pressure coolant jet [**Ezugwu et al. 2005**].

Lo´pez de Lacalle1 et al. [**2000**] examine the results of machining tests carried out on two extremely difficult to machine alloys commonly used in the aircraft industry, specifically, alpha–beta type titanium alloy Ti6A14V and nickel-based superalloy of type 718. They are, however, for various reasons. The aim of this paper is to consider how their drilling, turning, and milling could be made more productive. It is effective in the cutting of titanium to use a high-pressure water-jet system. Cutting speeds are double the conventional speed with a good drill life.

Dahlman [**2004**] showed that High-pressure cooling in turning operations is an effective method for achieving higher productivity. The use of HPC significantly improved chip control compared to dry machining, especially when using the wiper insert geometry.

The highest impact on chip control is achieved at low cutting feed rates. Chip control was not affected by cutting speed. A reduction of the Surface roughness value by about 80% can be observed when using HPC instead of dry turning. It can be concluded that wear can be drastically reduced by using HPC with tooling sensitive to thermal cracking.

Cozzens et al. [**1995**] conducted an experimental investigation on single point boring aiming to study the role of cutting fluid, tool and workpiece material, tool geometry and cutting conditions on machinability. The results indicated that the cutting fluid conditions have no significant effect on surface texture, forces and built-up edge. Since boring is a high-speed operation and lubrication is ineffective, no effect was seen on the forces. However, the cutting fluid was found to have a significant effect on surface integrity.

In drilling operations when temperature is increased a large amount of tool wear appears at the drill bit. Such high cutting temperature not only reduces dimensional accuracy and tool life but also impairs the surface integrity of the product; either it affects roundness of the hole or chip shape and color of chip. High-pressure coolant has reduced temperature as well as improving roundness and also provides lubrication in the tool tip and surface interface [**Dhar[c] et al. 2006**]. In Grinding operation material is generally removed by shearing and ploughing in the form of micro sized chips by the abrasive grits of the grinding wheel. As a result, high temperature is produced in the grinding zone due to large negative rake and high cutting speed of the grinding wheel. High-pressure coolant jet effectively reduces cutting zone temperature entering into chip tool interface maintaining a good surface integrity [**Dhar[d] et al. 2006**].

The effectiveness of high-pressure coolant in End milling can be evaluated in terms of improvement of surface finish, reduction in tool wear and cutting forces, and control of chip shape. Kumar et al. [**2002**] showed that in end milling ASSAB 718 supreme pre-hardened and tempered plastic mould steel, the application of high-pressure coolant produces a great reduction in flank wear and hence tool life and produces a significant improvement in surface finish for both uncoated and coated inserts. It is found that the cutting force is reduced, surface finish improved, and chip width is reduced with the use of high-pressure coolant.

1.4 Literature Review

1.4.1 Modeling of Cutting Temperature

The importance of temperature prediction for the machining processes has been well recognized in the machining research community primarily due to its effects on tool wear and its constraints on the productivity, tool life, part quality, chip morphology, etc. It is well observed that particularly the rate of wear is greatly dependent on the tool–chip interface temperature [**Usui et al. 1978**]. Temperature is one of the major concerns and, after chatter stability, perhaps is the main limitation in the selection of process parameters, such as cutting speed and feed rate, in the machinability and production of some advanced materials such as titanium and nickel-based alloys [**Klock et al. 1996**]. In these materials, due to their low thermal conductivity, most of the heat generated during the machining flows into the tool and, therefore, besides mechanical stresses on the cutting tools, severe thermal stresses occur. The thermal stresses accelerate tool fatigue and failures due to

fracture, wear or chipping. Furthermore, if the temperature exceeds the crystal binding limits, the tool rapidly wears due to accelerated loss of bindings between the crystals in the tool material.

The role of the cutting temperature in metal cutting has been studied in great detail, beginning as early as 1907 by Taylor [**1907**]. Since the early twentieth century, much of the work on the thermal aspects of metal cutting has been directly experimental, providing mostly temperature in an average sense. These works can be categorized as thermo-e.m.f (thermocouples), radiation (pyrometry, infrared photography, etc.) and thermo-chemical reactions (thermo-colours) [**Barrow 1973**]. Other experimental methods have included the metallographic method [**Wright and Trent 1973**] and the physical vapour deposition (PVD) film method [**Kato and Fujii 1996**] to name just a few. Alternatively, the reverse estimation scheme has been tried to solve the cutting temperature profile based on the indirectly measured temperature information [**Yen and Wright 1986**]. Numerical methods were also applied to determine the temperature distribution with some important results documented by Tay et al. [**1974**] and Dawson and Malkin [**1984**]. Apparently, experimental measurements are laborious and costly to carry out. As alternatives, numerical and analytical investigations have been receiving more and more attention.

1.4.1.1 Numerical Modelling of Cutting Temperature

Numerical methods (FEM or other computational methods) were also applied to determine the temperature distribution with some important results documented by Tay et al. [**1974**] and Dawson et al. [**1984**]. More recent progress has been reviewed by da Silva

et al. [**1999**] and Ng et al. [**1999**]. Although significant advances in computing technology have been witnessed recently, numerical methods are still time consuming and their accuracy depends on formulation methods, workpiece material constitutive models, the tool-chip condition, and boundary conditions. Most importantly, at present, they are not efficient when used in process optimization, especially when using an exhaustive searching method. As a much less computationally intensive approach, analytical modeling attracts a lot of interest in efforts to optimize the machining processes.

Usui et al. [**1978**] and Tlusty and Orady [**1981**] used the finite difference method to predict the steady-state temperature distribution in continuous machining by utilizing the predicted quantities, such as chip formation and cutting forces, through the energy method. The predicted temperatures were lower than the observed ones near the cutting edge and the chip leaving point. They correlated the crater wear of carbide tools to the predicted temperature and stresses in the tool. Smith and Armarego [**1981**] have predicted temperature in orthogonal cutting with a finite difference approach. Ren and Altintas [**2000**] applied a slip line field solution proposed by Oxley [**1989**] on high speed orthogonal turing of hardened mold steels with chamfered carbide and CBN tools. They evaluated the strain, strain rate and temperature dependent flow stress of the material, as well as the friction field at the rake face–chip contact zone from standard orthogonal cutting tests conducted with sharp tools. They showed a good correlation between the maximum temperature on the rake face and crater wear, which led to the identification of cutting speed limits for an acceptable tool life limits.

Strenkowski and Moon [**1990**] have developed an Eulerian finite element model to simulate the cutting temperature. This Eulerian formulation of the cutting model

requires a constitutive law between the viscosity, second invariant of the strain rate tensor and uniaxial yield stress. An iterative computational scheme is also required for the solution. Numerical solutions, especially Finite Element (FE) methods require accurate representation of material's constitutive properties during machining. However, since the strain rates and strains are several magnitudes higher than those evaluated from standard tensile and Hopkinson's bar tests, FE methods mainly suffer due to lack of accurate material models. Shatla et al. [**1999**] used the material properties evaluated from orthogonal cutting and milling tests in the FE simulation of metal cutting. He reported improvements in predicting the temperature and cutting forces in both continuous turning and transient milling operations using a Finite Element method. There has been less research reported in the prediction of tool temperature in milling, where the chip thickness vary continuously, and the process is intermittent (i.e., the tool periodically enters and exits the cut). As a result, the shear energy, shear angle, and the friction energy changes continuously with time. Hence, the process does not stay in steady-state equilibrium like in continuous machining operations.

McFeron and Chao [**1958**] have developed a model for the analytical calculations of average tool–chip interface temperature for the plain peripheral milling process. They have instrumented a face mill with a thermocouple to measure the average transient temperature on the rake face of a carbide tool. Stephenson and Ali [**1992**] analyzed a special case of interrupted cutting with constant chip thickness. They have developed a model by considering a semi-infinite rectangular corner heated by a time varying heat flux with various spatial distributions to predict the average temperature on the rake face. They concluded that tool temperatures are generally lower in interrupted cutting than in

continuous cutting under the same condition since temperature is dependent primarily on the duration of heating cycle and secondarily on the length of cooling time between cycles. As they noted, their analysis quantitatively underestimates the temperatures for short heating cycles.

Stephenson et al. [**1997**] have presented work on temperature prediction in contour turning. Redulescu and Kapoor [**1994**] analyzed the tool–chip interface temperature by solving the heat conduction problem with prescribed heat flux. The mechanistic force model was utilized in this analysis. Their results also indicate that the tool–chip interface temperature increases with cutting speed for both continuous and interrupted cutting. Jen and Lavine [**1994**] used a similar approach to Redulescu for tool temperature calculation and improved calculation speed relatively by using power law approximation for the exponential terms. For further information on the literature review and on methods to calculate the machining temperature, the publication by Tay [**1993**] is recommended. One of the biggest challenges in this research area is the lack of the experimental data to verify the mathematical models proposed in predicting the tool temperature. It is rather difficult to embed sensors close to the cutting edge. Infra-red temperature sensors provide average readings from the entire cutting zone. When the cutting is time varying like in milling, it is more challenging to put even simple sensors close to the cutting edge of the rotating tool. Most published articles rely on the few published experimental data from Trigger and Chao [**1951**], Boothroyd [**1963**] and Stephenson and Ali [**1992**]

Kim et al. [**1999**] presented a finite element method for predicting the temperature and the stress distributions in micromachining. The diamond cutting tool is used to

machine the work material oxygen-free-high-conductivity copper (OFHC copper) and its flow stress is taken as a function of strain, strain rate and temperature in order to reflect realistic behavior in machining process. From the simulation, a lot of information on the micro-machining process like the effects of temperature and friction on micro-machining are investigated.

A numerical model based on the finite difference method is presented by Lazoglu and Altintas [**2002**] to predict tool and chip temperature fields in continuous machining and time varying milling processes. Continuous or steady state machining operations like orthogonal cutting are studied by modeling the heat transfer between the tool and chip at the tool-rake face contact zone. The shear energy created in the primary zone, the friction energy produced at the rake face-chip contact zone and the heat balance between the moving chip and stationary tool are considered. The temperature distribution is solved using the finite difference method. Later, the model is extended to milling where the cutting is interrupted and the chip thickness varies with time. The proposed model combines the steady-state temperature prediction in continuous machining with transient temperature evaluation in interrupted cutting operations where the chip and the process change in a discontinuous manner. Heat balance equations were determined in partial differential equation forms for the chip and for the tool. The finite difference method was utilized for the solutions of the steady-state tool and chip temperature fields. The simulation results both for continuous and interrupted machining processes agreed well with experimentally measured temperatures for different materials under various cutting conditions. The proposed algorithm can be utilized in selecting cutting speed, feed rate and tool rake and clearance angles in order to avoid excessive thermal loading of the tool,

hence reducing the edge chipping and accelerated wear of the cutting tools. The mathematical models and simulation results are in satisfactory agreement with experimental temperature measurements reported in the literature.

Experiments carried out by Sundaram et al. [**2003**] investigate the influence of various grinding parameters like wheel speed, workspeed and depth of cut on the grinding temperature at the surface of the Al-SiCP composite workpiece with different grinding wheels. The temperature distribution within the workpiece was studied by simulating the grinding process and using finite element analysis package with transient thermal analysis. Specific energy as the input, the temperature distribution for dry grinding condition and with coolant was analyzed. Even though partition ratio is lower for diamond, but the temperature developed at the surface is more for diamond compared with other wheels. The affinity to wheel loading is more for diamond wheels than other wheels. The CBN shows better results than other wheels. The influence of coolant is significant.

Grzesik and Nieslony [**2004**] proposed a physics based modelling concept has been applied to both the individual layer and the composite layer approach to develop an estimate of the average and the maximum steady-state chip-tool interface temperatures in orthogonal turning. Different approaches for determining the heat partition coefficient for sliding bodies of defined thermal properties were tested.

A novel approach to cutting temperature prediction in multi-layer coated cutting tools is developed by Attia and Kops [**2004**]. This approach is not based on the commonly used assumption of perfect contact at the tool-chip interface, but rather the contact mechanics at asperity level and the resulting thermal constriction resistance. A Micro-

contact model was developed, and the correlation between the contact pressure and the thermal contact resistance of uncoated and multi-layer coated tools is established. The model was validated against analytical and experimental data. The thermal interaction and redistribution of heat between the workpiece, the chip and the tool were analyzed, supported by FE model, which considers thermal characteristics of multi-layer coating. It was found that coating causes reduction of the heat flow into the tool and reduction of the maximum temperature rise. These reductions can reach more than 50% and 120ºC, respectively. The importance of the present approach lies in the fact, that it can be used with a higher degree of confidence for the design of coated tools and other related issues, such as e.g. wear.

Grzesik et al. [**2005**] create a FEM simulation model in order to obtain numerical solutions of the cutting forces, specific cutting energy and adequate temperatures occurring at different points through the chip/tool contact region and the coating/substrate boundary for a range of coated tool materials and defined cutting conditions. Commercial explicit finite element code Thirdwave Advant Edge has been used in simulations of orthogonal cutting processes performed by means of uncoated carbide and coated tools. The various thermal simulation results obtained were compared with the measurements of the average interfacial temperature and discussed in terms of various literature data.

Carvalho et al. [**2006**] developed a thermal model which is obtained by a numerical solution of the transient three-dimensional heat diffusion equation that considers not just the insert tip but also the shim and tool holder assembly. To determine the solution equation the finite volume method is used. Changing in the thermal properties with the temperature and heat losses by convection are also considered. Several cutting tests using

cemented carbide tools were performed in order to check the model and to verify the influence of the cutting parameters on the temperature field.

Bareggi et al. [**2007**] present approaches for modelling the cooling influence of high velocity air jets using a supersonic nozzle during metal cutting on a lathe with the commercial package DEFORM 3D. Here, simulation results are consistent with the analytical results from other researchers. Cutting temperatures estimated with DEFORM 3D are consistent with simulation undertaken with ADVANTEDGE. While simulation offers insights into the process which are not easily measured in experiments, careful engineering scrutiny of approaches and results remains necessary.

Soo et al. [**2007**] follow a brief historical perspective on the development of orthogonal cutting model's, including key work by Merchant and Oxley and concentrates on the use of finite element techniques to simulate two-dimensional orthogonal turning and the subsequent transition to three-dimensional formulations, thus enabling milling and drilling to be realistically modelled.

The results reported in the paper by Mamalis et al. [**2008**] pertain to the simulation of high speed hard turning when using the finite element method. For the finite element modelling a commercial programme, namely the Third Wave Systems Advant-Edge, was used. This programme is specially designed for simulating cutting operations, offering to the user many designing and analysis tools. The orthogonal cutting models provide results such as workpiece and tool temperatures which were compared to experimental results from the relevant literature. The 3D oblique cutting models represent a situation where the chip deforms not in plane as in the ideal case of orthogonal cutting

but in all three dimensions; a more realistic approach is, thus, provided. Nevertheless, these models are more complicated and require the use of much more elements increasing this way the effort and the computational time required for the analysis. From the analysis it can be concluded that the proposed models are practical, since only a minimum amount of experimental work is needed, and produce reliable results, allowing for industrial use in pursue of optimal production.

Grzesik and Bartoszuk [**2009**] analyzed quantitatively heat transfer problem in the cutting tool in a steady-state orthogonal cutting when using uncoated carbide tools and the AISI 304 stainless steel as a work material. Finite Difference Approach (FDA) is applied to predict the changes of temperature distribution, and both average and maximum temperatures at the tool-chip interface, resulting from differentiating the heat flux configuration. It was found that the assumption of an asymmetrical trapezoidal shape of heat flux configuration, similar to the distribution of contact shear stress, provides the simulated results closer to the experimental data.

1.4.1.2 Analytical Modelling of Cutting Temperature

Analytical modeling approach can provide better insight to the underlying physical mechanisms. At the forefront of analytical modeling, based on the moving heat source method, the analytical modeling of steady-state temperature in metal cutting has been presented by Hahn [**1951**], Trigger and Chao [**1951, 1953, 1955, 1958**], Loewen and Shaw [**1954**]. Trigger and Chao [**1951**] made the first attempt to evaluate the cutting temperature analytically. They calculated the average tool–chip interface temperature by considering the mechanism of heat generation during the metal cutting operations. They

concluded that the tool–chip interface temperature is composed of two components: (a) that due to the plastic deformation associated with the chip formation at the shear zone; and (b) that due to friction between the chip and tool face along the contact region. Loewen and Shaw [**1954**] have stated that it is not possible to experimentally determine the influence of many of the variables on the cutting temperature, or to measure conveniently its components. They developed a simple analytical procedure to compute the interface temperature by making the assumptions that the fraction of heat flow into the chip is constant along the rake face in the tool–chip contact region, and the tool acts like a quarter infinite body.

Most recently Komanduri and Hou [**2000, 2001[a], 2001[b]**] and Huang and Liang [**2005**] model the temperature analytically based on the premise of a moving heat source [**Jaeger 1942, Carslaw and Jaeger 1959**]. The commonalties of these models are the consideration of heat sources at the primary and the secondary shear zones with related boundary conditions and the assumption that the bulk of the deformation energy is converted into heat while a negligible amount is stored as latent energy in the deformed metal. However, there are differences in these models in the way the heat source properties and boundary conditions were treated. In treating the primary heat source, the models are different in considering the nature, the moving direction, and velocity of the heat source, as well as in estimating the heat partition ratio and the boundary conditions.

When modeling the temperature rise on the chip side, the velocity of the moving heat source was treated differently as the chip velocity in work [**Hahn 1951, Trigger and Chao 1951**] as the cutting velocity in work [**Chao and Trigger 1953**], and as the shear velocity in work [**Loewen and Shaw 1954**]. Furthermore, except for those of work [**Hahn**

1951, Chao and Trigger 1953, Komanduri et al.2000], most models considered the primary heat source as the result of two bodies in sliding contact and used Blok's heat partition approach [**Blok 1938**] for the evaluation of the average temperature within the primary shear zone. Realizing the fact that there is actually only one body involved in the primary shear zone, Komanduri et al. [**2000**] proposed that the temperature rise on chip due to the primary heat source should be the effect of an oblique band heat source moving at chip velocity within a semi-infinite medium. They also argued that the temperature rise on the workpiece is the result of an oblique band heat source moving at the cutting velocity within a semi-infinite medium. No boundary along the tool-chip interface was considered when modeling the effect of the primary heat source, though an insulated boundary condition along the tool-chip interface was used when modeling the effect of the secondary heat source. In evaluating the combined effects of two heat sources, Komanduri et al. [**2001[b]**] considered the effect of the primary heat source on the final temperature rise within the tool by introducing an induced stationary rectangular heat source caused by the primary heat source. When modeling the effect of the secondary heat source, the heat partition approach is commonly applied by considering a contact pair of the tool and the chip.

Chao et al. [**1953**] used Blok's partition principle [**Blok 1938**] by assuming a uniform heat partition ratio along the tool-chip contact length, but failed to achieve a temperature rise on the chip in agreement with that on the tool along the interface. To resolve this issue, Chao et al. suggested there was a non-uniform distribution of the heat partition ratio along the contact length and tried the functional analysis method, the discrete numerical iterative method [**Chao and Trigger 1955**], and a method in which the

linear algebraic equations [**Chao and Trigger 1958**] are simultaneously solved. On the other hand, Chao et al. [**Chao and Trigger 1958**] simply assumed that the heat intensities along the tool-chip and tool-workpiece interfaces were uniform, which actually should have been the combination of plastic and elastic zones with different heat intensities, respectively.

Recently, Komanduri et al. [**2001[a]**] furthered the functional analysis approach based on the idea of Chao et al. [**1955**], but no perfect function has been found. Although those studies [**Chao and Trigger 1958, Komanduri and Hou 2001**] have adopted the concept of a non-uniform distribution of the heat partitionratio, they all treated heat intensity along the tool-chip interface as uniform. Wright et al. [**1980**] modeled the effect of the secondary heat source by applying non-uniform heat intensity, but applied a uniform heat partition ratio which was determined empirically. Until now, there is no documented model that considers both the non-uniform heat partition ratio and non-uniform heat intensity along the tool-chip interface. This better understanding of the temperature distribution along the tool–workpiece interface at the presence of tool wear helps to provide insight into several important issues in metal cutting, such as tool wear progression, dimensional tolerance and workpiece surface integrity, etc. Unfortunately, most of the analytical studies documented thus far focus on thermal modelling only for a fresh tool. The effect of tool wear on the cutting temperature distribution was first modelled by Chao and Trigger and there have been very few followers since [**Huang and Liang 2003**]. In the work of Chao and Trigger, the primary heat source was taken as having no effect on the workpiece temperature rise, and the temperature rise on the chip side was modelled as an average bulk quantity. This paper analytically quantifies the tool

wear effect by taking into account the contributions of the primary heat source and considering the distribution of chip temperature rise. However, the temperature rise due to the primary heat source on the workpiece surface underneath the tool flank face can be as high as 200^{o}C depending on the thermal number in conventional cutting [**Komanduri and Hou 2000**]. Furthermore, the temperature rise due to the primary heat source has been shown to be distributed, rather than constant, along the chip side [**Komanduri and Hou 2000**].

Huang and Liang [**2003**] proposed a model of the temperature distributions analytically, especially along the tool– workpiece contact length in orthogonal cutting for a worn tool. The study utilizes the heat source method [**Jaeger 1942, Carslaw and Jaeger 1959**] to treat the effects of heat sources. On the chip side, the effect of the primary shear zone is modelled as a uniform moving oblique band heat source and that of the secondary shear zone as a non-uniform moving band heat source within a semi-infinite medium. On the tool side, the effects of both the secondary and the rubbing heat sources are considered as non-uniform static rectangular heat sources within a semi-infinite medium. On the workpiece side, the primary shear zone is modelled as a uniform moving oblique band heat source and the rubbing heat source as a non-uniform moving rectangular heat source within a semi-infinite medium. The proposed model is verified based on the published experimental data of orthogonal cutting Armco iron. In addition, a case is presented to analyse the effects of cutting speed, feed rate and flank wear length on the temperature distributions.

It is found that the progression of flank wear does not change the average rake face temperature noticeably and both the average flank face temperature and average rake

face temperature increase with the flank wear length and cutting speed, but decrease with feed rate. The model-estimated ratio of average rake temperature to average flank temperature over a range of cutting conditions and flank wear lengths is in agreement with published experimental observations.

Analytical models for estimating the interface temperature and heat partition to the chip in continuous dry machining of steels with flat-faced tools treated with multilayer coatings are presented by Grzesik and Nieslony [**2003**]. The database for modeling includes changes in the thermal properties of both workpiece and substrate/coating materials and the Peclet and Fourier numbers occurring at actual interface temperatures. Process outputs involve the average tool–chip interface temperature, the tool–chip contact length, the friction energy and the heat balance between the moving chip and stationary tool.

Among many temperature modeling studies, uniform heat partition ratio and/or uniform heat intensity along the interface are frequently assumed. This assumption is not true in actual machining and can lead to ill-estimated results at the presence of sticking and sliding. Huang and Liang [**2005**] present a new analytical cutting temperature modeling approach to describe the temperature distribution along the tool-chip contact length in metal cutting. It addresses related boundary conditions, considers the combined effect of the primary and the secondary heat sources, and solves the temperature rise along the tool-chip interface based on the non-uniform heat partition ratio and non-uniform heat intensity along the interface.

Grzesik [**2006**] studied the temperature distribution in the cutting zone was determined by integrating thermal analytical and simulation models of orthogonal cutting process with uncoated and coated carbide tools. Primarily, 2D FEM simulations were run to provide numerical solutions of temperatures occurring at different points through the chip/tool contact region and the coating/substrate boundary under defined cutting conditions. The changes of the temperature distribution fields resulting from varying heat flux transfer conditions are the main findings of the FEM simulations. Finally, the analytically and numerically predicted average temperatures were validated against the tool-work thermocouple-based measurements and discussed in terms of relevant literature data.

Zhang and Liu [**2008**] have developed an analytical model with constant temperature at tool and chip interface of one-dimensional heat transfer in monolayer coated tools to investigate temperature distribution in metal cutting. The explicit form of temperature formulae were obtained by using the Laplace Transform technique and a Taylor series expansion. The transient temperature distributions have shown that the thermo-physical parameters of coating and substrate materials have huge influences on temperature distributions in monolayer coated tools. The coating thickness also has some influence on temperature distributions in coated tools.

Bono and Ni [**2002**] developed a model for predicting the heat flow into the workpiece and investigated the influence of the heat that emerges on hole diameter and cylindricity in dry drilling. Finally, he has presented a comparison between numerical and experimental results.

1.4.1.3 Other Approaches of Modelling Temperature

Al based models are developed using non-conventional approaches such as Artificial Neural network (ANN), Fuzzy Logic (FL) and Genetic Algorithm (GA). Machining process is very complex and does not permit pure analytical physical modeling. Thus, experimental and analytical models also known as explicit (empirical) models are developed by using conventional approaches such as Statistical Regression technique with combination of Response Surface Methodology (RSM) had remained as an alternative in mathematical modeling for machining processes. Although Statistical Regression technique may work well for machining process modeling, this technique may not describe precisely the underlying non linear complex relationship between decision variables and responses. Yu-Hsuan et al. [**1999**] in their study concluded that non conventional approach; ANN model gave a high accuracy rate (96-99%) for predicting surface roughness (response) in end milling operation compare to the result obtained from Statistical Regression model. Jiao et al. [**2004**] applied FL technique based on fuzzy adaptive network (FAN) model for surface roughness prediction in turning operation; concluded that FAN network can estimate many parameters and even tune the network structure and thus is much more powerful than the usual multiple variables regression analysis. Jian and Ongxing [**2003**] in their work, focusing on modeling the system error of workpieces under cutting tool setting based on GA technique; presented that GA based method was better than the regression-modeling method in terms of accuracy and generalization ability. Recently, AI based models have become the preferred trend which are applied by most researchers to develop model for near optimal conditions in machining process. However, difference techniques labeled as AI may be suitable and could work

well in certain modeling problems. Thus, this paper discusses the abilities, limitations with the applications of ANN technique in the modeling stage in order to find the optimal conditions in machining process. The features of the modeling approach and their application potentials are concluded based on the machining processes. The following section discusses one of the three non conventional approaches listed above, i.e. ANN technique in order to be used in developing the prediction models to predict the values of decision variables and responses in machining process.

1.4.2 Modeling of Cutting Forces

1.4.2.1 Numerical Modelling of Cutting Forces

It is important to study the various approaches for simulating cutting forces in orthogonal and oblique cutting operations since they give a clear overview of the modeling of forces in any machining operation. Typical approaches for numerical modeling of metal cutting are Lagrangian and Eulerian techniques. Lagrangian techniques, the tracking of discrete material points, have been applied to metal cutting [**Sehkon and Chenot 1993, Obikawa and Usui 1996, Obikawa et al. 1997**]. Techniques typically used a predetermined line of separation at the tool tip, propagating a fictitious crack ahead the tool. This method precludes the resolution of the cutting edge radius and accurate resolution of the secondary shear zone due to severe mesh distortion. To alleviate element distortions, others used adaptive remeshing techniques to resolve the cutting edge radius [**Sehkon and Chenot 1993, Marusich and Ortiz 1995**]. Eulerian approaches, tracking volumes rather than material particles, did not have the burden of rezoning distorted

meshes [**Strenkowski and Athavale 1997**]. However, steady state free-surface tracking algorithms were necessary and relied on assumptions such as uniform chip thickness, precluding the modeling of milling processes or segmented chip formation.

Özel et al. [**1998**] predicted chip formation, cutting temperatures, tool stresses and cutting forces from Finite Element Method (FEM) simulations. The experiments were conducted in a horizontal high speed milling center to measure cutting forces. Predicted cutting forces and chip shapes were compared with experimental results.

Ozel and Altan [**2000**] developed a methodology for simulating the cutting process in flat end milling operation and predicting chip flow, cutting forces, tool stresses and temperatures using finite element analysis (FEA). As an application, machining of P-20 mold steel at 30 HRC hardness using uncoated carbide tooling was investigated. Using the commercially available software DEFORM-2D, previously developed flow stress data of the workpiece material and friction at the chip–tool contact at high deformation rates and temperatures were used. Comparisons of predicted cutting forces with the measured forces showed reasonable agreement and indicate that the tool stresses and temperatures are also predicted with acceptable accuracy. The highest tool stresses were predicted at the secondary (around corner radius) cutting edge.

Marusich [**2001**] observes the influence of cutting speed and friction on cutting force by way of finite element modeling. Simulations are validated by comparison of cutting forces and chip morphologies for the Al6061-T6. Analysis of cutting forces over a wide range of cutting conditions suggests an important role of the secondary shear zone in the decrease of cutting force as a function of speed, even well into what is considered to be

the adiabatic machining regime. The proposition is supported by a decrease in chip thickness and significant increase in temperature at the tool-chip interface as the speed is increased. Temperatures in the primary shear zone rise only modestly and cannot account for the change in cutting force. Furthermore, the effect contributes to the nonlinear increase of forces with respect to feed as opposed to a plowing force by the cutting edge radius.

Patrascu and Carutasu [**2007**] presented a FEM model for 3D simulation of turning process with chip breaker tools. The model uses Oxley's machining theory to predict cutting forces for square inserts. Inserts were modeled with CATIA V5R8 and exported as STL files to import them in DEFORM 3DTM software. A comparison made between predicted and experimental results shows good agreement.

Otieno and Mirman [**2008**] presented a finite element analysis of the machining of aluminum T6061 alloys. The cutting forces and temperatures are predicted using AdvantagEdge™ software. The results are used to guide machining operators to select machining conditions that produce favorable stresses on the tools, thus avoiding tool breakage. The preliminary results from this study can be used in an optimization process to determine optimum cutting conditions. Moreover, by studying the stresses in the tool material, it is possible to determine what the maximum recommended feeds and depths of cut should be for given cutting speeds.

Aly et al. [**2004**] introduced the use of molecular dynamics and dislocation theory as a link between nano-scale and meso-scale modules with the finite element method calculations serving as a bridge between the modules. The purpose of this work is to fill

the void between the nanometric scale information required to model micro-cutting and the known macro-scale mechanical behaviour of materials in metal cutting. The proposed study suggests several future perspectives for the use of alternative modules aiming to further our knowledge of material behaviour modeling related to manufacturing processes.

1.4.2.2 Analytical Modelling of Cutting Forces

The analytical models are based upon the theory of mechanics of cutting, orthogonal or oblique but they are complicated and mostly, they demand the a-priori knowledge of response magnitudes, as shear angle and friction angle [**Shaw 1989**].

Many researchers have investigated forces in metal cutting operations in the past. Earlier cutting force models have been developed and simulated for orthogonal cutting operations by Merchant [**Merchant 1945**] who assumed the chip to be a rigid body held in equilibrium by the action of forces across the chip tool interface and shear plane. He also assumed that the shear plane angle would minimize the work done in cutting. Analytical models have been favored for the modeling of forces in metal cutting because they are easy to implement and can give much more insight about the physical behavior in metal cutting. To model the chip formation forces in metal cutting, two fundamental approaches have been extensively researched: minimum energy principle [**Lee and Shaffer 1945**] and slip line field theory [**Oxley 1989**]. Unfortunately, the solutions did not take into account factors such as flow stress varying with temperature, strain, and strain rate. Lee and Shaffer [**Lee and Shaffer 1951**] have applied slip line field theory to orthogonal metal cutting by assuming super plastic material behavior. Their solution required the construction of a slip-line field pattern and the shearing in the primary deformation zone is

assumed to be concentrated on a narrow shear plane. However neither of these models could incorporate the actual work piece behavior into the model structure in a realistic way. Therefore the predicted results were not quite in agreement with the experimental results obtained using different work piece material combinations. It is believed by Boothroyd [**1988**] that unique relationship of the form suggested by Merchant [**Merchant 1945**] or Shaffer [**Lee and Shaffer 1951**] for the prediction of shear and friction angle can never hold true for all materials. This is mainly due to the difference in the material properties, which have to be included into the relationship of shear plane and friction angle.

Alternatively, by using the plasticity theory for the plane strain case, slip line fields are constructed around the primary shear zone from experiments, and also by considering the effects of strain, strain rate and temperature on the flow stress a parallel-sided shear zone approach was presented by Oxley [**1989**]. Numerous researchers have applied or modified these two approaches to model the force profiles later in metal cutting. Furthermore, in order to generalize the modeling approach, a modified Johnson–Cook equation is applied in the chip formation model to represent the workpiece material properties as a function of strain, strain rate, and temperature.

Wright [**Wright 1982**] has attempted to include the work material strain hardening properties obtained through tension tests in calculating the shear plane and friction angle. However Bagci [**1973**] has shown that unless the secondary shear zone effects are included, Wright's [**1982**] model also would not hold for different combinations of tool geometries and work materials. Accordingly Bagci [**1973**] has proposed an experimental correction factor to take into account different cutting conditions. Similar

concepts have been applied by other researchers [**Baily and Bhavandia 1973, Black 1979, Yellowly 1985**]. However no model has yet been developed that can incorporate the work piece material properties into the machining models without requiring additional experimental cutting force data.

Work material properties can be appropriately incorporated into machining models by applying the more complicated plasticity theory. This requires that no specific form of deformation pattern be assumed prior to solution and work piece material properties should be known as to the ranges of strains, strain rates and temperatures generated during the cutting action. Several researchers have attempted to apply principles of plasticity theory in metal cutting. But there are several numerical and technical problems involved in plasticity applications to metal cutting operations. As a result of very high strains and strain rates, high temperatures are generated during the deformation and the material properties apparently change from isotropic to anisotropic. However it is very difficult to represent material properties at high ranges of strains, strain rates and temperatures that are involved in metal cutting, since the material testing methods at these ranges of operating conditions can only give qualitative results [**Baily and Bhavandia 1973, Campbell 1973**]. Therefore the results obtained from the plasticity analysis would also be qualitative. Thus, to improve the accuracy of the solutions obtained using plasticity theory, material property relationships and material testing methods at high strains, strain rates and temperatures must be improved.

Tulsty [**1975**] develop an analytical modeling of the End milling operations started with. In this work analytical expressions for tangential and radial cutting forces are framed and later these force components are resolved into the feed and normal direction

cutting forces at the center of the cutter. The analytical expressions thus obtained are evaluated and plotted for various combinations of the cutting parameters and were found to produce satisfactory results. But eventually this model when tried for Micro end milling operations didn't produce accurate simulated cutting forces in coincidence with experimental cutting forces.

Analytical cutting force model for end milling operation has been developed by Wang [**Junz and Zheng 2002**] considering the shearing and ploughing mechanisms. The elemental forces are defined as a linear combination of shearing and ploughing forces in six constants.

By thermal modeling of both the primary and secondary heat sources, modification to Oxley's predictive machining theory is made by Huang and Liang [**2003**] to model the metal cutting behaviors. Temperature distributions along the primary and secondary shear zones are modeled with the moving heat source method. To generalize the modeling approach, the modified Johnson–Cook equation is applied in the modified Oxley's approach to represent the workpiece material properties as the function of strain, strain rate, and temperature. Although the (modified) Johnson–Cook equation cannot capture blue brittle phenomenon and history effect, the prediction results from this study show that the Johnson–Cook equation works well as the material constitutive equation, at least within the normal machining condition range. The proposed approach describes the effect of tool thermal property on cutting forces and it can facilitate tool design and process optimization. The model predictions are compared to the published experimental process data of hard turning AISI H13 steel (52 HRC) when using the low CBN content tool and the high CBN con- tent tool. The proposed model and EM predict lower

tangential and thrust forces and higher tool–chip interface temperature when using the lower CBN content tool.

Jianwen Hu et al. [**2008**] developed an analytical model for cutting force simulations in finish hard turning by a worn tool, which includes both chip formation and flank wear-land contact forces. Due to the 3D nature of the cutting zone, both the uncut chip area and wear-land contact are considered as numerous thin slices and individually analysed for cutting forces modelling. Using coordinate transformations, cutting forces due to individual slices can be projected and further integrated from the lead to tail cutting edge to calculate three components of cutting forces. The methodology was applied to simulate process parameter effects on cutting forces. The radial component is the most sensitive force to the change of process parameters, especially, flank wear-land and tool nose radius. Among all parameters tested, flank wear-land shows the most dominant effects on cutting forces and its existence will also augment the effects of other parameters, for example, the tool nose radius.

The presence of flank wear-land accompanies additional cutting forces as well as heat generation to the thermo-mechanical process. There seems to be two schools of thought. One reported that total cutting forces can be treated as consisting of two uncoupled parts: forces due to chip formation regardless of the tool sharpness, and forces due to flank wear alone [**Waldorf et al. 1998, Smithey et al. 2000, Smithey et al. 2001, Elanayar and Shin 1996**]. But some other researchers still doubt the efficacy of this decoupling property. Wang and Liu suggested that chip formation forces are affected by wear-land interactions [**Wang and Liu 1998, Wang and Liu 1999**]. Elanayar and Shin also studied cutting forces due to wear-land using an indentation force model [**Elanayar**

and Shin 1996]. The authors also reported that wear-land effects on chip formation forces are insignificant. Huang and Liang have applied the worn tool model from [**Waldorf et al. 1998, Smithey et al. 2000, Smithey et al. 2001**], expanding to three dimensional cutting, to model wear-land forces in hard turning [**Huang and Liang 2004**]. Wang and Liu [**1998**] developed a method to decouple wear-land forces and chip formation forces. The authors further characterized wear-land effects on heat transfer of chip formation and part surface microstructural alterations in orthogonal cutting [**Wang and Liu 1999**].

1.4.2.3 Other Approaches of Modelling Cutting Forces

The semi-empirical expressions contain constants that are experimentally predicted and they can be classified as linear, power and exponential functions. The most established cutting force relationship although old is that proposed by Kienzle and Victor, also known as the specific cutting resistance model [**Kienzle and Victor 1957**]; it will be considered in the following. Over the last years, empirical models for the machinability parameters in various machining processes have been developed using data mining techniques, such as statistical design of experiments (Taguchi method) [**Davim 2003**], response surface methodology), computational neural networks[**Luo et al. 1998**] and genetic algorithms [**Suresh et al. 2002**]. All these techniques are, more or less, ‘’black box’’ approaches but possess the advantage of providing the impact of each individual factor and factor interactions, after an appropriate design of the experiment. Especially, for the Taguchi and response surface methodology, a minimum amount of experimental trials is combined to a reliable global examination of the variables interconnection, instead of one- factor- at- a –time experimental approach and interpretation [**Ross 1988**]. Turning

operations are widely used in workshop practice for applications carried out in conventional machine tools, as well as in NC and CNC machine tools, machining centres and related manufacturing systems. All three cutting force components are of interest because apart from the tangential (main) component that gives the cutting power and its determination is apparently necessary, the radial and in-feed components control dimensional and form errors in case of workpiece and tool deflections and tool wear.

When quantitative knowledge about metal cutting operations is required, experimental techniques should be employed to improve the accuracy of the force predictions. If the results of the experimental methods are expressed in the equation, these methods are called empirical methods. Since any metal cutting process involves many variables, empirical techniques require large number of experiments to arrive at a credible model. Empirical models cannot be extrapolated outside the experimentally tested domain. However forces can be related to the mechanics of the operation through a set of experimentally obtained model parameters [**Shaw et al. 1952, Nigm et al. 1977, Ueda and Mastsuo 1986, Rosenberg and Rosenberg 1987**]. These model parameters would be functions of a smaller number of variables than forces, and thus require a smaller number of experiments to obtain the parametric relationships. For example, the cutting forces are a function of the radial and axial engagements whereas the model parameters may not be affected by these geometric cutting conditions. These types of models are commonly called mechanistic force models. These mechanistic model parameters can be selected in multiple ways. For instance, shear plane angle, shear strength, friction, pressure, chip flow angle, direction of friction force, radial, tangential and axial force components are some of the commonly used model parameters in the mechanistic force models. The accuracy of

mechanistic force models depends upon the accuracy of the empirical parametric relationships obtained through experiments.

Petropoulos et al. [**2005**] developed a predictive model for cutting force components in longitudinal turning of constructional steel with a coated carbide tool. The model is formulated in terms of the cutting conditions. Taguchi method is used for the plan of experiments and the analysis is performed using response surface methodology. Next, a related comparison is attempted to results obtained using the Kienzle -Victor cutting force model.

The wearland force and edge force models are developed by Song and Wenge [**2006**] in empirical form for force prediction purpose. The orthogonal cutting force model allowing for the effects of flank wear is developed and verified by the experimental data. A comprehensive analysis of the mechanics of cutting in the oblique cutting process is then carried out. Based on this analysis, predictive cutting force models for oblique cutting allowing for the effects of flank wear are proposed. The predictive force models are qualitatively and quantitatively assessed by oblique cutting tests. The modelling approach is then used to develop the cutting force models for a more general machining process, turning operation. By using the concept of an equivalent cutting edge, the tool nose radius is allowed for under both orthogonal and oblique cutting conditions.

Empirical models for tool life, surface roughness and cutting force are developed by Al-Ahmari [**2007**] for turning operations. Process parameters (cutting speed, feed rate, depth of cut and tool nose radius) are used as inputs to the developed machinability models. Two important data mining techniques are used; they are response surface

methodology and neural networks. Data of 28 experiments when turning austenitic AISI 302 have been used to generate, compare and evaluate the proposed models of tool life, cutting force and surface roughness for the considered material.

Sarma et al. [**2008**] developed a model to correlate the cutting parameters with cutting force, using response surface methodology. The results indicate that the developed model is suitable for prediction of cutting forces in turning of GFRP composites. The effect of different parameters on cutting forces are analyzed and presented in this study.

Sharma et al. [**2008**] constructed a model of cutting forces using neural networks. The data cutting forces at different cutting parameters such as approaching angle, speed, feed and depth of cut obtained by experimentation is analyzed and used to construct the model. Then the models are compared for their prediction capability with the actual values. The model gave overall 76.4% accuracy.

Ibraheem et al. [**2008**] predicted cutting force by Genetic network technique. The prediction accuracy of the cutting force values in this research when (GN) are used is 92%. 3. Genetic network (GN) has proved to be a successful technique that can be used to predict the longitudinal cutting force produced in end milling.

A new approach to obtain the specific coefficients for a mechanistic model from virtual FEM models has been presented by Gonzalo et al. [**2009**]. The main objective is the elimination of the experimental machining test to characterize the specific cutting coefficients needed in the mechanistic milling models. Two ways to get coefficients have been proposed: (i) The direct way, with improved accuracy but high computational costs

and (ii) The hybrid way through Armarego spatial conversions, less accurate but faster for successive tests due to the use of 2D orthogonal cutting models The results of both methods have been presented and discussed. The two ways proposed provide the same precision for the calculation of milling forces. The use of numerical FEM models instead of experimental data for the calculation of specific cutting coefficients only introduces an additional error of 4% in the calculation of the cutting forces in milling operations.

Khidhir et al [**2010**] described a modification approach applied to a fuzzy logic based model for predicting cutting force where the machining parameters for cutting speed ranges, feed rate, depth of cut and approach angle are not overlapping. For this study, data were selected depending on the design of experiments. Response surface methodology was applied to predict the cutting force and to examine the fuzzy logic based model. The modification approach fuzzy logic based model produced the cutting force data providing good correlation with response surface data. In this situation the cutting force data were superimposed and results were adjusted according to their own ranges.

1.5 Summary of the Review

A review of the literature on machinability of different commercial steels highlights the immense potential of the control of machining temperature and its detrimental effects. It is realized that the machining temperature has a critical influence on chip formation, cutting forces, tool wear and tool life. All these responses are very important in deciding the overall performance of the tool. The conventional cutting fluids are not that effective in high speed machining particularly in continuous cutting of materials likes steels. Further the conventional cutting fluids are not environment friendly.

Cryogenic machining can improve the machinability index as well as provide environmental friendliness machining but cryogenic machining is costly due to high cost of liquid nitrogen. Application of minimum quantity lubricant (MQL) jet not only can reduce cutting fluid requirement but also substantial technological benefits has been observed in machining different steels by different inserts. Though MQL gives some advantages during the turning operation, it presents some limits due to the difficulty of lubricant reaching the cutting surface.

From all these investigations, it is evident that applying cutting fluid in the form of a jet at higher pressure into the cutting zone is more beneficial than conventional cooling techniques. In general, low pressure the cutting fluids is not capable of penetrating deep enough into the tool-chip interface to dissipate heat as quickly as possible from the appropriate regions in the cutting zone. Further, all these investigations are limited to stationary single edge cutting tool operations. However there is a great need to improve machining performance by improving cooling methods in the case of turning, drilling and milling especially while machining difficult to machine materials.

High-pressure coolant (HPC) jet cooling is a promising technology in high speed machining, which economically addresses the current processes, environmental and health concerns. In this unique process cutting oil is impinged through a nozzle precisely at the narrow cutting zone. The success of implementing this technology across the metal removal industries is therefore depend on increased research activities providing credible data for in depth understanding of high-pressure coolant supplies at the chip-tool interface and integrity of machined components. The growing demands for high MRR, precision and effective machining of exotic materials is restrained mainly by the high cutting

temperature. It is revealed from the aforesaid literature survey that the cutting temperature, which is the cause of several problems restraining productivity, quality and hence machining economy, can be substantially controlled by high-pressure coolant jet.

Efficient quantitative and predictive models that establish the relationship between a big group of input independent parameters like speed, feed and depth of cut and resultant performance in terms of cutting temperature and force are required for the wide spectrum of manufacturing processes, cutting tools and engineering materials currently used in the industry could contribute in industrial applications along with theoretical understanding. This research aims to develop Predictive models for cutting temperature and force for turning medium carbon steel with uncoated carbide insert by industrially recommended process parameters under high-pressure coolant (HPC) condition. The proposed model is verified based on the published experimental data.

1.6 Scope of the Thesis

The cutting temperature, which is the cause of several problems restraining productivity, quality and hence machining economy, can be controlled by the application of high-pressure coolant (HPC) jet. The growing demands for high MRR, precision and effective machining of exotic materials is restrained mainly by the high cutting temperature. Keeping that in view, the present research work has been taken up to explore the role of high pressure coolant (HPC) system on the major machinability characteristics in machining (turning) steels by uncoated carbide tools under different machining conditions as well as to predict cutting temperature and cutting force in machining when machining under HPC condition.

Chapter 1 presents the survey of previous work regarding general requirements in machining industries, effect of cutting temperature and controlling method of the cutting temperature, technological-economical-environmental problems associated with the conventional cooling practices and expected role of high pressure cooling (HPC) jet machining, various methodologies and recent techniques in predictive modeling of cutting temperature and forces. Literature review on the effect of cutting temperature, beneficial effects of high pressure coolant jet machining, cutting temperature and cutting force modeling provide a basic idea regarding contemporary research activities in metal cutting.

Chapter 2 presents specific objectives of this thesis work and also outline the methods which have been followed to draw effective results that commensurate with the goals of the thesis.

Chapter 3 presents the experimental conditions and procedure of the machining experiments carried out and the experimental results on the effects of HPC, relative to dry machining on chip formation, chip-reduction coefficient, cutting zone temperature, cutting forces in turning AISI 1060 steel by uncoated carbide SNMM inserts under different cutting conditions.

Chapter 4 provides development of an analytical predictive model for cutting temperature at the chip-tool interface from the characterization of the physical processes taking place during machining and its validation.

Chapter 5 provides development of a statistical predictive model for cutting force correlating with the various cutting conditions such as speed feed and depth of cut.Model validation has also been carried out in this chapter.

Chapter 6 focuses on the finite element modeling of cutting temperature which has been developed by ABAQUS/CAE. It contains model creation, mesh generation, application of load & boundary condition, analysis techniques, post processing, FEM results in terms of nodal temperature finally validation has been carried out by comparing actual data with predicted data.

Chapter 7 contains the detailed discussions on the experimental results, possible interpretations on the results obtained, analytical modeling of cutting temperature, statistical modeling of cutting force and finite element modeling of temperature distribution.

Finally, a summary of major contributions and recommendation for the future work is given in **Chapter 8** and references are provided at the end.

Chapter-2

Objectives of the Present Work

2.1 Objectives of the Present Work

It is revealed from the aforesaid literature survey that the cutting temperature, which is the cause of several problems restraining productivity, quality and hence machining economy, can be controlled by the application of high-pressure coolant jet. The growing demands for high MRR, precision and effective machining of exotic materials is restrained mainly by the high cutting temperature. The objectives of the present investigation, keeping in view the overall improvement in productivity and quality in machining steel by the industrially used uncoated carbide insert at different speeds and feed rates combinations, are

(a) Experimental investigation on the role of high-pressure coolant jet in respect of

   i. average chip-tool interface temperature

   ii. cutting force

(b) Develop predictive models for cutting temperature and cutting force from the characterization of the physical processes.

(c) Validation of developed mathematical model.

2.2 Methodology

The research work was mainly analytical and partly experimental which is required to develop the analytical and finite element models and for its validation. Proper design of experiment has been done for reasonably quantitative assessment of the role of the machining and the high-pressure coolant (HPC) jet parameters on the technological responses and satisfactory prediction of machining responses in terms of cutting temperature and cutting force. The methodology was as follows:

i. A high-pressure coolant delivery system has been analyzed for supplying coolant at high pressure from the coolant tank and impinged at high speed through the nozzle into the chip-tool interface. Considering the conditions required for the present research work and uninterrupted supply of coolant at variable pressure and flow rate, a coolant tank of capacity of 200 liter has been used. The coolant tank comprises of motor-pump assemble, flow control valve, relief valve and directional control valve. The nozzle of 0.50 mm bore diameter has been fixed to the tool post and was connected with standard connecting end to supply high-pressure cutting oil in the form of thin jet at the chip-tool interface.

ii. A nozzle for application of the high-pressure coolant jet has been analyzed and used for controlling the spray pattern, covering area and coolant flow rate.

iii. Chip shape, chip color and chip thickness ratio under high-pressure coolant conditions have been studied.

iv. The average chip-tool interface temperatures have been monitored by tool-work thermocouple technique. Cutting temperature data are simultaneously recorded with tool wear aggravation.

v. Main cutting force (P_z) under high-pressure coolant conditions has been recorded with the help of lathe tool dynamometer, charge amplifier and computer. Computer was used for monitoring the profile of the cutting force.

vi. An analytical model has been developed for cutting temperature in turning AISI 1060 steel under high pressure coolant condition. Two different statistical models (second order response surface model and non-linear equation model) for the cutting froce have been developed correlating with the cutting process parameter such as cutting speed, feed and depth of cut.

vii. The proposed models have been verified by experimental data of turning AISI 1060 steel under high-pressure coolant condition.

Chapter-3

Experimental Investigations

3.1 Introduction

Based on cutting condition and work/tool material the physical behavior during metal cutting has been changed. For cost savings, increasing productivity and for preventing any hazard occurring to the machine, cutting tool or the deterioration of the product quality it is highly desirable to have an idea about the behaviour of machining. For optimizatioin of process parameters, the prediction of the ralation of process responses such as cutting temperature, cutting forces, surface roughness and tool life with the process parameter is necessary. In this research work AISI 1060 steel were turned in a lathe with tungsten carbide inserts at industrial cutting speed, feed and Depth of cut combination under high-pressure coolant (HPC) condition. Generation of high cutting temperature during machining is one of the most critical and primary level response during turning which not only reduces tool life but also impairs the product quality. The temperature behaves proportionally with the increased values of cutting process parameters and increased strength and hardenability of the work piece materials. Cutting force is another primary level machining response which directly relates the amount of cutting power requirements. Chips morphology has also been studied in order to examine and relate cutting temperature and cutting force effects on chip's color, breakability and shear angle. Cutting fluids are widely used to improve the machining responses. But due to its ineffectiveness in desired cooling and lubrication and corresponding health hazards,

corrosion and contamination of natural environment, High pressure coolant jet has been applied in machining through specially designed external nozzle in order to have better experimental results.

3.2 Experimental Procedure and Conditions

For high production machining of steel, effective control of the cutting zone temperature is very essential. The concept of high-pressure coolant presents itself as a possible solution for high speed machining in achieving slow tool wear while maintaining cutting forces/power at reasonable levels, provided that the high-pressure cooling parameters can be strategically tuned. It has the benefits of a powerful stream that can reach the cutting area, it provides strong chip removal, and in some cases enough pressure to debur. High-pressure coolant injection technique not only provided reduction in cutting forces and temperature but also reduced the consumption of cutting fluid. A coolant applied at the cutting zone through a high-pressure jet nozzle could reduce the contact length and coefficient of friction at chip-tool interface and thus could reduce cutting forces and increase tool life to some extent. It has been reported that the cooling and lubrication is improved in high speed machining of difficult-to-machine materials by the use of high-pressurized coolant/lubricant jet. The purpose of the experimental investigation in this present research work is to investigate on the behavior of cutting temperature, force and chips morphology experimentally under high-pressure coolant which is a pre-requisite in order to predict different machining phenomenon through predictive modelling.

The machining tests were carried out by straight turning of AISI 1060 steel, in a reasonably rigid and powered (10 hp) centre lathe (China) at different cutting speeds (V_c) and feeds (S_o) under high-pressure coolant environment. Keeping in view less significant role of depth of cut (t) on cutting temperature, saving of work material and avoidance of

dominating effect of nose radius on cutting temperature, the depth of cut was kept fixed to only 1.0 mm and 1.5 mm. The tool geometry is reasonably expected to play significant role on such cooling effectiveness. SNMM 120408, WIDIA has been undertaken for the present investigation. The material of the cutting tool is tungsten carbide. The insert was clamped in a PSBNR-2525 M12 (Sandvik) type tool holder.

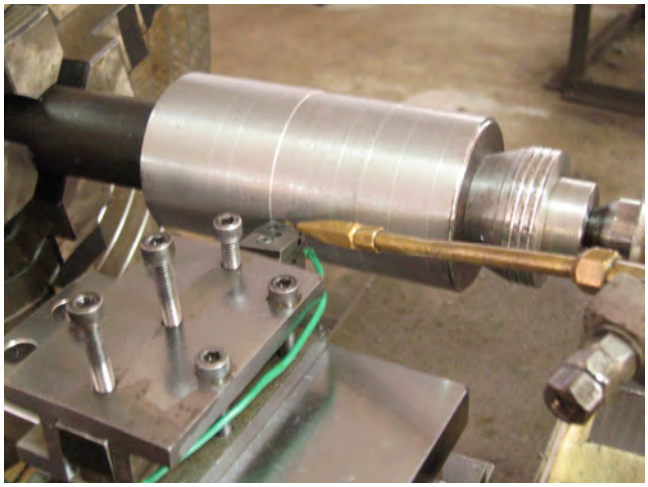

Fig.3.1 Photographic view of high-pressure coolant delivery nozzle injecting coolant during machining [**Kamruzzaman 2009**]

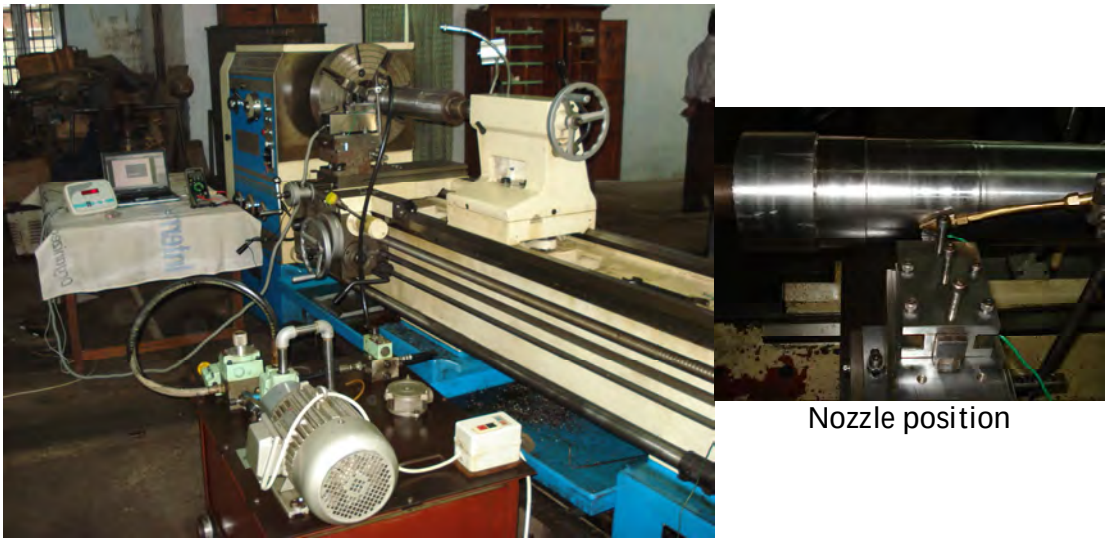

Fig.3.2 Photographic view of experimental set-up [**Kamruzzaman 2009**]

The positioning of the nozzle tip with respect to the cutting insert has been settled after a number of trials. The final arrangement made and used has been shown in Fig.3.1.

The high pressure coolant jet is directed along the auxiliary cutting edge at an angle 30^o to reach at the principal flank and partially under the flowing chips through the in-built groove parallel to the cutting edges. The photographic view of the experimental set-up is shown in Fig.3.2.

The ranges of cutting speed and feed rate chosen in the present investigation are representative of the current industrial practice for the tool-work material combination that has been investigated. The conditions under which the machining tests have been carried out are briefly given in Table 3.1.

Table 3.1 Experimental conditions

Machine tool	: Lathe (10 hp), China
Work materials	: AISI 1060 Steel (Size: Ø178 X 580 mm, BHN: 195)
Cutting insert	: SNMM 120408 TTS, WIDIA (ISO Specification)
Tool holder	: PSBNR 2525 M12, Sandvik
Working tool geometry	: -6^o, -6^o, 6^o, 6^o, 15^o, 75^o, 0. 8 mm
Process parameters	
Cutting speed, V_c	: 93,133, 186 and 266 m/min
Feed rate, S_o	: 0.10, 0.14, 0.18 and 0.22 mm/rev
Depth of cut, t	: 1.0 mm and 1.50 mm
High pressure coolant (HPC)	: 80 bar, Coolant: 3.5 l/min through external nozzle
Coolant type	: VG-68 (ISO grade)
Environment	: ➢ Dry and ➢ High pressure coolant (HPC) condition

3.3 Experimental Results

3.3.1 Chip Formation

The machining chips were collected during all the treatments for studying their shape, colour and nature of interaction with the cutting insert at its rake surface. Shape and color of chip during turning AISI 1060 steel by SNMM insert under Dry and HPC conditions are incorporated in Fig.3.3.

Cutting speed, V_c (m/min)	Feed rates, S_o (mm/rev)							
	0.10		0.14		0.18		0.22	
	Environment							
	Dry	HPC	Dry	HPC	Dry	HPC	Dry	HPC
93	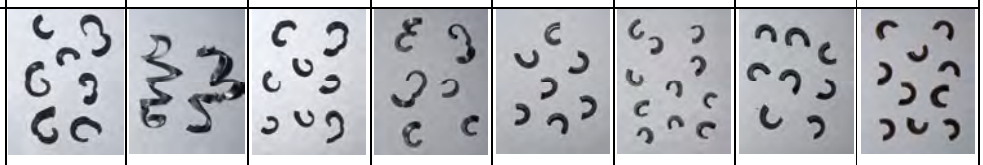							
133	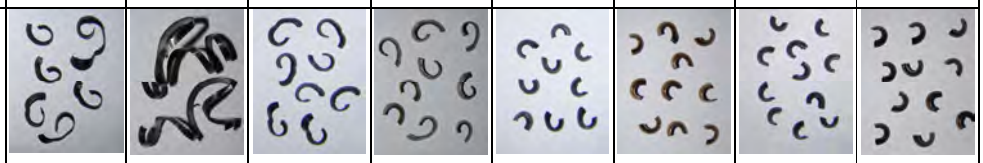							
186	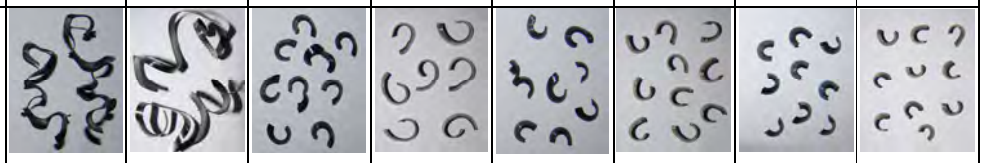							
266	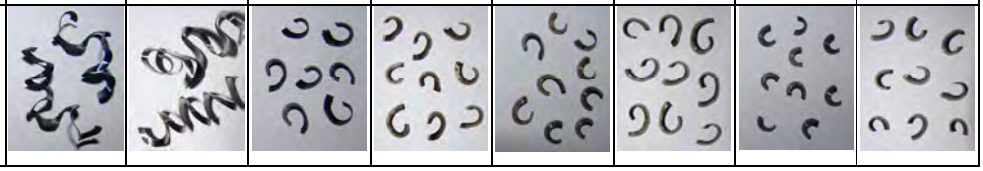							

Fig.3.3 Shape and color of chip during turning of AISI 1060 steel by SNMM insert under Dry and HPC conditions

Fig.3.3 shows that when machined under high-pressure coolant condition the form of some ductile chips did not change but their back surface appeared much brighter and smoother. This indicates that the amount of reduction of temperature due to high-pressure coolant enabled favourable chip-tool interaction and elimination of even trace of

built-up edge formation. The colour of the chips have also become much lighter i.e. metallic from blue due to reduction in cutting temperature due to high-pressure coolant jet. It is important to note that the role of high-pressure coolant jet has been more effective in respect of form and colour of the chips when the same steel was machined by the groove type SNMM inserts. Such improvement can be attributed to effectively larger positive rake of the tool and better cooling by the jet coming along the groove parallel to the cutting edges.

3.3.2 Chip Reduction Coefficient

The chip reduction coefficient, ξ (ratio of chip thickness after and before cut) is an important index of chip formation and specific energy consumption for a given tool-work combination. For given tool geometry and cutting conditions, the value of chip reduction coefficient depends upon the nature of chip-tool interaction, chip contact length, curl radius and form of the chips all of which expected to be influenced by high-pressure coolant in addition to the level of cutting speeds and feeds. In machining conventional ductile metals and alloys producing continuous chips, the value of ξ is generally greater than 1.0 because chip thickness after cut (a_2) becomes greater than chip thickness before cut (a_1) due to almost all sided compression and friction at the chip-tool interface. Larger of ξ means larger cutting forces and friction and is hence undesirable. The thickness of the chips was repeatedly measured by a slide caliper to determine the value of chip thickness.

The schematic view of the formation of chip is shown in Fig.3.4. The machining chips were collected during all the treatments for studying their shape, colour and nature of interaction with the cutting insert at its rake surface. Chips have been visually examined and their thickness has been measured by slide callipers at every run.

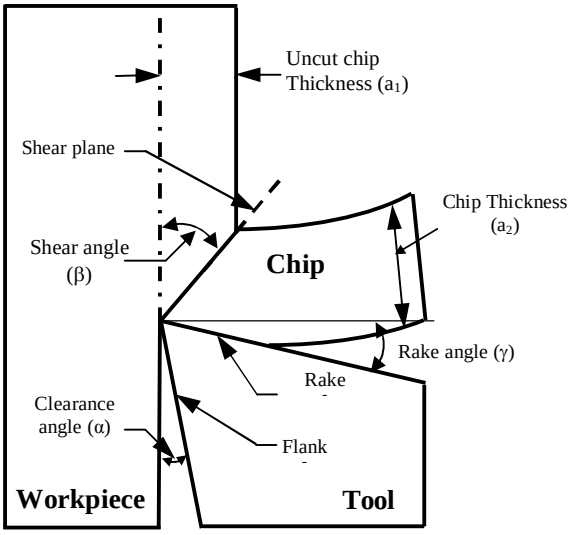

Fig.3.4 Schematic view of the chip formation mechanism

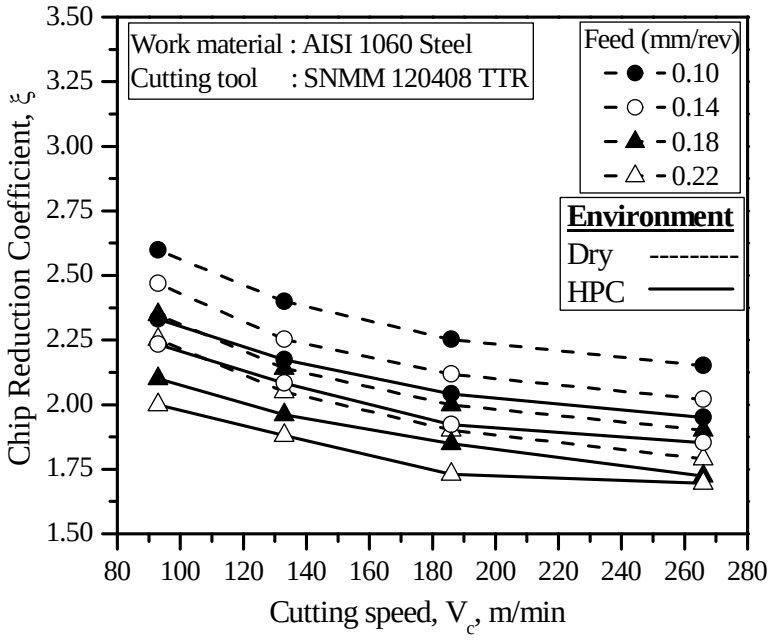

Fig.3.5 Variation of chip reduction coefficient with that of cutting speeds and feed rates under dry and HPC conditions at depth of cut 1.0 mm

The variation in value of chip reduction coefficient, ξ with change in cutting speeds and feed rates as well as machining environment evaluated for AISI 1060 steel have been plotted and shown in Fig.3.5 and Fig.3.6 which depict some significant facts;

i. values of ξ has all along been greater than 1.0

ii. the value of ξ reduced by the application of High pressure coolant

iii. the value of ξ decreased with increase in V_c and S_o

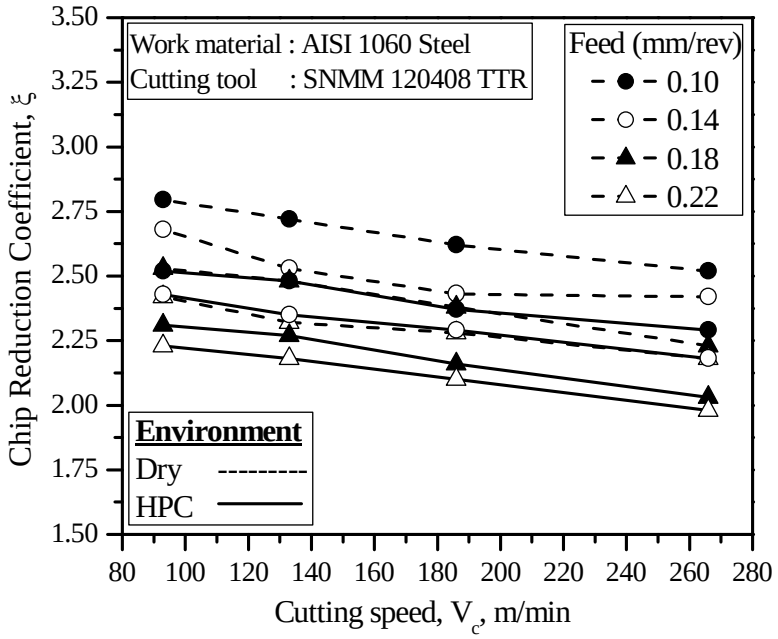

Fig.3.6 Variation of chip reduction coefficient with that of cutting speeds and feed rates under dry and HPC conditions at depth of cut 1.5 mm

Fig.3.5 and Fig.3.6 clearly show that throughout the present experimental domain the value of ξ gradually decreased with the increase in V_c though in different degree for the different tool-work combinations, under both dry and HPC conditions. The value of ξ usually decreases with the increase in V_c particularly at its lower range due to plasticization and shrinkage of the shear zone for reduction in friction and built-up edge formation at the chip-tool interface due to increase in temperature and sliding velocity. With the increase in feed (i.e. uncut chip thickness) also the value of ξ decreases due to increase in effective rake angle of the tool with edge radiusing or beveling as schematically shown in Fig.3.5 and Fig.3.6. In machining steels by tools like carbide, usually the possibility of built-up edge formation and size and strength of the built-up edge, if formed gradually increase with the increase in temperature due to increase in V_c

and also S_o and then decrease with the further increase in V_c due to too much softening of the chip material and its removal by high sliding speed.

3.3.3 Cutting Temperature

The specific energy required in machining converted into heat and the heat generated during machining raises the temperature of the cutting tool tips and the work-surface near the cutting zone.The machining temperature at the cutting zone is an important index of machinability and needs to be controlled as far as possible. Cutting temperature increases with the increase in specific energy consumption and material removal rate (MRR). Such high cutting temperature adversely affects, directly and indirectly, chip formation, cutting forces, tool life and dimensional accuracy and surface integrity of the products.

Therefore, application of HPC jet is expected to improve upon the aforesaid machinability characteristics which play vital role on productivity, product quality and overall economy. The lubricating effect on cutting temperatures in high-pressure coolant machining is considered by the change of cutting forces which lead to different heat intensities in the cutting zone. For the temperature rise in the chip on the tool-chip interface, the effects of the shearing heat source on the shear plane and the frictional heat source on the tool-chip interface are considered. For the temperature rise in the tool on the tool-chip interface, the effects of the secondary heat source due to friction and the heat loss due to cooling on the tool rake face are influential.

The average cutting temperature (θ) was measured under all the machining conditions undertaken by simple but reliable tool-work thermocouple technique with proper calibration. The evaluated role of high-pressure coolant on average chip-tool

interface temperature in turning AISI 1060 steel by uncoated carbide SNMM inserts at different V_c–S_o combinations compared to dry condition have been shown in Fig.3.7 and Fig.3.8.

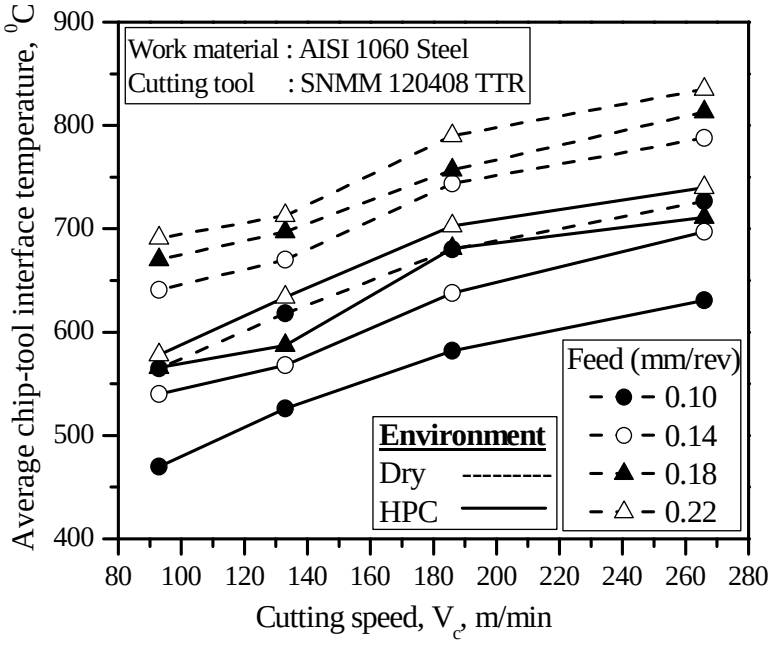

Fig.3.7 Variation of average chip tool interface temperature with that of cutting speeds and feed rates under dry and HPC conditions at depth of cut 1.0 mm

The cutting temperature generally increases with the increase in V_c and S_o, though in different degree, due to increased energy input and it could be expected that high-pressure coolant would be more effective at higher values of V_c and S_o. The average chip-tool interface temperature (θ) have been determined by using tool-work thermocouple technique and plotted against cutting speed for different work-tool combinations, feed rates and environments undertaken. Fig.3.7. and Fig.3.8 is showing how and to what extent θ has decreased due to high-pressure coolant application under the different experimental conditions. With the increase in V_c and S_o, θ increased as usual, even under high-pressure coolant condition, due to increase in energy input.

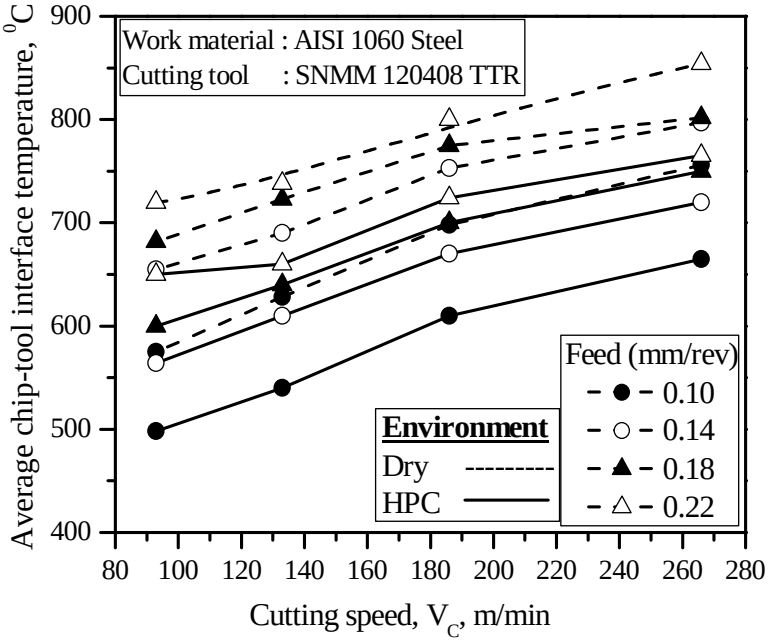

Fig.3.8 Variation of average chip tool interface temperature with that of cutting speeds and feed rates under dry and HPC conditions at depth of cut 1.5 mm

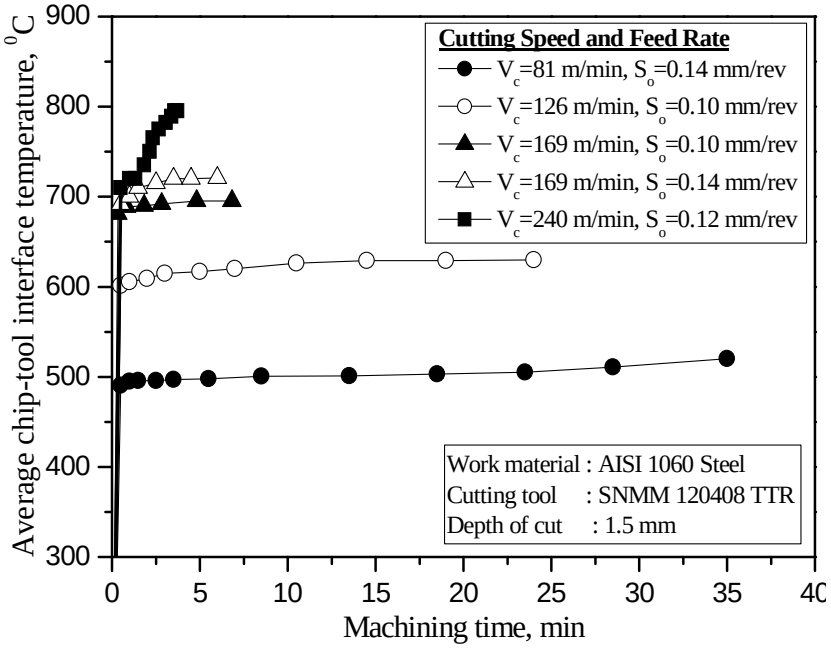

Fig.3.9 Variation of average chip tool interface temperature with machining time at different V_c-S_o combination under HPC condition

Temperature is drastically reduced under low speed-feed condition and apparently a small reduction is observed under high speed-feed condition. Even such apparently small

reduction in the cutting temperature is expected to have some favorable influence on other machinability indices. With the increase in cutting velocity, plastic contact is increased and made the jet less effective to enter into the interface. Due to this, temperature reduction rate is lower under high speed-feed condition.

Fig.3.9 shows the variation of average chip tool interface temperature with machining time at different speed-feed combinations when machining under high-pressure coolant condition.

3.3.4 Cutting Force

Cutting force is generally resolved into components in mutual perpendicular directions for convenience of measurement, analysis, estimation of power consumption and for design of Machine-Fixture-Tool-Work systems. In turning by single point tools like inserts, the single cutting force generated is resolved into three components namely; tangential force or main cutting force, P_z, axial force or feed force, P_x and transverse force, P_y. Each of those interrelated forces has got specific significance. In the present work, the magnitude of P_z has been monitored by dynamometer for all the combinations of steel specimens, tool configurations, cutting velocities, feeds and environments undertaken.

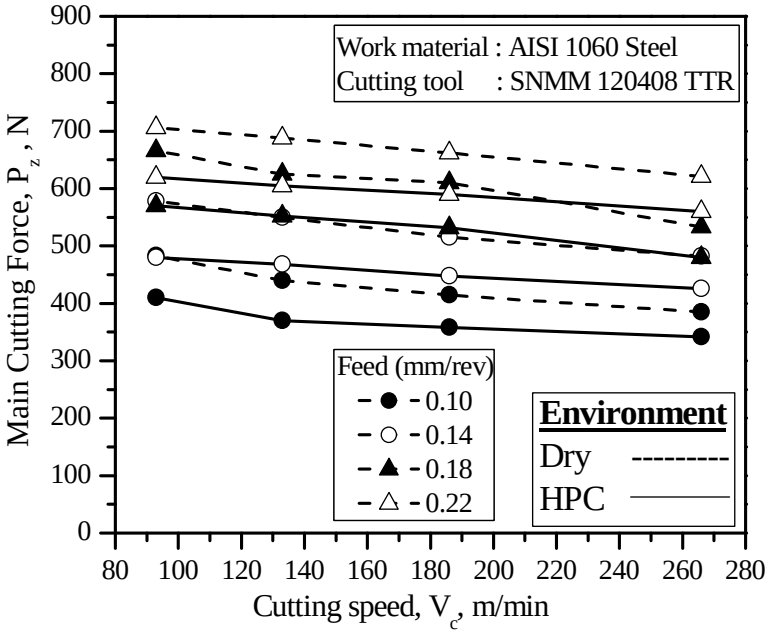

Fig.3.10 Variation of main cutting force with that of cutting speeds and feed rates under dry and HPC conditions at depth of cut 1.0 mm

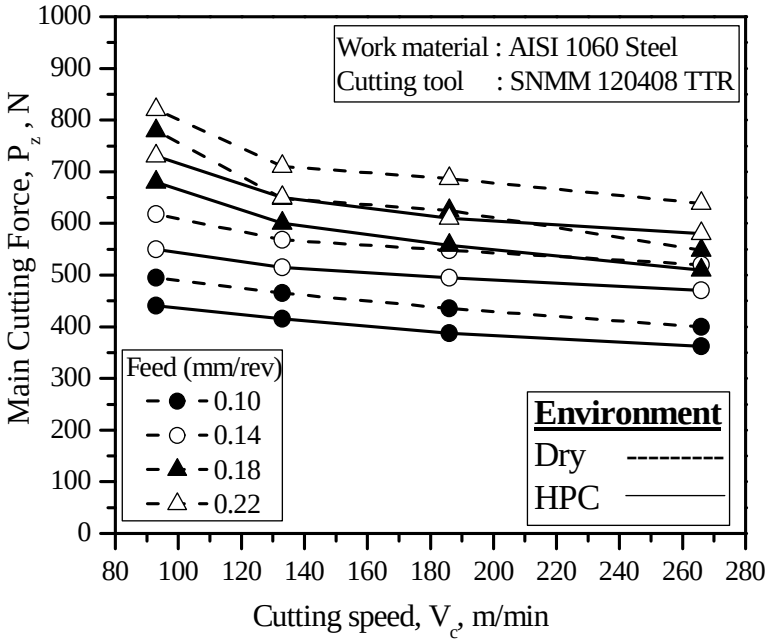

Fig.3.11 Variation of main cutting force with that of cutting speeds and feed rates under dry and HPC conditions at depth of cut 1.5 mm

In the present work, the magnitude of P_z has been monitored by dynamometer (Kistler) for all the combinations of steel specimen, tool configuration, cutting speeds, feed

rates and environments undertaken. The effect of high-pressure coolant on P_z that have been observed while turning AISI 1060 steel specimen by the SNMM carbide at different V_c-S_o-t have been graphically shown in Fig.3.10 and Fig.3.11 respectively.

Such sizeable reduction in the cutting force, P_z is reasonably attributed mainly to retention of the cutting tools sharpness and favorable change in chip-tool interaction resulting lesser friction and built-up edge formation. More or less similar results were noted in case of the other steels and tools undertaken.

Chapter-4

Modeling of Cutting Temperature

4.1 Introduction

Machining is inherently characterized by generation of heat and high cutting temperature. At such elevated temperature the cutting tool if not enough hot hard may lose their form stability quickly or wear out rapidly resulting in increased cutting forces, dimensional inaccuracy of the product and shorter tool life. The magnitude of this cutting temperature increases, though in different degree, with the increase of cutting velocity, feed and depth of cut and as a result, high production machining is constrained by rise in temperature. This problem increases further with the increase in strength and hardness of the work material. Knowledge of the cutting temperature is important because it

- affects the wear of the cutting tool resulting in increased cutting forces. Cutting temperature is the primary factor affecting the cutting tool wear.

- can induce thermal damage to the machined surface. High surface temperatures promote the process of oxidation of the machined surface. The oxidation layer has worse mechanical properties than the base material, which may result in shorter service life.

- causes dimensional errors in the machined surface. The cutting tool elongates as a result of the increased temperature, and the position of the

cutting tool edge shifts toward the machined surface, resulting in a dimensional error.

Studies in metal cutting have focused on determining the heat generation, its distribution in the cutting area, the cutting temperature and the cutting force. Cutting temperature and force are either measured in the real machining process, or predicted in the machining process design. For cutting temperature and force prediction, several approaches are used:

i. Analytical methods: there are several analytical methods to predict the mean temperature. In the analytical studies, empirical correlations have been used to determine heat generation and temperature distribution. Analytical calculations have been done under simplified assumptions.

ii. Statistical methods: in the statistical method the trend analysis is done with the help of few experimental data. By this method cutting parameters can be predicted almost accurately within a specific range of process parameters because the trend of data may be different in different ranges.

iii. Numerical methods: These methods are usually based on the finite element, finite difference and boundary element modelling of metal cutting. The numerical methods, even though more complex than the analytical approaches, allow for prediction not only of the mean cutting temperature along the tool face but also the temperature field in orthogonal and oblique cutting.

4.2 Mechanics of Machining

Two types of cutting are used in analysis of metal cutting mechanics: Orthogonal and oblique cutting. Most industrial metal cutting processes are three-dimensional or oblique. The machining geometry can be simplified from three-dimensional geometry to a two-dimensional or orthogonal geometry. Models of orthogonal machining are useful for understanding the basics of machining and can model an extensive number of production processes.

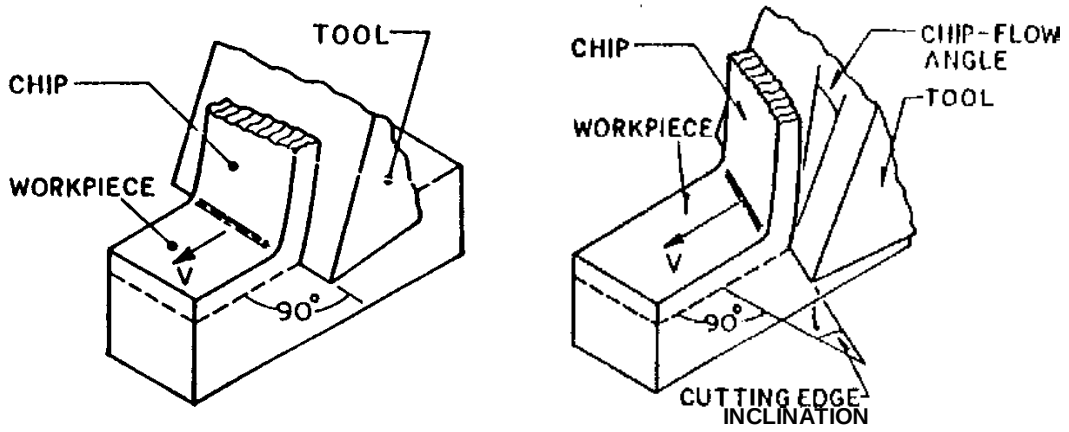

(a) Orthogonal machining (b) Oblique machining

Fig.4.1 Type of machining process

In orthogonal cutting, the material removal process is assumed to be uniform along the cutting edge that is perpendicular to the direction of relative motion between tool and the work piece; therefore it is a two dimensional plane strain problem. In oblique cutting, the major cutting edge is inclined to direction of the cutting velocity with an inclination angle as shown in Fig.4.1. Although most of the metal cutting operations are oblique, orthogonal cutting has been extensively studied because of its simplicity and

giving good approximations. The chip formation of oblique and orthogonal cutting is approximately identical. The orthogonal model is experimentally advantageous and produces a reasonably good approximation of the cutting process. Due to these facts it will be adopted in the present research.

A process of orthogonal cutting has been shown in the Fig.4.2 the process cosist of a rotational workpiece with a cutting tool having translational motion along the axis of rotation and a fixed depth of cut.when the tool is engaged with the rotational workpiece material start to remove from the work piece. The point where the tool touches the material is called machining zone. The rotational speed of the workpiece is expressed in rpm and the distance moved by the tool per unit revolution of the work piece is called feed rate expressed in mm/rev.the distance between the outer most surface to the finished surface in the measured in the radial direction is called depth of cut which is expressed in mm.

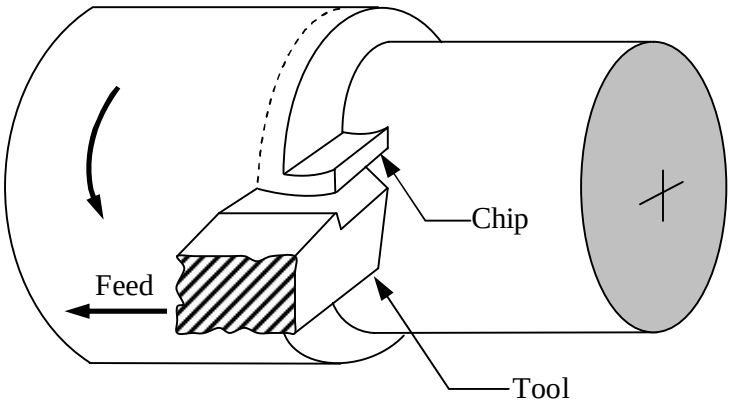

Fig.4.2 Orthogonal machining

A more idealized view of the cutting process that completely suppresses the concept of inhomogeneous strain by assuming the material to behave in a completely homogeneous fashion is shown in Fig.4.3. This figure shows the schematic view of the chip formation process where a tool engaged with the workpiece. The shear plane, chip-

tool interface and the work-tool interface (which formed after some time to start the metal cutting) and the tool will be of particular interest.

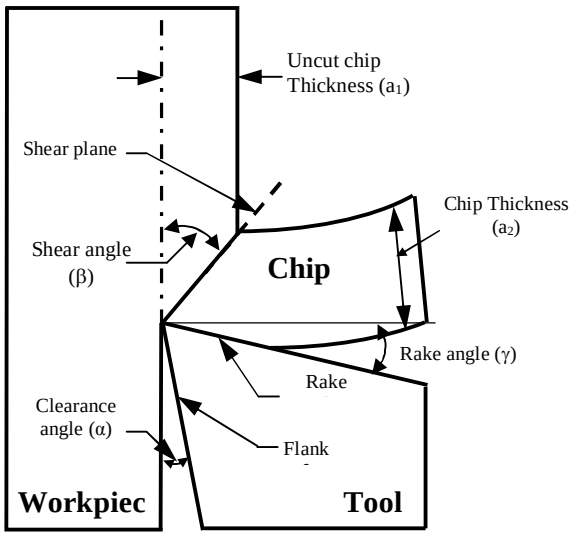

Fig.4.3 Schematic view of the chip formation mechanism

Orthogonal cutting and tool geometry variables are shown in Fig.4.3. Here, a_1 is the uncut chip thickness and it is sometimes called depth of cut, a_2 is the chip thickness. Rake face is the face where chip and tool in contact. Rake angle (γ) is an angle between the rake face and newly machined surface normal. Clearance face is a surface which the machined surface passes over. Clearance angle (α) is an angle between newly machined surface and clearance face and shear angle (β) is an angle between newly machined surface and shear plane. These variables are important because they determine the characteristics of the process. The orthogonal model is based on the following assumptions:

- the tool is sharp
- there is no clearance face contact
- the shear surface extends upward from the cutting edge

- the cutting edge is perpendicular to the direction of cutting
- the chip does not flow to either side (plane strain)
- the depth of cut is constant
- the width of the tool is greater than the width of the workpiece
- the work moves with uniformed velocity relative to the tool
- a continuous chip is formed without a built-up edge (BUE)
- the shear and normal stresses along the shear plane and tool are uniform

In orthogonal cutting, the relationship between the depth of cut, the chip thickness and the shear angle can be derived from the geometry of a two-dimensional model. Chip reduction coefficient, ξ (ratio of chip thickness after and before cut) is an important machinability index of chip formation and specific energy consumption for a given tool-work combination. For given cutting conditions, the value of Chip reduction coefficient depends upon the nature of chip-tool interaction, chip contact length and chip form in addition to the levels of cutting speed and feed. Chip reduction coefficient, ξ is evaluated from the ratio,

$$\xi = \frac{a_2}{a_1} = \frac{\cos(\beta - \gamma)}{\sin \beta} \quad \text{.....(4.1)}$$

where,

a_1 = Chip thickness before cut

a_2 = Chip thickness after cut

β = Shear angle

γ = Rake angle

In machining conventional ductile metals and alloys producing continuous chips, the value of ξ is generally greater than 1.0 because chip thickness after cut (a_2) becomes greater than chip thickness before cut (a_1) due to almost all sided compression and friction at the chip-tool interface. Larger value of ξ means larger cutting forces and friction and is hence undesirable.

In machining any conventional ductile metals like steels also ξ decreases with increases in V_c due to plasticization and shrinkage of shear zone. With the increase in feed (i.e. uncut chip thickness) also the value of ξ decreases due to increase in effective rake angle of the tool with edge beveling and its effect on ξ is given by,

$$\xi = e^{-\mu\left(\frac{\pi}{2} - \gamma\right)} \quad \text{.....(4.2)}$$

where,

μ = Apparent co-efficient of friction at the chip-tool interface

γ = Effective tool rake angle

Shear angle β can be determined by means of the chip reduction coefficient (ξ) and the rake angle of the cutting tool as follows:

$$\beta = \tan^{-1}\left(\frac{\cos\gamma}{\xi - \sin\gamma}\right) \quad \text{.....(4.3)}$$

where,

ξ = Apparent co-efficient of friction at the chip-tool interface

The shear plane length (L_{sh}) can be determined by the following equation,

$$L_{sh} = \left(\frac{a_1}{\sin \beta} \right) \quad \text{.....(4.4)}$$

The contact length, C_N were obtained by,

$$C_N = a_2 \left[1 + \tan (\beta - \gamma) \right] \quad \text{.....(4.5)}$$

The value of the shear strain (ε) is an indication of the amount of deformation that the metal undergoes during the process of chip formation. The shear strain that occurs along the shear plane can be expressed as follows:

$$\varepsilon = \cot \beta + \tan(\beta - \gamma) = \frac{\cos \gamma}{\sin \beta . \cos (\beta - \gamma)} \quad \text{.....(4.6)}$$

The following figure shows the velocity relation in metal cutting. As the tool advances, the metal gets cut and chip is formed. The chip slides over the rake surface of the tool. With the advancement of the tool, the shear plane also moves. There are three velocities of interest in the cutting process which include:

V_c = velocity of the tool relative to the workpiece. It is called cutting velocity.

V_f = velocity of the chip (over the tool rake) relative to the tool. It is called chip flow velocity.

V_s = velocity of displacement of formation of the newly cut chip elements, relative to the workpiece along the shear plane. It is called velocity of shear.

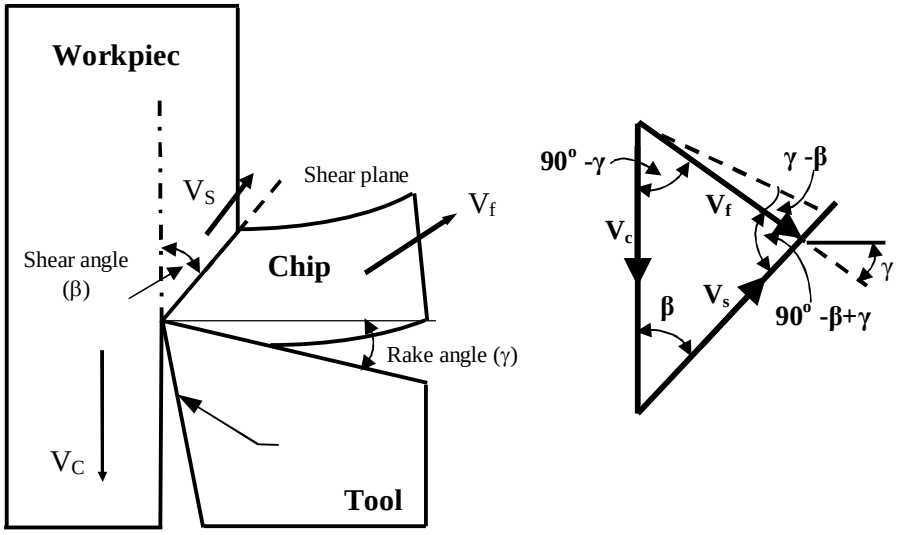

Fig.4.4 velocity of the cutting process

According to principles of kinematics, these three velocities, i.e. their vectors must form a closed velocity diagram. The vector sum of the cutting velocity, V_c and the shear velocity, V_s is equal to chip velocity, V_f . Thus,

$$V_s = \frac{\cos\gamma}{\cos(\beta - \gamma)} V_c \quad \text{.....(4.7)}$$

$$V_f = \frac{\sin\beta}{\cos(\beta - \gamma)} V_c \quad \text{.....(4.8)}$$

Using Eq. (4.1) and Eq. (4.4) the above equations may also be written as

$$V_s = \varepsilon \sin\beta\, V_c \quad \text{.....(4.9)}$$

$$V_f = V_c / \xi \quad \text{.....(4.10)}$$

where,

β = Shear angle

γ = Rake angle

ε = Shear strain

The force acting on a cutting tool during the process of metal cutting are the fundamental importance in the design of cutting tools. The determination of cutting forces necessary for deformation the work material at the shear zone is essential for several important requirements:

i. to estimate the power requirements of a machine tool

ii. to estimate the straining actions that must be resisted by the machine tool components, bearings, jigs and fixtures

iii. to evaluate the role of various parameters in cutting forces

iv. to evaluate the performance of any new work material, tool material, environment, techniques etc. with respect to machinability (cutting forces)

The force system in the general case of conventional turning process is shown in the following Figure.

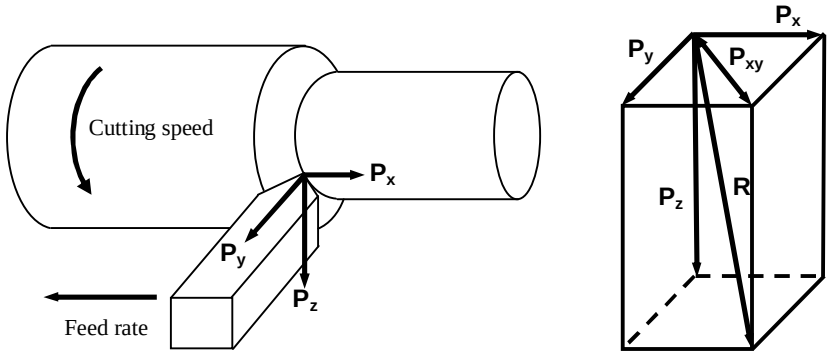

Fig.4.5 Forces in machining

P_x = feed force in the direction of the tool travel

P_y = thrust force in the direction perpendicular to the produced surface

P_z = cutting force or main force acting in the direction of the cutting velocity.

$$P_x = P_{xy} \sin \varphi \quad \text{.....(4.11)}$$

$$P_y = P_{xy} \cos \varphi \quad \text{.....(4.12)}$$

where,

φ = Principle cutting edge angle

Several forces can be defined relative to the orthogonal cutting model. Based on these forces, shear stress, coefficient of friction, and certain other relationships can be defined by using the Merchant Circle Diagram (MCD).

.

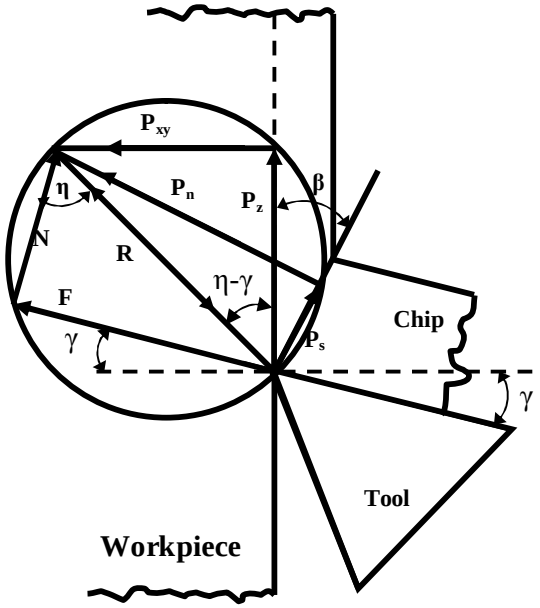

Fig.4.6 Merchant Circle Diagram (MCD)

$$\left.\begin{aligned} F &= P_z \sin\gamma + P_{xy} \cos\gamma \\ N &= P_z \cos\gamma - P_{xy} \sin\gamma \end{aligned}\right\} \quad \text{.....(4.13)}$$

$$\left.\begin{aligned} P_s &= P_z \cos\beta - P_{xy} \sin\beta \\ P_n &= P_z \sin\beta + P_{xy} \cos\beta \end{aligned}\right\} \quad \text{.....(4.14)}$$

where,

F = Friction force along the tool rake face

N = Friction force along the tool rake face

P_s = Component of force directed along the shear plane

P_n = Component of force perpendicular the shear plane

Now,

$$\mu = \frac{F}{N} = \frac{P_z \sin\gamma + P_{xy}\cos\gamma}{P_z \cos\gamma - P_{xy}\sin\gamma} = \tan\eta \quad \text{.....(4.15)}$$

where,

μ = Kinetic coefficient of friction

η = Mean angle of friction at the rake surface

Again, from the geometry of force relations of MCD

$$\left.\begin{aligned} P_z &= R\cos(\eta-\gamma) \\ P_s &= R\cos(\beta+\eta-\gamma) \\ P_z &= P_s\left[\frac{\cos(\eta-\gamma)}{\cos(\beta+\eta-\gamma)}\right] \end{aligned}\right\} \quad \text{.....(4.16)}$$

where,

η = Mean angle of friction at the rake surface

Based on the shear force, the shear stress (τ_s) which acts along the shear plane between the work and the chip is:

$$\tau_s = \frac{P_s}{A_s} \quad \text{.....(4.17)}$$

where,

$A_s = \frac{S_o t}{\sin \beta}$ = Area of the shear plane

S_o = Feed rate

t = Depth of cut

So, from Eq. (4.16) and Eq. (4.17) we get the following relation,

$$P_z = \tau_s S_o t \left[\frac{\cos(\eta - \gamma)}{\sin \beta \cos(\beta + \eta - \gamma)} \right] \quad \text{.....(4.18)}$$

$$P_{xy} = \tau_s S_o t \left[\frac{\sin(\eta - \gamma)}{\sin \beta \cos(\beta + \eta - \gamma)} \right] \quad \text{.....(4.19)}$$

According to Lee and Shaffer theory the shear occurs on a single plane. So for a cutting process according to this theory, the following are supposed to hold good:

i. The material ahead of the cutting tool behaved as ideal plastic material

ii. The chip does not get hardened

iii. The chip and parent work material are separated by a shear plane.

Lee and Shaffer derived the following relationship as:

$$\beta + \eta - \gamma = \frac{\pi}{4} \quad \text{.....(4.20)}$$

The expression for cutting force with this relation becomes,

$$P_z = \tau_s S_o t (\cot \beta + 1) \quad \text{.....(4.21)}$$

P_z is the major component, which also decides power consumption. For machining conventional materials producing continuous chips the shear angle β can be replaced by ξ as,

$$\cot \beta = \frac{1}{\tan \beta} = \frac{\xi - \sin \gamma}{\cos \gamma} \cong \xi - \tan \gamma \quad \text{.....(4.22)}$$

$$\left.\begin{aligned} P_z &= \tau_s S_o t (\xi - \tan \gamma + 1) \\ P_{xy} &= \tau_s S_o t (\xi - \tan \gamma - 1) \end{aligned}\right\} \text{.....(4.23)}$$

In machining ductile metals, particularly steels, the actual value of τ_s can be derived by the following equation,

$$\tau_s = 0.74 \sigma_u \varepsilon^{0.6\Delta} \quad \text{.....(4.24)}$$

where,

σ_u = Ultimate tensile strength of the work material at normal condition

Δ = Percentage elongation of the work material

ε = Average cutting strain

Earnest and Merchant extended their analysis and studied the relationship between the shear angle and the cutting conditions. They suggested that the shear angle always takes the value that reduces the total energy consumed in cutting to a minimum. Because the total work done in cutting is dependent upon and is a direct function of the component P_z of the cutting force, they developed an expression for P_z in terms of β and the constant properties of the workpiece material. By applying principle of minimum energy Earnest and Merchant derived the relationship,

$$\beta = \frac{\pi}{4} - \frac{\eta}{2} + \frac{\gamma}{2} \quad \text{.....(4.25)}$$

The expression for cutting force with this relation becomes,

$$P_z = 2\tau_s S_o t \cot\beta \quad \text{.....(4.26)}$$

4.3 Heat Generation in Machining

Machining involves considerable plastic deformation in the primary shear zone as well as sliding friction between the chip and the tool. This mechanical work is converted into thermal energy or heat and results in high temperatures at the tool/chip interface and the chip. In orthogonal cutting, the total energy consumed per unit time is

$$U = P_z V_c \quad \text{.....(4.27)}$$

where,

P_z = Main force acting in the direction of the cutting velocity

V_c = Cutting velocity

The total energy per unit volume of chip formed (or specific energy) is then

$$u = \frac{U}{V_c a_1 b} = \frac{P_z}{a_1 b} \quad \text{.....(4.28)}$$

where,

P_z = Main force acting in the direction of the cutting velocity

V_c = Cutting velocity

a_1 = Undeformed chip thickness

b = Width of cut

The total energy per unit volume of chip is composed of:

- the shear energy per unit volume (u_s) on the shear plane

- the friction energy per unit volume (u_f) on the rake face
- the surface energy per unit volume (u_a) as a result of the formation of new surface areas
- the momentum energy per unit volume (u_m) as a result of the momentum change associated with the metal changing direction as it crosses the shear plane.

The surface energy per unit volume (u_a) and the momentum energy per unit volume (u_m) are usually considered negligible in comparison to the other two components. Therefore the total energy per unit volume can be approximated as follows:

$$u = u_s + u_f \quad \text{.....(4.29)}$$

The shear energy per unit volume can be obtained in the following way:

$$u_s = \frac{P_s V_s}{V_c a_1 b} \quad \text{.....(4.30)}$$

where,

P_s = Component of force directed along the shear plane

V_s = Shear velocity

In a similar way the frictional energy per unit volume can be found as:

$$u_f = \frac{F V_f}{V_c a_1 b} \quad \text{.....(4.31)}$$

where,

F = Component of frictional force directed along the tool rake face

V_f = Chip velocity

4.4 Temperature Rise due to Heat Source (Stationary and Moving)

The partial differential equation that relates the temperature and energy input is as follows:

$$\frac{k}{\rho c}\left(\frac{\partial^2 \theta}{\partial x^2}+\frac{\partial^2 \theta}{\partial y^2}+\frac{\partial^2 \theta}{\partial z^2}\right)+\frac{Q}{\rho c}=\frac{d\theta}{dt} \quad \text{.....(4.32)}$$

where,

θ = Temperature at any location x, y, z

Q = Strength of an instantaneous point heat source

ρ = Density

c = Specific heat

k = Thermal conductivity

t = Time

When a quantity of heat Q is liberated instantaneously at a point x', y', z' in an infinite body the temperature at any point $P(x, y, z)$ in the body after a time t will be

$$\theta(x,y,z,t)=\left(\frac{Q\,K}{8k(\pi\,K\,t)^{3/2}}\right)e^{-r^{2/4Kt}}$$
$$\Rightarrow \theta(x,y,z,t)=\left(\frac{Q}{8\,\rho\,c(\pi\,K\,t)^{3/2}}\right)e^{-r^{2/4Kt}} \quad \text{.....(4.33)}$$

where,

$$r^2=(x-x')^2+(y-y')^2+(z-z')^2$$

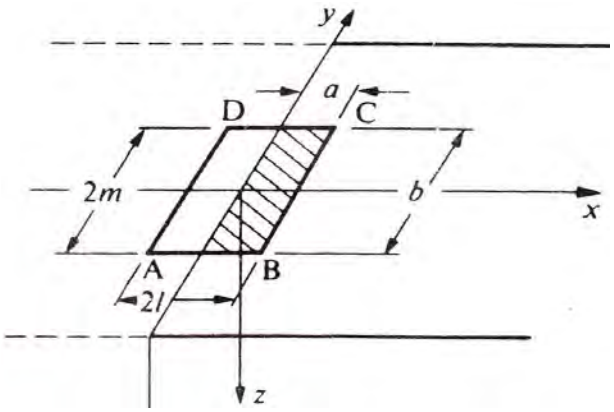

Fig.4.7 Stationary heat source

For the case of a continuous stationary heat source extending over a finite area, and for a steady state condition, i.e. at $T \to \infty$ the equation for the rise of temperature due to a uniform heat source extending over $-l < x' < l$ and $-m < y' < m$ as shown in Fig.4.7 is given by

$$\Delta\theta = \frac{Q}{2\pi k}\int_{-l}^{l} dx' \int_{-m}^{m} \frac{dy'}{\sqrt{(x-x')^2 + (y-y')^2 + (z-z')^2}} \quad \text{.....(4.34)}$$

The mean surface temperature rise over the area of the source may be obtained by the following equation,

$$\Delta\bar{\theta} = \frac{\int_{-l}^{l}\int_{-m}^{m} (\Delta\theta)\, dx\, dy}{4\, l\, m} \quad \text{.....(4.35)}$$

$$\Delta\bar{\theta} = \frac{Ql}{k}\frac{2}{\pi}\left[\begin{array}{l} \sinh^{-1}\left(\frac{l}{m}\right) + \left(\frac{m}{l}\right)\sinh^{-1}\left(\frac{l}{m}\right) - \frac{1}{3}\left(\frac{m}{l}\right)^2 \\ + \frac{1}{3}\left(\frac{l}{m}\right) - \frac{1}{3}\left\{\left(\frac{l}{m}\right) + \left(\frac{m}{l}\right)\right\}\left\{1 + \left(\frac{m}{l}\right)^{1/2}\right\} \end{array}\right] \quad \text{.....(4.36)}$$

This equation may be written,

$$\Delta\bar{\theta} = \frac{Ql}{k}\,\bar{A} \quad \text{.....(4.37)}$$

where,

$\overline{A}$ = Area factor (a function of the aspect ratio of the surface are $\frac{m}{l}$ only)

The approximate value of $\overline{A}$ may be written as

$$\overline{A} = \frac{2}{\pi}\left(\ln \frac{2m}{l} + \frac{1}{3}\frac{l}{m} + \frac{1}{2}\right) \quad \text{.....(4.38)}$$

A friction slider corresponding to a moving rectangular heat source of dimension $2m \times 2l$ of uniform strength q moving over a semi infinite body insulated everywhere except across the interface

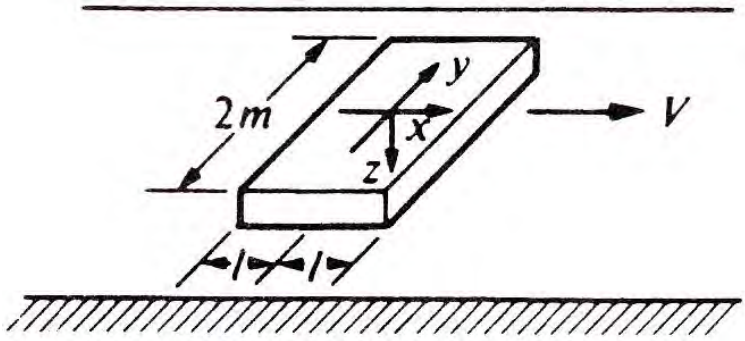

Fig.4.8 Schemetic diagram of moving heat source

For acontinuous moving point heat source when the heat is liberated at the rate of Q cal/sec at x, y, z = 0 for a time dT' and an infinite slider moves past this source with a velocity V parallel to axis of x, the temperature at a point x, y, z at time T can be calculated from

$$d\theta = \left(\frac{Q\,dT'}{8\rho c\left[\pi K (T - T')\right]^{3/2}}\right) e^{-r^2/4Kt} \quad \text{.....(4.39)}$$

where,

$$r^2 = \{ x - V(T - T') \}^2 + (y - y')^2 + (z - z')^2$$

By integrating the above equation between the period 0 and T and for steady state solution, i.e. at $T \to \infty$

$$d\theta = \left(\frac{Q}{4 \pi K R} \right) e^{-V(R-x)/(2K)} \quad \text{.....(4.40)}$$

where,

$R^2 = x^2 + y^2 + z^2$

The equation for the average temperature due to an infinite strip heat source extending over $-l < x' < l$ and $-\infty < y' < \infty$ at the surface z = 0, when heat flux is Q and the surrounding medium moves with a velocity V in the direction of x can be derived as follows:

$$\Delta\bar{\theta} = 0.754 \frac{Q\,l}{k\sqrt{L}} \quad \text{.....(4.41)}$$

where,

$L = \frac{V\,l}{2\,K}$ = Dimensionless velocity parameter

K = Thermal diffusivity

4.5 Predictive Modeling of Cutting Temperature

Machinability of materials usually judged mainly in respect of chip morphology, chip-tool interaction, cutting temperature, cutting forces, dimensional accuracy, surface integrity and wear and life of cutting tool with using cutting fluid and without using cutting fluid. In cutting, nearly all of energy dissipated in plastic deformation is converted into heat that in turn raises the temperature in the cutting zone. Since the heat generation is closely related to the plastic deformation and friction, we can specify three main sources of heat when cutting,

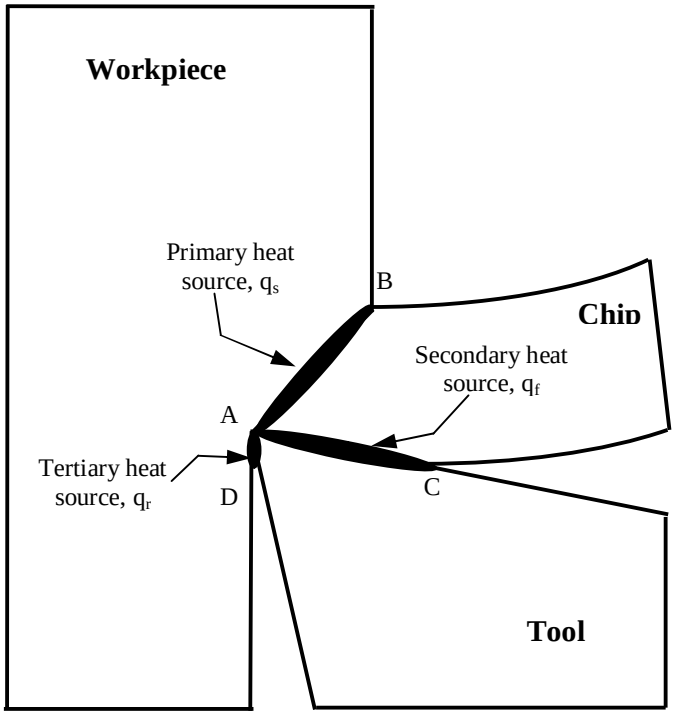

Fig.4.9 Heat sources in metal cutting process

i. Primary shear zone (A-B): The chip formation takes place firstly and mainly in this zone as the edge of the tool penetrates into the work-piece. Material on this zone has been deformed by a concentrated shearing process. q_s is the heat, generated in the primary zone due to intensive plastic deformation. The shear plane temperature is very important because it influences flow stress of work piece material and temperatures on the tool face. In this area local heating due to plastic work can cause the temperature to become very high. This leads to softening of the material and allows greater deformation and further heating, which can lead to periodic shear band formation and serrated chips.

ii. Secondary shear zone (A-C): The chip and the rake face of the tool are in contact from A to C. When the frictional stress on the rake face reaches a

value equal to the shear yield stress of the work-piece material, material flow also occur on this zone. Frictional heat source q_f localises at the tool-chip interface heat source. The friction in this area causes generation of heat, whichcan lead to high temperatures. Temperature of rake face is the maximum temperature in real machining operations and it causes tool wear.

iii. Tertiary shear zone (A-D): When the clearance face of the tool rubs the newly machined surface deformation can occur on this zone. Heat source q_r is generated due to tip radius of the cutting tool.The surface roughness and integrity of the finished surface, produced by the cutting process, are of interest in this area.

The main assumptions employed in the model development are:

i. The cutting edge is assumed to be sharp so that the tertiary zone can be neglected.

ii. All energy involved in plastic deformation (in the shear zone and at the chip-tool interface) is converted into heat.

iii. The primary and secondary zones are plane surfaces.

iv. The heat generated along the friction interface and the heat generated along the shear zone is evenly distributed.

v. The chip formation takes place along a thin shear zone and moves as a rigid body along the rake face of the tool. The chip leaves the shear zone at a constant temperature equal to the shear plane temperature.

vi. Part of energy at the shear plane will be convected away by the chip and part will flow into the work. Also, part of the energy at the chip-tool interface will usually go to the chip and part to the tool. There are thus two partition coefficients to be evaluated. R_1 is the fraction of energy of the shear plane going to the chip; R_2 is the fraction of energy at chip-tool interface going to the chip.

vii. Another assumption is that none of the energy per unit volume going to the chip on the shear plane is $u_{cs} = R_1 u_s$ while the enegy per unit volume going to the chip at chip-tool interface is $u_{cf} = R_2 u_f$ where u_s and u_f are the specific energies involved in shear and friction, respectively.

4.5.1 Shear Plane Temperature

The first analytical treatment of cutting tool temperature was that of Trigger and Chao (1951). The treatment that follows was originally presented by Loewen and Shaw (1954). Somewhat different treatments of shear-plane temperature than that presented here were presented by Hahn (1951) and Leone (1954).

The rate at which shear energy is expended along the shear plane will be

$$U_s = P_s V_s \quad \text{.....(4.42)}$$

where,

P_s = Component of force directed along the shear plane

V_s = velocity of the chip relative to the workpiece, which also is directed along the shear plane (shear velocity)

The rate at which energy is expended per unit area on the shear plane for orthogonal cutting conditions will be,

$$U_s' = \frac{P_s V_s}{a_1 b \csc \beta} \quad \text{.....(4.43)}$$

where,

a_1 = Undeformed chip thickness

b = Width of cut

β = Shear angle

To a good approximation, it may be assumed that all of the mechanical energy associated with the shearing process is converted into thermal energy, and the heat flows from the shear zone per unit time per unit area will be

$$q_s = \frac{P_s V_s}{J a_1 b \csc \beta} = \frac{u_s V_c \sin\beta}{J} \quad \text{.....(4.44)}$$

where,

J = Mechanical equivalent of heat

u_s = Shear energy per unit volume

V_c = Cutting speed

If $R_1 q_s$ is the heat per unit time per unit area which leaves the shear zone with the chip, then $(1\text{-}R_1)q_s$ is the heat per unit time per unit area that flows into the work piece. The mean temperature of the metal in the chip, in the vicinity of the shear plane, will be

$$\bar{\theta}_s = \frac{R_1 q_s (a_1 b \csc\beta)}{V_c a_1 b \rho_w c_w} + \theta_o = \frac{R_1 u_s}{J \rho_w c_w} + \theta_o \quad \text{.....(4.45)}$$

where,

θ_o = Ambient workpiece temperature

$\rho_w c_w$ = volume specific heat at the mean temperature between θ_s and θ_o

Eq. (4.41) can be used to compute the shear plane temperature rise. Here the chip may be considered to be a perfect insulator if the total heat flowing from the interface is $(1\text{-}R_1)q_s$. The velocity of sliding is taken as V_s. When Eq. (4.41) is used to compute the shear plane temperature, it is found that

$$\bar{\theta}_s = 0.754 \frac{(1-R_1) q_s \left(\frac{a_1 \csc\beta}{2}\right)}{k_w \sqrt{L_1}} + \theta_o \quad \text{.....(4.46)}$$

And

$$L_1 = \frac{V_s \left(\frac{a_1 \csc\beta}{2}\right)}{2K_w} = \frac{V_c \varepsilon a_1}{4K_w} \quad \text{.....(4.47)}$$

where,

k_w = Thermal conductivity of the workpiece

K_w = Diffusivity of the workpiece material at temperature θ_s

ε = Strain in the chip

Then equating the Eq. (4.45) and Eq. (4.46) solving for R_1, it is found that

$$R_1 = \frac{1}{1+1.328\left[\frac{K_w \varepsilon}{V_c\ a_1}\right]^{1/2}} \quad \text{.....(4.48)}$$

Once R_1 is known, $\bar{\theta}_s$ may be calculated from Eq. (4.47). It is evident that the percentage of energy going to the chip (R_1) does not increase with increased cutting speed (V_c) alone, but rather with the non-dimensional quantity $\left[\frac{K_w \varepsilon}{V_c\ a_1}\right]$. From Eq. (4.47) it may be seen that the temperature rise at the shear plane varies directly with the shear energy per unit volume going into the chip ($R_1\ q_s$), and inversely with the volume specific heat of the workpiece ($\rho_w\ c_w$).

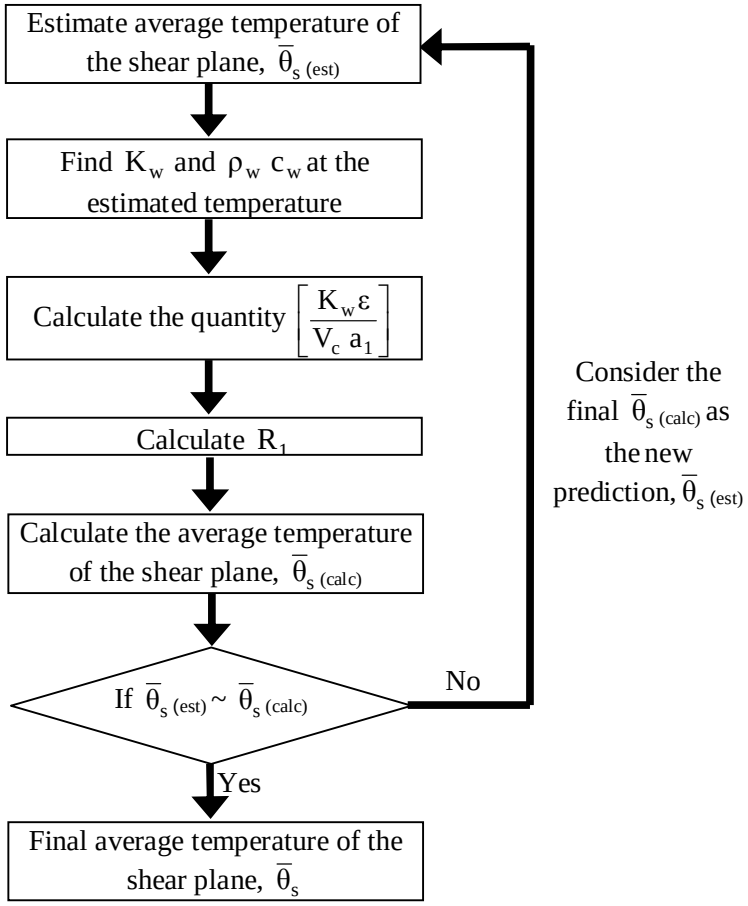

Fig.4.10 Flow chart for calculating the average shear plane temperature

4.5.2 Chip-tool Interface Temperature

From an analytical view point, the friction between chip and tool can be regarded as a heat source that is moving in relation to the tool. As before, it is a double treatment that allows calculation of the partition of friction energy between chip and tool, and hence the resulting temperature.the tool friction energy q_f that will be dissipated at the chip-tool interface per unit time per unit area will be

$$q_f = \frac{F V_f}{J C_N b} = \frac{u_f V_c a_1}{J C_N} \quad \text{.....(4.49)}$$

where,

F = Component of frictional force directed along the tool rake face

V_f = Chip velocityrelative to the tool

C_N = Chip-tool interface length

V_c = Cutting velocity

a_1 = Undeformed chip thickness

b = Width of cut

If R_2 is the fraction of q_f that flows into the chip, then the average temperature rise in the surface of the chip due to friction $\Delta\bar{\theta}_f$ is from Eq. (4.41)

$$\Delta\bar{\theta}_f = 0.754 \frac{R_2 q_f \left(\frac{C_N}{2}\right)}{k_{ch}\sqrt{L_2}} \quad \text{.....(4.50)}$$

And,

$$L_2 = \frac{V_f \left(\frac{C_N}{2}\right)}{2K_{ch}} \quad \text{.....(4.51)}$$

where,

k_{ch} = Thermal conductivity of the chip at its final temperature

K_{ch} = Diffusivity of the chip at its final temperature

The mean temperature of the chip surface along the tool face ($\bar{\theta}_T$) will be the sum of the mean shear- plane temperature ($\bar{\theta}_s$) and the mean temperature rise due to friction $\Delta\bar{\theta}_f$, and

$$\bar{\theta}_T = \bar{\theta}_s + \Delta\bar{\theta}_f = \bar{\theta}_s + 0.377\frac{R_2 q_f C_N}{k_{ch}\sqrt{L_2}} \quad \text{.....(4.52)}$$

To find R_2, the stationary heat source solution must be applied to the tool.

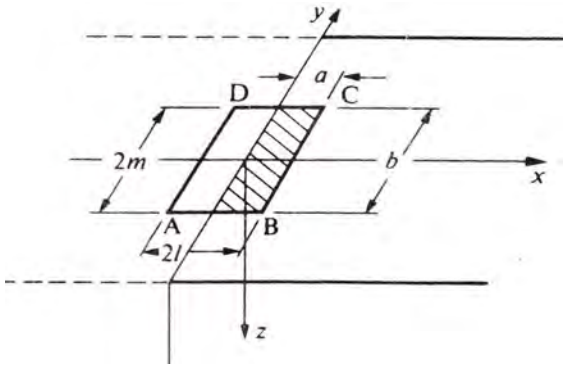

Fig.4.11 Stationary heat source at chip tool interface

The hatched area in Fig.4.11 represents the area of contact between a chip and a two dimensional cutting tool, the cutting edge being along the y-axis and the tool face in the xy-plane. The tool represented by the solid lines may be considered a quarter infinite body relative to the shaded area of contact. This is seen to represent a good approximation of an orthogonal cutting. Tool, provided the rake and clearance angle angles are not too large. By symmetry it is evident that the temperature at any point in the surface of the quarter infinite body subjected to the uniform heat source represented by the shaded area would be the same as the temperature of the corresponding point in the semi infinite body when subjected to a uniform heat source extending over ABCD, provided that the yz-plane is a perfect insulator, just as the xy-plane, which is a valid assumption.thus, the aspect ratio

to be used in obtaining the mean tool-face temperature rise is,

$$\frac{m}{l} = \frac{b}{2C_N} \quad \text{.....(4.53)}$$

With the aspect ratio thus defined for any tool, the shape fator $\overline{A}$ may be determined and the temperature $\overline{\theta}_T$ solved for as a point in the tool from Eq. (4.37)

$$\overline{\theta}_T = \frac{(1 - R_2) q_f C_N \overline{A}}{k_t} + \theta'_o \quad \text{.....(4.54)}$$

where,

k_t = Thermal conductivity of the tool at its final temperature $\overline{\theta}_T$

θ'_o = Ambient temperature of the tool

By equating the two values of $\overline{\theta}_T$ given in Eq. (4.52) and Eq. (4.54) it is found that,

$$R_2 = \frac{q_f \left(\frac{C_N \overline{A}}{k_t}\right) - \overline{\theta}_s + \theta'_o}{q_f \left(\frac{C_N \overline{A}}{k_t}\right) + q_f \left(\frac{0.377 C_N}{k_t \sqrt{L_2}}\right)} \quad \text{.....(4.55)}$$

$$R_2 = \frac{\left(\frac{u_f V_c a_1 \overline{A}}{J k_t}\right) - \overline{\theta}_s + \theta'_o}{\left(\frac{u_f V_c a_1 \overline{A}}{J k_t}\right) + \frac{0.754 u_f}{J \rho_{ch} c_{ch}} \left(\frac{V_c a_1 \xi}{C_N K_{ch}}\right)} \quad \text{.....(4.56)}$$

where,

$\rho_{ch} c_{ch}$ = Volume specific heat of chip at its final temperature $\overline{\theta}_T$

So, the quantity C' and B' can be written as,

$$C' = \left(\frac{u_f V_c a_1 \overline{A}}{J k_t}\right) \text{ and } B' = \frac{0.754 u_f}{J \rho_{ch} c_{ch}} \left(\frac{V_c a_1 \xi}{C_N K_{ch}}\right) \quad \text{.....(4.57)}$$

When R_2 is finally determined, $\overline{\theta}_T$ may be found readily from Eq. (4.52).

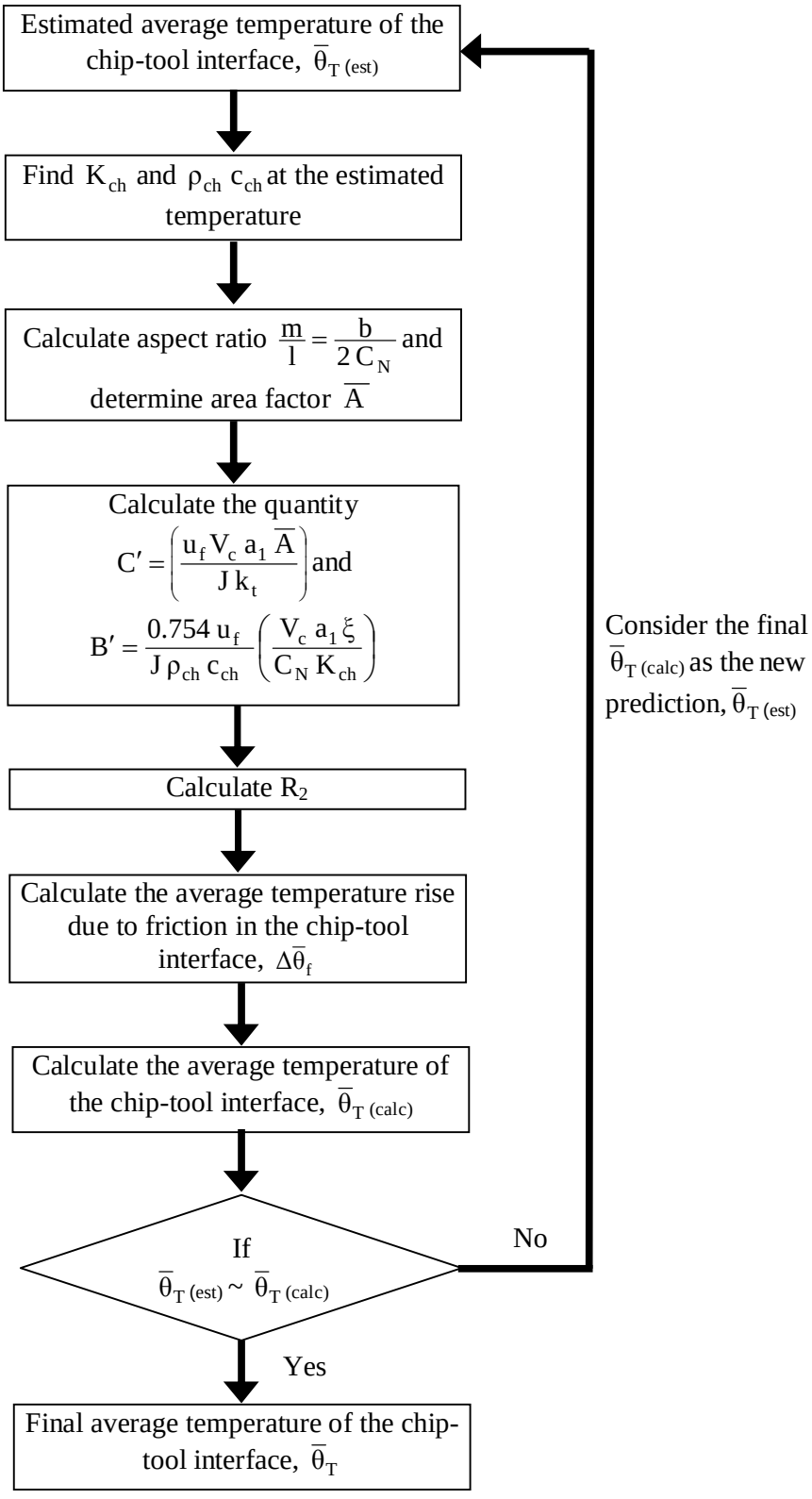

Fig.4.12 Flow chart for calculating the average chip-tool interface temperature

4.6 Model Validation of Cutting Temperature

In order to validate the model, the measured cutting temperature for turning AISI 1060 steel by uncoated SNMM insert (120408) at different V_c-S_o-t combinations has been compared with the predicted temperature.The pressure and flow rate of the high pressure coolant are maintained at 80 bar and 3.5 l/min respectively. Table 4.1 shows the combination of V_c-S_o-t for different test conditions.

Table 4.1 Test conditions for temperature validation

Test No.	V_c (m/min)	S_o (mm/rev)	t (mm)
1	93	0.10	1.5
2	93	0.14	1.5
3	93	0.18	1.5
4	93	0.22	1.5
5	133	0.10	1.5
6	133	0.14	1.5
7	133	0.18	1.5
8	133	0.22	1.5
9	186	0.10	1.5
10	186	0.14	1.5
11	186	0.18	1.5
12	186	0.22	1.5
13	266	0.10	1.5
14	266	0.14	1.5
15	266	0.18	1.5
16	266	0.22	1.5

In the Fig.4.13 predicted values from the analytical model and the measured values have been compared. Fig.4.13(b) shows that the predicted values can follow the trend of the measured values very efficiently and can predict the value of the cutting temperature within reasonable error level.

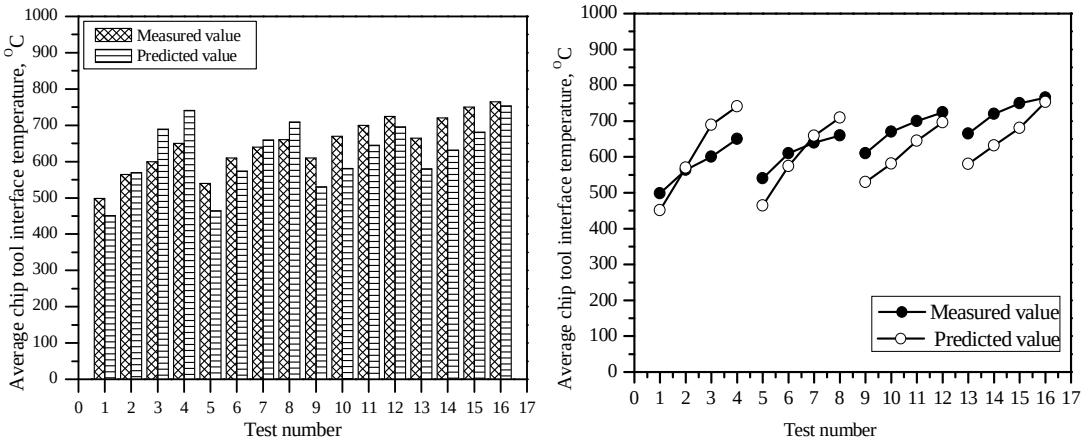

Fig.4.13 Comparison of measured and predicted cutting temperature for different tests when turning AISI 1060 steel by SNMM insert under HPC condition.

Chapter-5

Modeling of Cutting Force

5.1 Introduction

The knowledge of cutting forces developing in the various machining processes under given cutting factors is of great importance, being a dominating criterion of material machinability, to both: the designer-manufacturer of machine tools, as well as to user. Furthermore, their prediction helps in the analysis of optimisation problems in machining economics, in adaptive control applications, in the formulation of simulation models used in cutting databases. In this regard, cutting forces being a substantial dependent variable of the machining system has been investigated by many researchers in various cutting processes through formulation of appropriate models for their estimation. These models are analytical, semi-empirical and empirical relationships, which connect cutting factors to forces.

Over the last years, empirical models for the machinability parameters in various machining processes have been developed using data mining techniques, such as statistical design of experiments (Taguchi method, response surface methodology), computational neural networks and genetic algorithms. All these techniques possess the advantage of providing the impact of each individual factor and factor interactions, after an appropriate design of the experiment. Especially, for the Taguchi and response surface methodology, a minimum amount of experimental trials is combined to a reliable global examination of the

variables interconnection, instead of one- factor- at- a –time experimental approach and interpretation.

The Response Surface Methodology (RSM) is a collection of mathematical and statistical techniques useful for the modeling and analysis of problems in which a response of interest is influenced by several variables and the objective is to optimize this response [**Montgomery. 2005**]. The most extensive applications of RSM are in the particular situations where several input variables potentially influence some performance measure or quality characteristic of the process. The performance measure or quality characteristic is called the response. The input variables are sometimes called independent variables. The field of response surface methodology consists of the experimental strategy for exploring the space of the process or independent variables, empirical statistical modeling to develop an appropriate approximating relationship between the yield and the process variables, and optimization methods for finding the values of the process variables that produce desirable values of the response. In this work we will concentrate on the second strategy: statistical modeling to develop an appropriate approximating model between. The concept of the response surface involves a dependent variable (Y) called the response variable and several independent variables X_o, X1, X2, X3 ….X_n. If all of these variables are assumed to be measurable, the response surface can be expressed as Eq. (5.1):

$$Y = f(X_o, X_1, X_2, X_3 ... X_n.) + e \quad \text{…….....(5.1)}$$

Where, f is the response function which is unknown and perhaps very complicated and ‘e’ is the error which is normally distributed with zero mean according to the observed response. It is assumed that the independent variables are continuous and controllable by the experimenter with negligible error. Usually they are called the natural variables, because they are expressed in the natural units of measurement, such as degrees

Celsius, pounds per square inch, etc. In much RSM work it is convenient to transform the natural variables to coded variables, which are usually defined to be dimensionless with mean zero and the same standard deviation.

Because the form of the true response function f is unknown, we must approximate it. In fact, successful use of RSM is critically dependent upon the experimenter's ability to develop a suitable approximation for f. In many cases, either a first-order or a second order model is used.

The first-order model is likely to be appropriate when the experimenter is interested in approximating the true response surface over a relatively small region of the independent variable space in a location where there is little curvature in f. The form of the first-order model in Eq. (5.2) is sometimes called a main effects model, because it includes only the main effects of the variables.

$$Y = \left\{ b_o X_o + b_1 X_1 + b_2 X_2 + b_3 X_3 + ... \right\} + e \quad \text{.....(5.2)}$$

If there is an interaction between these variables, it can be added to the model easily as follows:

$$Y = \begin{Bmatrix} b_o X_o + b_1 X_1 + b_2 X_2 + b_3 X_3 + b_{12} X_1 X_2 \\ + b_{23} X_2 X_3 + b_{13} X_1 X_3 + ... \end{Bmatrix} + e \quad \text{.....(5.3)}$$

This is the first-order model with interaction. Adding the interaction term introduces curvature into the response function. Often the curvature in the true response surface is strong enough that the first-order model (even with the interaction term included) is inadequate. A second-order model will likely be required in these situations. The general second-order model is as given below:

$$Y = \left\{ \begin{matrix} b_o X_o + b_1 X_1 + b_2 X_2 + b_3 X_3 + b_{12} X_1 X_2 + b_{23} X_2 X_3 + \\ b_{13} X_1 X_3 + b_{11} X_1^2 + b_{22} X_2^2 + b_{33} X_3^2 + ... \end{matrix} \right\} + e \quad \text{.....(5.4)}$$

Where Y is the estimate response based on second order equation. The parameters b_0, b_1, b_2, b_3, b_{12}, b_{23}, b_{13}, b_{11}, b_{22} and b_{33} are to be calculated by the method of least squares.

Response surface method is found the successful technique to perform the trend analysis of cutting force with respect to various combinations of design variables include the cutting speed, feed rate and depth of cut. It is a combination of experimental and regression analysis and statistical inferences. The concept of the response surface involves a dependent variable (P_z) called the response variable and several independent variables. If all of these variables are assumed to be measurable, the response surface can be expressed as Eq. (5.5):

$$P_z = f(V_c, S_o, t) + e \quad \text{.....(5.5)}$$

Where, f is the response function and V_c, S_o, t are the cutting speed, feed and depth of cut and 'e' is the error which is normally distributed with zero mean according to the observed response. The observed response P_z as a function of the speed, feed and depth of cut can be written as in Eq. (5.6).

$$P_z = b_o + b_1 V_c + b_2 S_o + b_3 t \quad \text{.....(5.6)}$$

Where P_z is the response, b_0, b_1, b_2 and b_3 are the constants.

The non-linear relationship between the cutting force and machining independent variables represented in the following equation. The equation is,

$$P_z = C\, V_c^{\,a}\, S_o^{\,b}\, t^c \quad \text{.....(5.7)}$$

Where C is a constant and a, b and c are the exponents. A logarithmic data transformation can be applied to convert the nonlinear form of equation into to the linear form. This is one of most popularly used data transformation techniques in empirical model building.The above function can be represented in linear mathematical form as follows:

$$\ln P_z = \ln C + a \ln V_c + b \ln S_o + c \ln t \quad \text{.....(5.8)}$$

The above equation can be compared with the first order linear model like Eq. (5.2). The constants and exponents C, a, b and c can be determined by the method of least squares.

5.2 Predictive Model of Cutting Force Correlating with Speed, Feed and Depth of Cut

The main effect plot for cutting force has been shown in Fig.5.1(a). The plots show the variation of individual responses with the three parameters i.e. cutting speed, feed rate and depth of cut separately. In the plots, x-axis shows the value of each parameter at three levels and y-axis the response values. Horizontal line in the plot shows the mean value of the response. The results show that increasing cutting speed there is a continuous decrease in cutting force. Cutting force increases with increase of feed rate and depth of cut, but in different degrees.

Fig.5.1(b) shows the interaction plot, that means the variation of main cutting force due to interaction between cutting speed and feed rate ($V_c \times S_o$), feed rate and depth

of cut ($S_o \times t$), cutting speed and depth of cut ($V_c \times t$) etc. Fig.5.2(a), Fig.5.2(b) and Fig.5.2(c) show the three dimensional surface plot for cutting force.

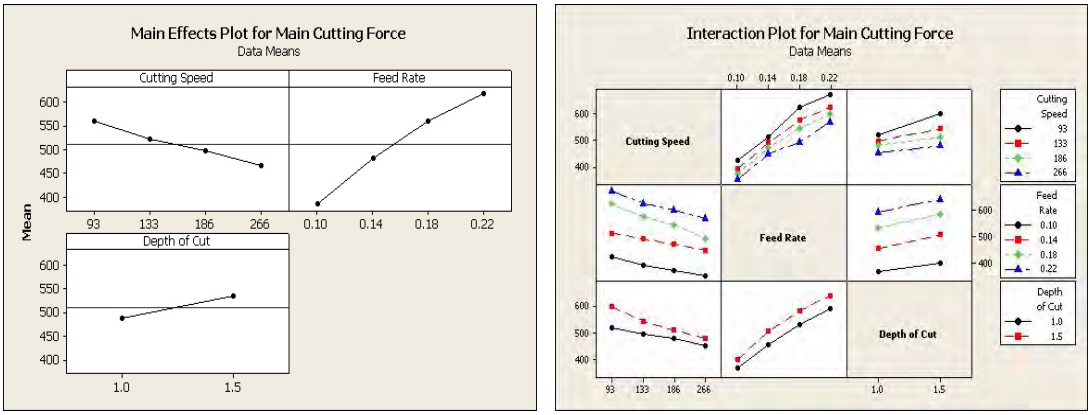

(a) (b)

Fig.5.1 (a) Main effect plot and (b) interaction plot for cutting force

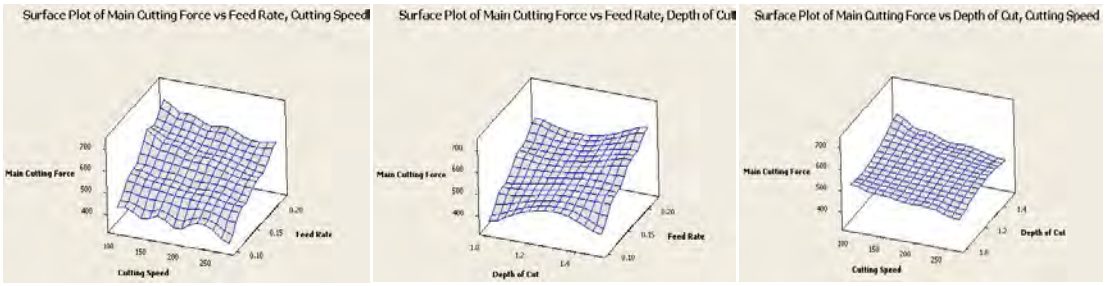

(a) (b) (c)

Fig.5.2 Surface plot for cutting force

From the above figures it can be decided that since there is significant interaction effect of the variables on the response cutting force, first order model is not formulated to predict the cutting force. In the first order regression model the interaction effect is not considered and so, it can't predict the actual cutting force value. Here the second order regression model and the non-linear model (with the help of logarithmic transformation) is developed and compared with each other.

The second order model was postulated in obtaining the relationship between the main cutting force and the machining independent variables. The developed second order mathematical model is given in Eq. (5.8).

$$P_z = 0.29 - 0.20\,V_c + 3590.84\,S_o + 127.39\,t - 5036.13\,S_o^{\,2} - 1.88\,V_c\,S_o - 0.44\,V_c\,t + 212.74\,S_o\,t \quad \text{……...…..……(5.8)}$$

where,

P_z = Cutting force

V_c = Cutting speed

S_o = feed rate

t = depth of cut

The total analysis was done using uncoded units. The co-efficient of correlation R-Sq(pred) = 96.98% indicating that the equation is able to predict the cutting force values with 96.98% accuracy. The detailed statistical analysis of the variables that are used in the equation has been given in Table 5.1.

Table 5.1 Regression table for the second order mathematical model

Term	Co-efficient	SE Co-efficient	T	P
Constant	0.29	67.26	0.004	0.997
V_c	0.20	0.32	0.627	0.537
S_o	3590.84	529.07	6.787	0.000
t	127.39	40.21	3.168	0.004
$V_c^{\,2}$	0.00	0.00	2.241	0.035
$S_o^{\,2}$	-5036.13	1401.84	-3.593	0.002
$V_c \times S_o$	-1.88	0.76	-2.464	0.022
$V_c \times t$	-0.44	0.14	-3.147	0.005
$S_o \times t$	212.74	197.43	1.078	0.293

R-Sq(pred) = 96.98% R-Sq(adj) = 98.33%

Here, the P-values are used to determine which of the effects in the model are statistically significant. The α value is assumed as 0.05. From Table 5.2, it can be clearly stated that, linear, square and the interaction effects of the cutting process variables are statistically significant since their P-values are less than 0.05.

Table 5.2 Analysis of Variance for the second order mathematical model

Source	DF	Seq SS	Adj SS	Adj MS	F	P
Regression	8	274946	274946.08	34368.26	222.25	0.000
Linear	3	270057	7517.76	2505.92	16.20	0.000
Square	2	2325	2671.77	1335.88	8.64	0.002
Interaction	3	2564	2564.01	854.67	5.53	0.006
Residual error	22	3402	3402.08	154.64		
Total	30	278348				

The check of the normality assumptions of the data is conducted; it can be seen in Fig.5.3(a) that all the points on the normal plot come to close to forming a straight line. This implies that the data are fairly normal and there is no deviation from the normality. This shows the effectiveness of the developed model. Notice that the residuals are falling on a straight line, which means that the errors are normally distributed. In addition, Fig.5.3(b) illustrates that there is no noticeable pattern or unusual structure in residual VS fitted value plot. This implies that the proposed second order model is adequate to illustrate the pattern of the cutting force.

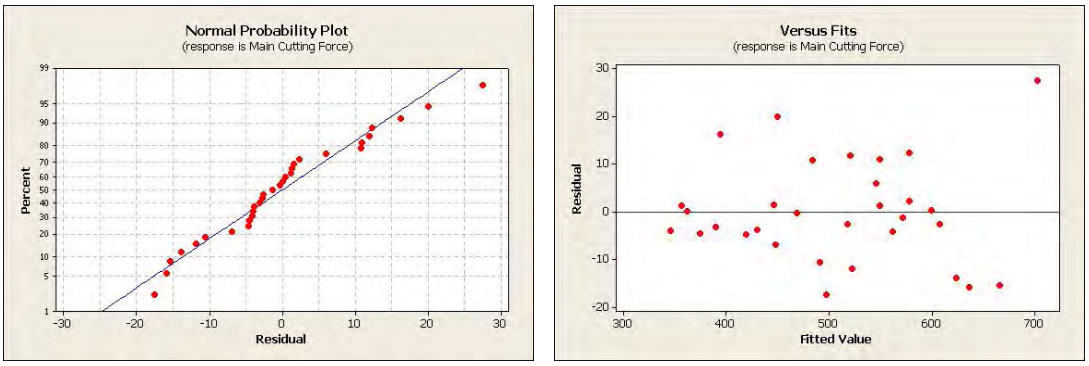

(a) (b)

Fig.5.3 Second order mathematical model (a)Normal probability plot for residuals (b) Residual VS fitted value plot

The logarithmic transformed linear equation of cutting force prediction in terms of metal cutting parameters (cutting speed, feed rate and depth of cut) is as follows:

$$\ln P_z = 8.16 - 0.169 \ln V_c + 0.602 \ln S_o + 0.219 \ln t \quad \text{……...…..……(5.9)}$$

The coefficient of the coded values of cutting speed, feed rate and depth of cut in terms of ln V_c, ln S_o and ln t is derived by first order regression analysis. Since all the three parameters are under the same logarithmic scale, the factor with highest value of coefficient possesses the most dominating effect over the response. From the Eq. (5.9) the non-linear model of the cutting force can be expressed as the following equation,

$$P_z = \frac{3498.187\ S_o^{0.602}\ t^{0.219}}{V_c^{0.169}} \quad \text{…….....…..……(5.10)}$$

Table 5.3 Regression table for the non-linear model

Predictor	Co-efficient	SE Co-efficient	T	P
Constant	8.15956	0.07233	112.81	0.000
ln V_c	-0.16936	0.01278	-13.26	0.000
ln S_o	0.60246	0.01692	35.61	0.000
ln t	0.21943	0.02458	8.93	0.000

R-Sq = 98.2% R-Sq(adj) = 98.0%

The value of regression co-efficient for this data analysis has been found as 98.2%. Table 5.4 shows the analysis of variance for the non-linear model.

Table 5.4 Analysis of variance for the non-linear model

Source	DF	SS	MS	F	P
Regression	3	1.21057	0.40352	507.88	0.000
Residual Error	28	0.02225	0.00079		
Total	31	1.23282			

Here, the α value is assumed as 0.05 and from the Table 5.4 it is clear that the P-value, which is used to determine the model significance, is less than the α value.

The check of the normality assumptions of the data is conducted; it can be seen that the data are fairly normal and there is a no deviation from the normalityand the errors are normally distributed. In addition, Fig.5.4(b) illustrates that there is no noticeable pattern or unusual structure in residual VS fitted value plot. This implies that the proposed logarithmic model is also adequate to illustrate the pattern of the cutting force.

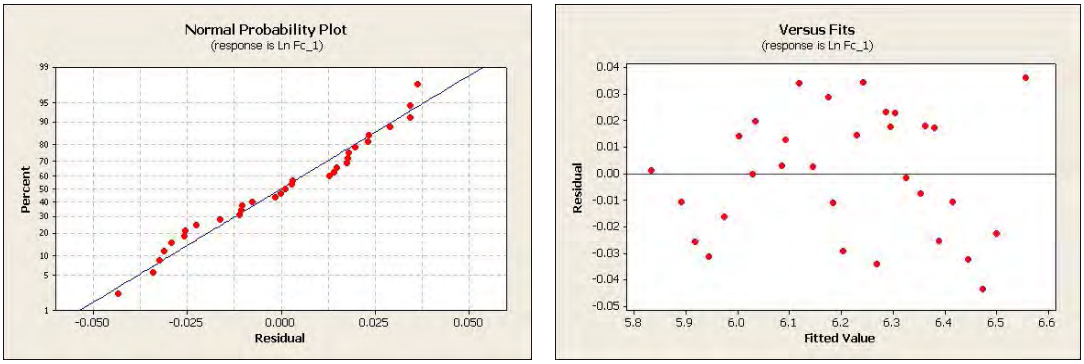

(a) (b)

Fig.5.4 Non-linear model (a) Normal probability plot for residuals (b) Residual VS fitted value plot

5.3 Model Validation of Cutting Force

In order to validate the model, the cutting force obtained during turning AISI 1060 steel at different V_c-S_o-t combinations has been compared with the predicted value. The pressure and flow rate of the high pressure coolant are maintained at 80 bar and 3.5 l/min respectively. Table 5.5 shows the combination of V_c-S_o-t for different test conditions.

Table 5.5 Test conditions for force validation

Test No.	V_c (m/min)	S_o (mm/rev)	t (mm)
1	93	0.10	1.0
2	186	0.10	1.0
3	133	0.14	1.0
4	266	0.14	1.0
5	93	0.18	1.0
6	186	0.18	1.0
7	133	0.22	1.0
8	266	0.22	1.0
9	93	0.10	1.5
10	186	0.10	1.5
11	133	0.14	1.5
12	266	0.14	1.5
13	93	0.18	1.5
14	186	0.18	1.5
15	133	0.22	1.5
16	266	0.22	1.5

In Fig.5.5 and Fig.5.6, predicted values from two models have been compared with the experimental values. From these figures both the model can predict the trend of the experimental data but, between the two predictive models the non-linear model can predict cutting force accurately.

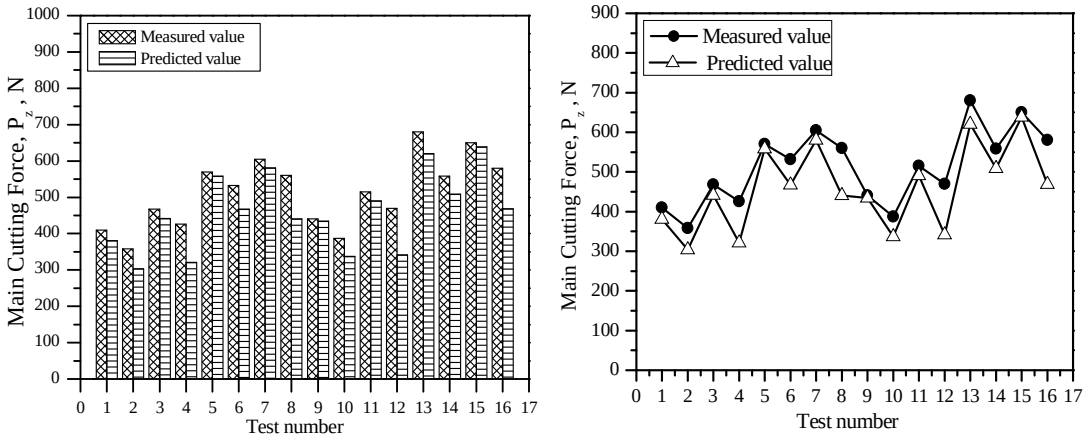

Fig.5.5 Comparison of measured and predicted cutting force from the second order mathematical model for different tests when turning AISI 1060 steel by SNMM insert under HPC condition.

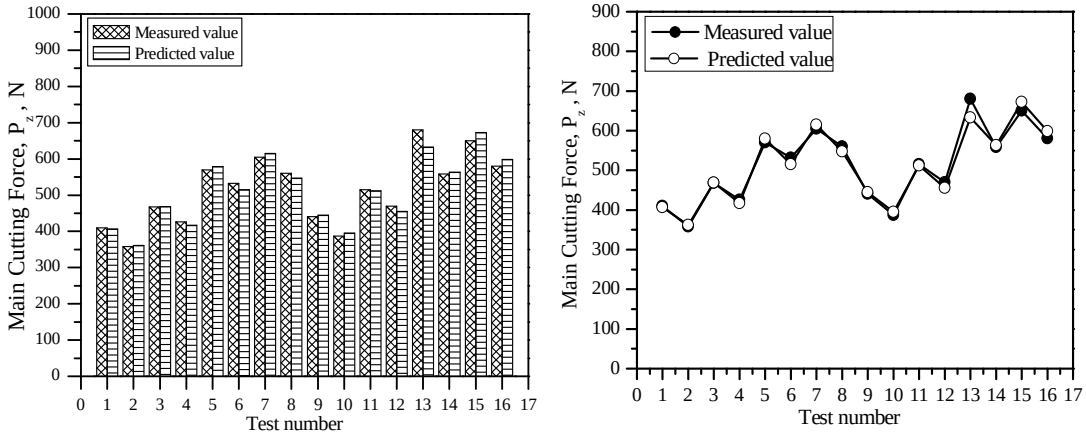

Fig.5.6 Comparison of measured and predicted cutting force from non-linear equation model for different tests when turning AISI 1060 steel by SNMM insert under HPC condition.

Chapter-6

Finite Element Modeling (FEM) of Cutting Zone Temperature

6.1 Introduction

Metal cutting is one of the most widely used manufacturing techniques in the industry and there are lots of studies to investigate this complex process in both academic and industrial world. Predictions of important process variables such as temperature, cutting forces and stress distributions play significant role on designing tool geometries and optimizing cutting conditions which is very necessary for process efficiency. The objective of metal cutting studies is to establish a predictive theory that would enable us to predict cutting performance such as chip formation, cutting force, cutting temperature, tool wear and surface finish. Experimental works are needed to obtain results but they are expensive and time consuming. At this point numerical methods become important. Finite element (FE) analysis is a powerful numerical modeling approach that can provide valuable insight into the behavior of metal cutting processes. In recent years, finite element analysis has become the main tool for simulating of metal cutting processes and a lot of research activities were done in simulating both the cutting process and the machine tool. Various outputs and characteristics of the metal cutting processes such as cutting forces, stresses, temperatures, chip shape, etc. can be predicted by using FEM without doing any experiment. FEM is a formal computational method and, consequently, its results depend entirely on the input. Many studies on FEM of the orthogonal cutting process have been

published until now for predicting the stress, strain and temperature with reasonable accuracy.

The ABAQUS Unified FEA product suite offers powerfull and complete solution for both routine and sophisticated engineering problems covering a vast spectrum of industrial applications. Analysis method with ABAQUS can be described as follows:

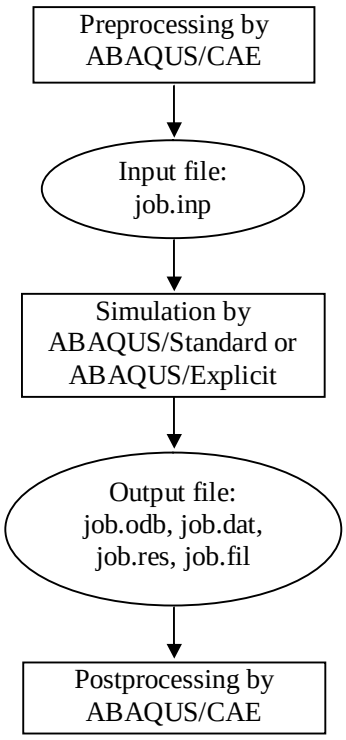

Fig.6.1 Flow chart for the analysis by ABAQUS

By ABAQUS/CAE a model is generated and an input file is generated with ABAQUS/CAE after completing the model. Then the input file is submitted to the ABAQUS/ analysis product ABAQUS/Standard or ABAQUS/Explicit. By reading the input file Abaqus analysis product perform analysis and then send information to ABAQUS/CAE to monitor the progress of the job and generates an output database.

This chapter covers a study on modeling and simulation of orthogonal metal cutting of AISI 1060 steel by a uncoated tungsten carbide tool by finite element method. The general-purpose FEA software ABAQUS/CAE (version 6.9-EF1) has been used to set up the finite element model in two dimensions (2D, orthogonal cutting). The model takes into account only the area closer to the cutting edge, where the chip is formed. Work piece is defined as a deformable body, while the tool is considered rigid. Input requirements for the model included tool and workpiece geometry, tool and workpiece mechanical and thermal properties and boundary conditions.

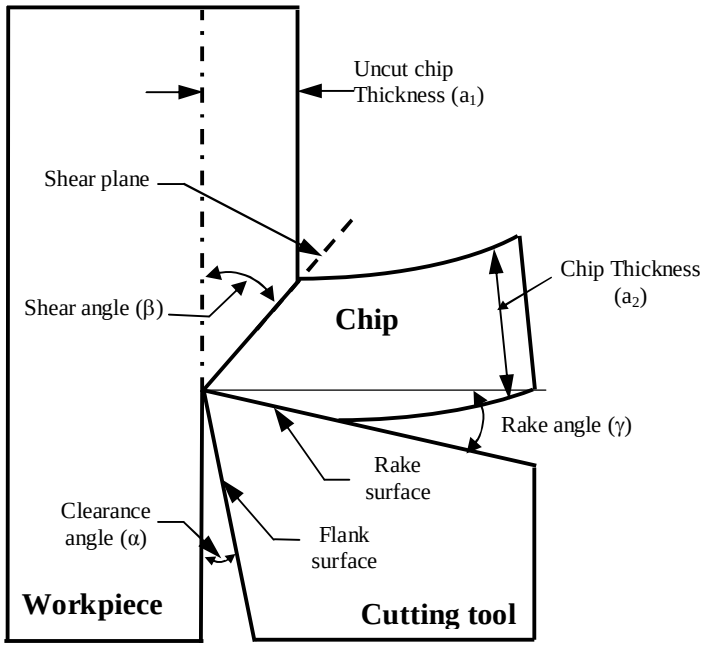

Fig. 6.2 Schematic view of chip formation mechanism

A Schematic view of chip formation mechanism is shown in Fig.6.2. This figure shows the enlarged sectinal view of the cutting zone where a tool engaged with the workpiece. The shear plane, chip-tool interface and the work-tool interface (which formed after some time to start the metal cutting) and the tool wil are of particular interest.

2D analysis is a restrictive approach from an industrial point of view, but it is considered accurate enough to make a sensitivity analysis in order to validate numerical results. Furthermore, it reduces significantly the computational time.

Fully coupled thermo-mechanical FE simulations are not able to follow the machining process up to steady-state conditions, as in order to keep the CPU time within reasonable limits, only a few milliseconds of the process can be simulated. The cutting tool had a clearance angle of 6°, rake angle of -6°. The simulations were performed at different cutting speeds and feed rate and a fixed depth of cut of 1.5 mm. To verify the simulation the results in terms of cutting temperature compared with the results obtained from experiments. The investigation indicates that the simulation results are consistent with the experiments and this finite element simulation method presented can be used to predict the cutting temperature accurately during machining of steel.

6.2 Modeling Procedures

6.2.1 Creating Parts

Total metal cutting model is created in to three parts as work material, cutting tool and chip by ABAQUS software.Two dimensional planer (modeling space) view of the cutting tool has been drawn having deformable type and shell base feature. Here sectional view of the work material is cosidered and cutting tool rake angle, clearance angle are shown in the figure.The shear plane(work-piece and chip), chip-tool interface (chip and cutting tool) and rubbing surface (flank surface of the tool) have been segmented using partitioning the edges. Around ten partition points along the shear plane and chip tool

interface and five partition points along the rubbing surface have been created to properly distribute the heat load.

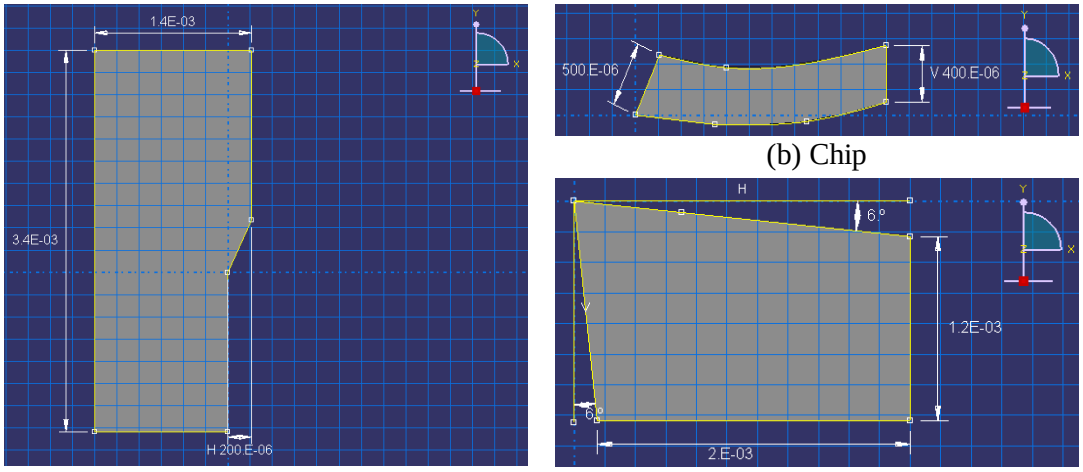

(a) Work piece (b) Chip (c) Cutting tool

Fig.6.3 Workpiece-chip-tool for FEM

6.2.2 Defining the Assembly

Each part, created in the first step is oriented in its own coordinate system and is independent of the other parts in the model.

Table 6.1 Defining the assembly

Part name	Created instances	Type
Work piece	Work piece-1	Dependent(mesh on part)
Chip	Chip-1	Dependent(mesh on part)
Cutting tool	Cutting tool-1	Dependent(mesh on part)

Merged instance	Primary instances	Merged part	Type
Total model-1	Work piece -1 Chip-1 Cutting tool-1	Total model	Dependent(mesh on part)

Although a model may contain many parts, it contains only one assembly. The geometry of the assembly is defined by creating instances of a part and then positioned the instances relative to each other in a global coordinate system. The part instances have been declared as dependent for manipulating mesh generation on part rather than instance. ABAQUS/CAE positions the instance so that the origin of the sketch that defined the frame overlays the origin of the assembly's default coordinates system. Then instances are mergerd to create total metal cutting model. The 'Merge Instance' function creates new part and automatically instance it into the assembly.

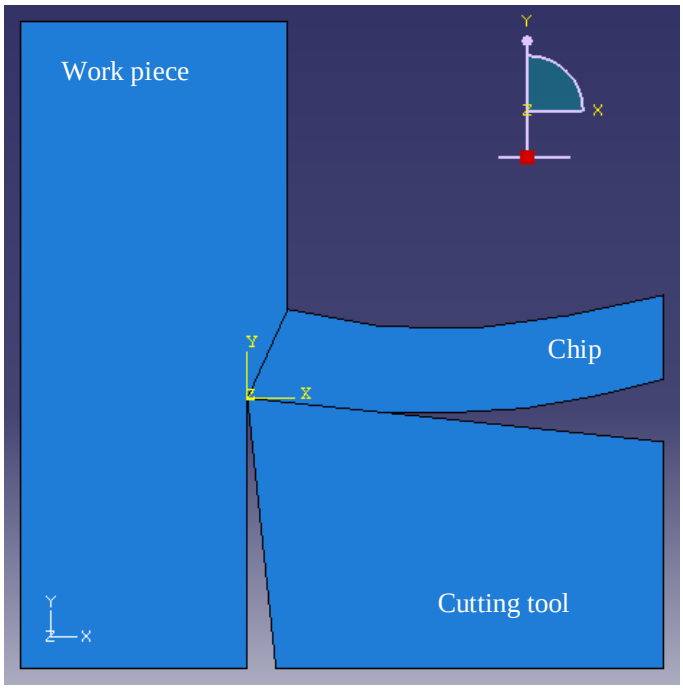

Fig.6.4 Assembly model of workpiece-chip-tool

6.2.3 Defining Materials

In this problem the work material and the chip material (as it is a part of work material) is AISI 1060 steel and the cutting tool is Tungsten carbide. So, two materials named AISI 1060 and Tungsten carbide are created with their specific propeties.

Table 6.2 Thermal-mechanical properties of materials

Property	AISI 1060 Steel	Tungsten Carbide
Young's modulus, E (GPa)	200	630
Poisson's ratio, ν	0.29	0.24
Density, ρ (kg/m^3)	7865	14700
Thermal conductivity, k (W/mmK)	0.052-(1.9E-5)Θ	0.047
Specific heat, c (J/kgK)	420+0.66*Θ	251
Yield Stress,σ (GPa)	0.42	6
Plastic Strain,ε	0.0	0.0

Where, Θ is the temperature in ^{o}C.

6.2.4 Defining and Assigning Section Properties

The properties of a part were defined through different sections. Three solid homogeneous sections have been created using previously defined materials and then the sections have been assigned to the specific parts instances which were created at the first step.

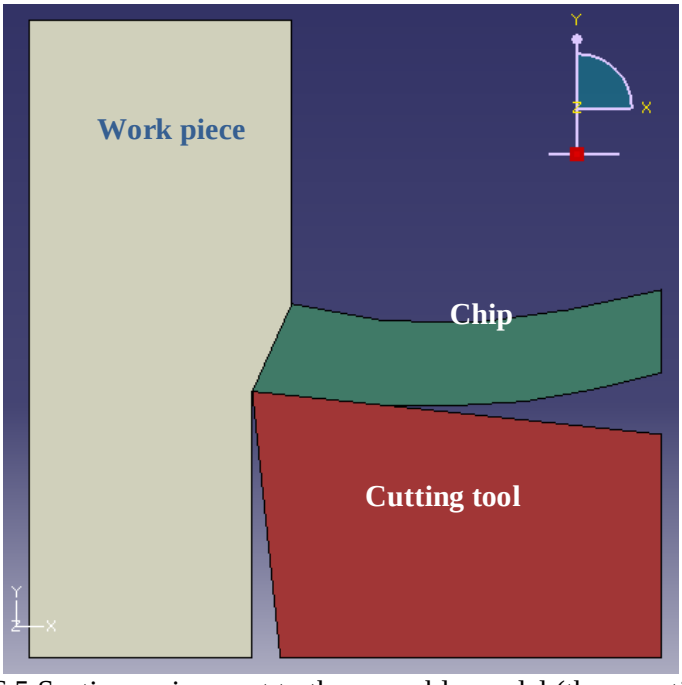

Fig.6.5 Section assignment to the assembly model (three sections)

Table 6.3 Defining and asigning section properties

Created sections	Type	Material	Assigned to the part
Work piece section	Solid, homogeneous	AISI 1060 steel	Work piece
Chip section	Solid, homogeneous	AISI 1060 steel	Chip
Cutting tool section	Solid, homogeneous	Tungsten carbide	Cutting tool

After assigning the section the material on the different section of the assembly can be viewed as follows,

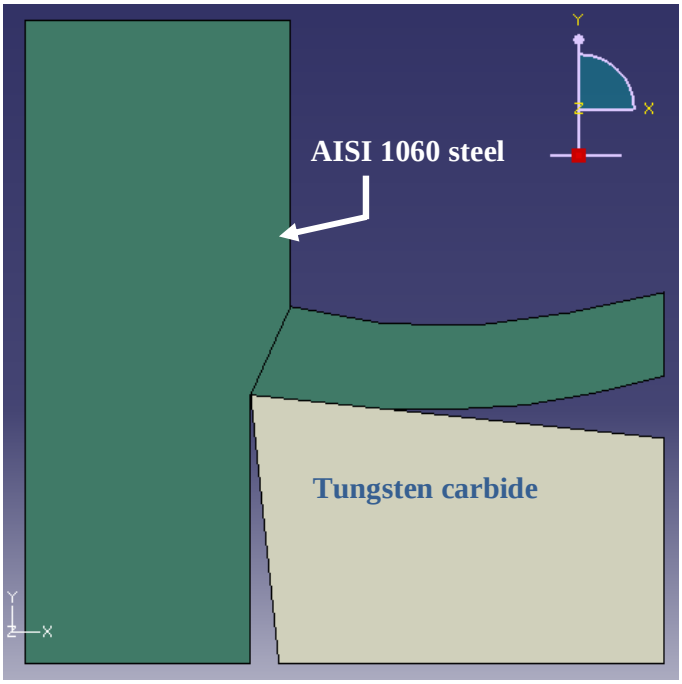

Fig.6.6 Materials on the assembly model (two materials)

6.2.5 Meshing the Model

To generate the finite element mesh by ABAQUS/CAE the mesh control, the element type and seeding need to be defined. In the present research work, under mesh control quadratic element shape with free meshing technique and medial axis algorithm have been selected for the mesh. Free meshing presumes no specific mesh pattern and can

generate mesh as the model state necessitates. Fig.6.7 shows mesh generation of the present part instance of the cutting tool.

The most important aspect during mesh generation completion is to assign mesh element to the part. Mesh elements are different depending on the use of standard or explicit method. Element assignment also depends on the nature of analysis techniques. Considering theses two things, CPE4RT (A 4-node plane strain thermally coupled quadrilateral, bilinear displacement and temperature, reduced integration, hourglass control.) element of quadratic formation has been used for analysis. The mesh density has been specified by creating proper seeding.

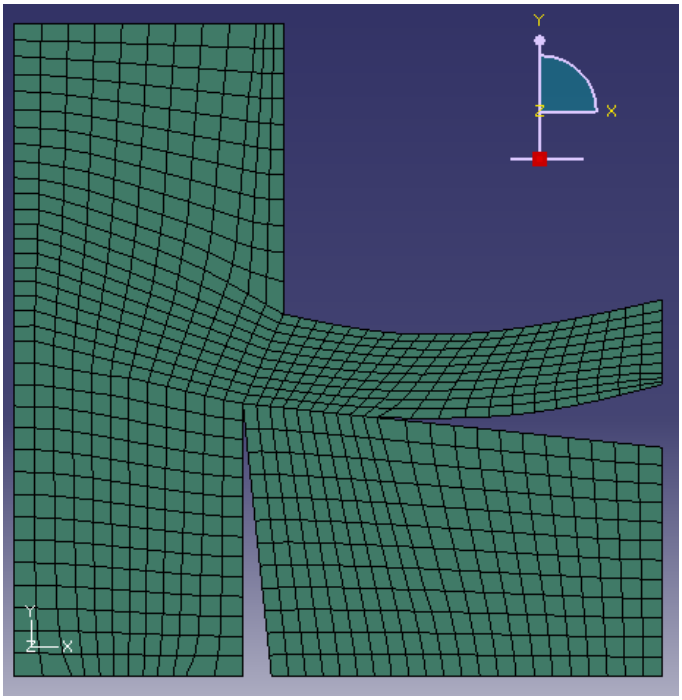

Fig.6.7 Mesh generation on the workpiece-chip-tool

6.2.6 Configuring Analysis

The simulation, which normally is run as a background process, is the stage in which Abaqus/Standard or Abaqus/Explicit solves the numerical problem defined in the

model. Different types of analysis techniques can be used to solve the problem numerically. The analysis will consist of two types of steps such as initial step and analysis step. ABAQUS/CAE generates the initial step automatically, but the analysis step is needed to be created.

After the initial step, boundary conditions are propagated to the next analysis step. In the present research work, the simulation is conducted using several analysis steps. Each analysis step incorporates output requests, interaction properties, loads, boundary conditions and pre-defined field. For the analysis step, coupled temperature displacement techniques have been considered. Fully coupled thermal-stress analysis is considered here because the stress analysis is dependent on the temperature distribution and the temperature distribution depends on the stress solution. During turning, significant heating is generated due to inelastic deformation of the material which, in turn, changes material properties. Fully coupled thermal-stress analysis is needed for such cases where the thermal and mechanical solutions must be obtained simultaneously rather than sequentially. Coupled temperature-displacement elements are provided for this purpose in both Abaqus/Standard and Abaqus/Explicit; however, each program uses different algorithms to solve coupled thermal-stress problems. In brief, fully coupled thermal-stress analysis is performed because

- Mechanical and thermal solutions affect each other and therefore must be obtained simultaneously.

- The model necessitates the existence of elements with both temperature and displacement degrees of freedom.

- Time dependent material response is analyzed.

Though coupled temperature displacement analysis can be performed by ABAQUS/Standard and explicit method, standard method has been used here with steady-state response and the Nlgeom setting is turned off.

In Abaqus/Standard the temperatures are integrated using a backward-difference scheme, and the nonlinear coupled system is solved using Newton's method. Abaqus/Standard offers an exact as well as an approximate implementation of Newton's method for fully coupled temperature-displacement analysis.

An exact implementation of Newton's method involves a nonsymmetric Jacobian matrix as is illustrated in the following matrix representation of the coupled equations:

$$\begin{bmatrix} K_{uu} & K_{u\theta} \\ K_{\theta u} & K_{\theta\theta} \end{bmatrix} \begin{Bmatrix} \Delta u \\ \Delta\theta \end{Bmatrix} = \begin{Bmatrix} R_u \\ R_\theta \end{Bmatrix} \qquad \text{.....(6.1)}$$

where,

Δu = corrections to the incremental displacement

$\Delta\theta$ = corrections to the incremental temperature

R_u = mechanical residual vector

R_θ = thermal residual vector

Solving this system of equations requires the use of the unsymmetric matrix storage and solution scheme. Furthermore, the mechanical and thermal equations must be solved simultaneously. The method provides quadratic convergence when the solution estimate is within the radius of convergence of the algorithm. The exact implementation is used by default.

Some problems require a fully coupled analysis in the sense that the mechanical and thermal solutions evolve simultaneously, but with a weak coupling between the two solutions. In other words, the components in the off-diagonal submatrices $K_{u\theta}, K_{\theta u}$ are small compared to the components in the diagonal submatrices $K_{uu}, K_{\theta\theta}$. For these problems a less costly solution may be obtained by setting the off-diagonal submatrices to zero so that we obtain an approximate set of equations:

$$\begin{bmatrix} K_{uu} & 0 \\ 0 & K_{\theta\theta} \end{bmatrix} \begin{Bmatrix} \Delta u \\ \Delta\theta \end{Bmatrix} = \begin{Bmatrix} R_u \\ R_\theta \end{Bmatrix} \quad \text{.....(6.2)}$$

where,

Δu = corrections to the incremental displacement

$\Delta\theta$ = corrections to the incremental temperature

R_u = mechanical residual vector

R_θ = thermal residual vector

As a result of this approximation the thermal and mechanical equations can be solved separately, with fewer equations to consider in each subproblem. The savings due to this approximation, measured as solver time per iteration, will be of the order of a factor of two, with similar significant savings in solver storage of the factored stiffness matrix. Further, in many situations the subproblems may be fully symmetric or approximated as symmetric, so that the less costly symmetric storage and solution scheme can be used. The solver time savings for a symmetric solution is an additional factor of two.

This modified form of Newton's method does not affect solution accuracy since the fully coupled effect is considered through the residual vector R_j at each increment in time. However, the rate of convergence is no longer quadratic and depends strongly on the

magnitude of the coupling effect, so more iterations are generally needed to achieve equilibrium than with the exact implementation of Newton's method. When the coupling is significant, the convergence rate becomes very slow and may prohibit obtaining a solution. In such cases the exact implementation of Newton's method is required. In cases where it is possible to use this approximation, the convergence in an increment will depend strongly on the quality of the first guess to the incremental solution, which you can control by selecting the extrapolation method used for the step. The time increment used in an analysis must be smaller than the stability limit. Time increment can either be automatic or fixed. In the present research work, fixed time incrementation is considered in order to save time of computation. Since, time increment is less than the stability limit; simulation can be performed with stability.

6.2.7 Applying Boundary Conditions and Loads to the Model

At the anlysis step, proper boundary conditions are created. Fig. 6.8 shows the boundary conditions of the model. Here only temperature boundary conditions are applied.

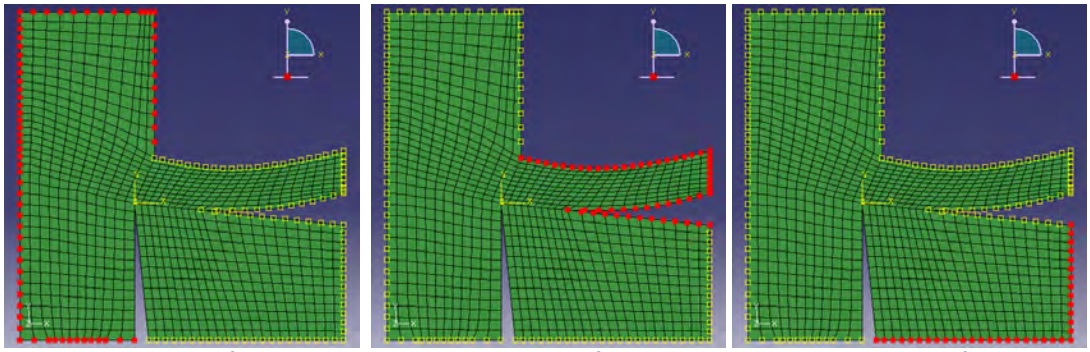

(a) 35°C (b) 20°C (c) 35°C

Fig.6.8 Boundary conditions of the model

Fig.6.9 shows the load cases that take place at the cutting zone during turning. Among all the forces P_z and P_x are taken from the experimental data and the other forces are calculated by using these forse and the data of the tool geometry.

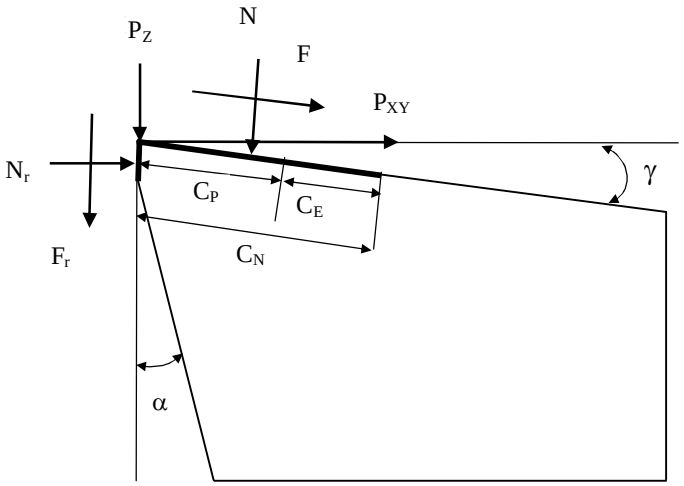

Fig. 6.9 Mechanical loads in metal cutting

The following equations have been used to calculate the mechanical loads. For orthogonal cutting,

$$P_x = P_{xy} \sin \varphi \quad \text{.....(6.3)}$$

where,

P_x = Feed force

P_{xy} = Resultant force of P_x and P_y

φ = Principal cutting edge angle

Frictional force and normal force on the rake is calculated by

$$\left.\begin{aligned} F &= P_z \sin \gamma + P_{xy} \cos \gamma \\ N &= P_z \cos \gamma - P_{xy} \sin \gamma \end{aligned}\right\} \quad \text{.....(6.4)}$$

where,

F = Friction force along the tool rake face

N = Friction force along the tool rake face

γ = Rake angle

Hence, the frictional co-efficient μ can be calculated by

$$\mu = \frac{F}{N} = \frac{P_z \sin\gamma + P_{xy}\cos\gamma}{P_z \cos\gamma - P_{xy}\sin\gamma} = \tan\eta \quad \text{.....(6.5)}$$

where,

μ = Kinetic coefficient of friction

η = Mean angle of friction at the rake surface

Frictional force and normal force that are working on the flank face are calculated by

$$\left.\begin{aligned} F_r &= C_1(BHN)\frac{t}{\cos\varphi} \\ N_r &= C_2(BHN)\frac{t}{\sin\varphi} \end{aligned}\right\} \quad \text{.....(6.6)}$$

where,

C_1 ,C_2 = Constant

BHN = Hardness of tungsten carbide

t = Depth of cut

φ = Principle cutting edge angle

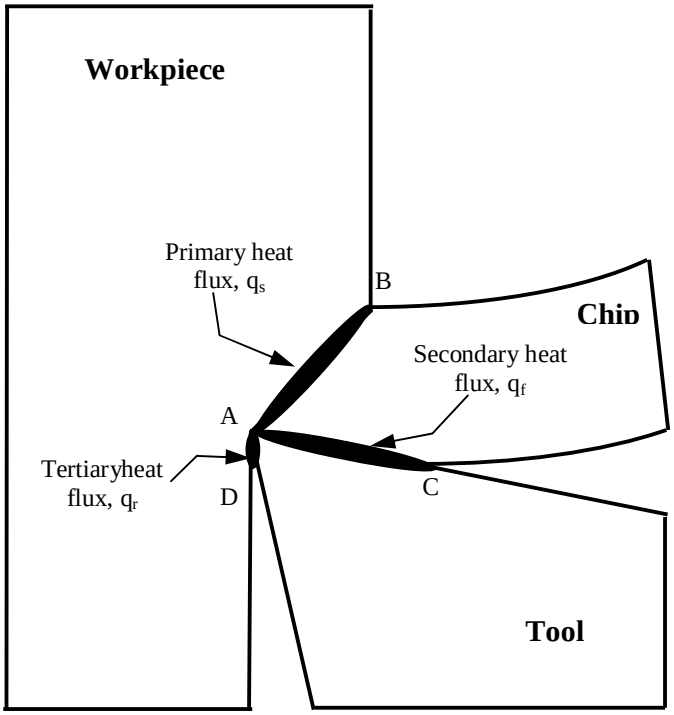

Fig.6.10 Thermal loads in metal cutting

Thermal load in metal cutting can be calculated using experimental force data and the experimental cutting condition data. The concentrated shear heat flux that is applied as thermal load is calculated by

$$q_s = \frac{F_s V_s}{b L_{sh}} \quad \text{.....(6.7)}$$

where,

q_s = Shear plane/ primary heat flux in W/m^2

F_s = Shear force

V_s = Shear velocity

b = Width of cut

L_{sh} = Shear length

Frictional heat flux is derived by the following equation,

$$q_f = \frac{F_f V_f}{bC_N} \quad \text{.....(6.8)}$$

where,

q_f = Frictional/ secondary heat flux

F_f = Frictional froce

V_f = Chip velocity

b = Width of cut

C_N = Chip-tool contact length

Tertiary heat flux can be calculated as,

$$q_r = \frac{F_r V_C}{bL_{VB}} \quad \text{.....(6.9)}$$

where,

q_r = Rubbing/ tertiary heat flux

F_r = Rubbing force

V_C = Cutting velocity

b = Width of cut

L_{VB} = Flank wear length

The quantity C_N and L_{sh} can be calculated by using Eq. (4.4) and Eq. (4.5). The different heat generations in the cutting zones for dry and high-pressure coolant conditions are conveyed by the measured cutting forces which represent the lubricating effect in different circumstances. With the oil lubrication, the measured cutting forces in high-pressure coolant machining are expected smaller than those in dry cutting. The secondary

and the tertiary heat flux are stationary and the primary heat flux moves continuously at a velocity which is called shear velocity. Fig.6.11 shows the mechanical and thermal loads applied in ABAQUS/Standard.

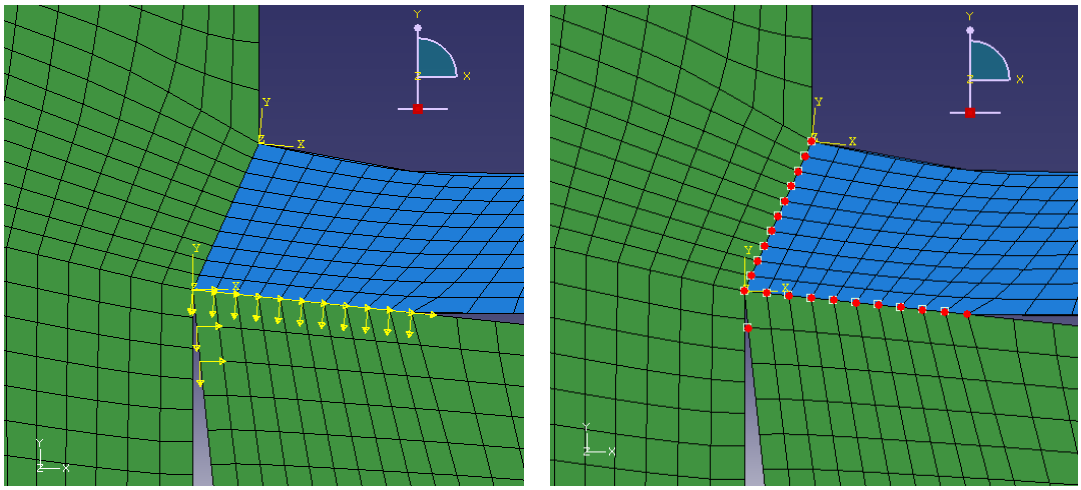

Fig.6.11 Mechanical and thermal loads applied in the model

6.2.8 Creating an Analysis Job & Running the Analysis

After configuring analysis, a job was created that is associated with the model. Before running the simulation, a data check analysis is necessary, because there may have some errors in the model for incorrect or missing data. However, it is possible to combine the data check and analysis phases of the simulation by setting the Job Type to Full analysis. So, a full analysis type job was created and submitted for analysis.

6.2.9 Postprocessing with Abaqus/CAE

Graphical postprocessing is important because of the great volume of data created during a simulation. When the job completes successfully, the results of the analysis can be viewed with the Visualization module of Abaqus/Viewer graphically using a variety of

methods, including deformed shape plots, contour plots, vector plots, animations, and X–Y plots.

6.3 Finite Element Modeling Results

The finite element analysis provided distribution of temperature assuming steady state heat transfer in the work piece, chip and tool. Such analyses have been carried out for different combinations of speed and feed when turning AISI 1060 steel by uncoated carbide insert under HPC condition. By the visualization module of Abaqus/Viewer the analysis results is viewed. Fig.6.12 shows the FEM results in terms of nodal temperature distribution.

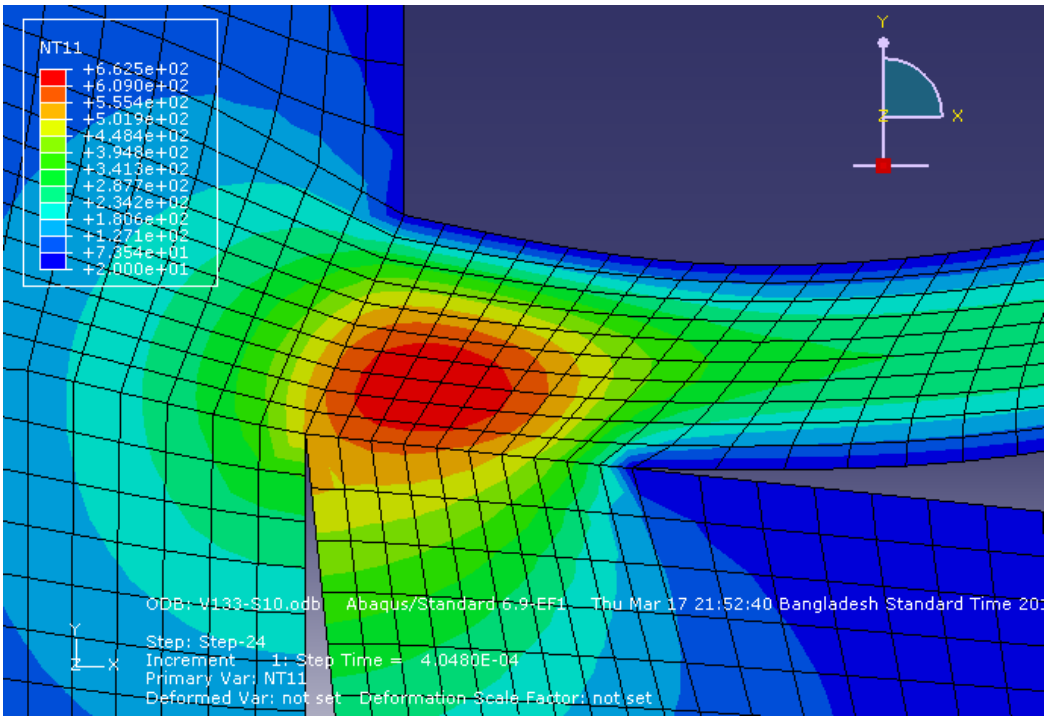

Fig.6.12 Pattern of temperature distribution in work piece, chip and tool in turning AISI 1060 steel by SNMM insert under HPC condition

In Fig.6.13 shows that the pattern of estimated temperature distribution in the work piece, chip and cutting tool is quite similar for all the cases but the values of

temperature are different for different cases. It clearly appears from the figure that compared to chip-tool interface temperature the shear plane temperature has all along been much less average values.Temperature distribution can help us to know the highest temperature zone that means high heat affected zone in the chip-tool interface.

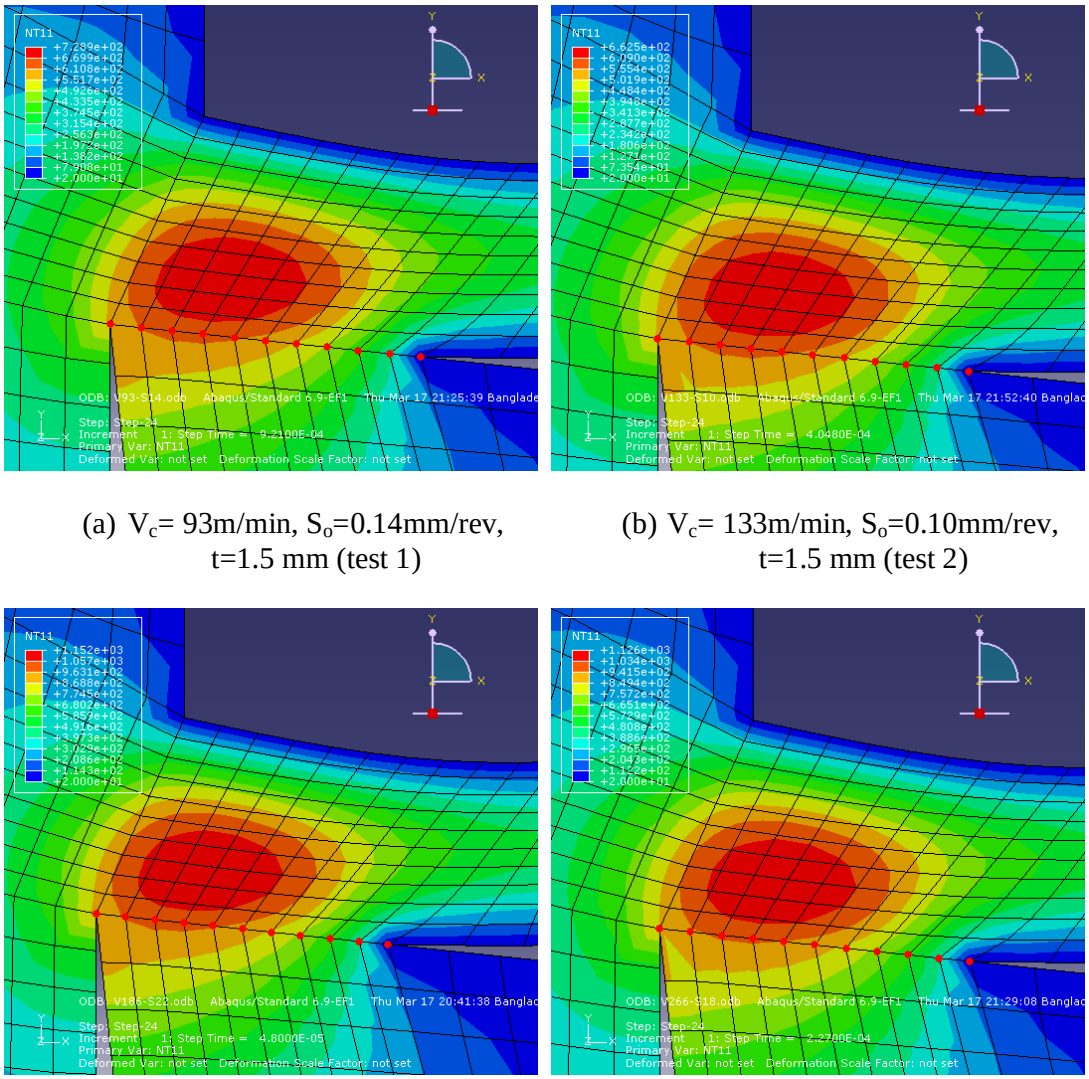

(a) V_c= 93m/min, S_o=0.14mm/rev, t=1.5 mm (test 1)

(b) V_c= 133m/min, S_o=0.10mm/rev, t=1.5 mm (test 2)

(c) V_c=186m/min, S_o=0.22mm/rev, t=1.5 mm (test 3)

(d) V_c= 266m/min, S_o=0.18mm/rev, t=1.5 mm (test 4)

Fig.6.13 Temperature distribution in work piece, chip and tool in turning AISI 1060 steel by SNMM insert under HPC condition at different cutting conditions

Average chip-tool interface temperature have been determined from the temperature distribution and plotted against the measured value. Fig.6.14 shows a far better agreement of predicted data with the measured value.

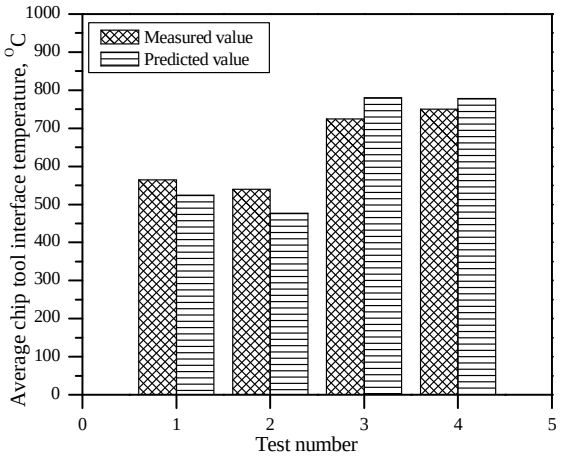

Fig.6.14 Comparison of measured and predicted average chip-tool interface temperature for different tests when turning AISI 1060 steel by SNMM insert under HPC condition

Chapter-7

Discussion on Results

7.1 Cutting Temperature

With the increase in V_c, S_o and t generally cutting zone temperature increases due to increased energy input and it could be expected that high-pressure coolant would be more effective at higher values of V_c, S_o and t. The average chip-tool interface temperature (θ) has been plotted against cutting speed for different work-tool combinations, feed rates and environments undertaken. Fig.3.7. and Fig.3.8 is showing how and to what extent θ has decreased due to high-pressure coolant application under the different experimental conditions. With the increase in V_c, S_o and t, θ increased as usual, even under high-pressure coolant condition cutting temperature shows the similar trend. Under high-pressure coolant condition cutting temperature reduced for all the cases but in different degree.

Temperature is drastically reduced under low speed-feed condition and apparently a small reduction is observed under high speed-feed condition. Even such apparently small reduction in the cutting temperature is expected to have some favorable influence on other machinability indices. With the increase in cutting velocity, plastic contact is increased and made the jet less effective to enter into the interface. Due to this, temperature reduction rate is lower under high speed-feed condition.

The effect of HPC jet on machining performance is always dominant over machining under dry condition due to internal mechanics of HPC jet. As HPC jet is pressurized enough to gain huge velocity, it is able to penetrate in the chip-tool interface zone thus reducing chip-tool contact length resulting lower values of frictional co-efficient due to less sliding contact. It can be stated undoubtedly that cutting temperature is greatly influenced by the changes of cutting process parameters and environment. Changing any of the variables among cutting speed, feed, depth of cut, coolant pressure and flow rate of HPC jet enables the variation of cutting temperature at the chip tool interface.

The difference of color and shape of the chip when turning under both dry and HPC conditions can be correlated with the cutting zone temperature. Fig.3.3 shows that the back surface of the chips appeared much brighter and smoother and the colour have also become much lighter i.e. metallic or golden from blue when turning under HPC condition which indicates that the amount of reduction of temperature due to high-pressure coolant enabled favourable chip-tool interaction and elimination of even trace of built-up edge formation.

Fig.3.9 shows the variation of average chip tool interface temperature with machining time at different speed-feed combinations when machining under high-pressure coolant condition. It is very clear from the graph that level of cutting temperature varies slightly due to rubbing heat source during turning at the work tool interface. Average cutting temperature is the ultimate outcome of heat generated at shear plane, chip-tool interface and work-tool interface. For a particular speed, feed condition, heat generation at shear plane and at the chip tool interface are expected to be constant. For as the time progresses, due to the development of wear land at the tool flank face, cutting temperature may shift upward.

There are several analytical methods to predict the mean temperature. In turning, nearly all of energy dissipated in plastic deformation is converted into heat that in turn raises the temperature in the cutting zone. In the analytical studies, empirical correlations have been used to determine heat generation and cutting zone temperature. Fig.4.13 and Table 7.1 shows the comparison of measured and predicted average chip-tool interface temperature for different tests when turning AISI 1060 steel by SNMM insert under HPC condition. In the model the tool is considered as sharp with no rubbing heat source. But in real case, tool cannot remain sharp during cutting. The predictive values show a good agreement with the measured value with some deviation.

Table 7.1 % error for the cutting temperature prediction

Test No.	V_c (m/min)	S_o (mm/rev)	t (mm)	Measured cutting temperature(^oC)	Predicted cutting temperature (^oC)	% error
1	93	0.10	1.5	498	451	9
2	93	0.14	1.5	564	570	1
3	93	0.18	1.5	600	689	14
4	93	0.22	1.5	650	741	14
5	133	0.10	1.5	540	464	14
6	133	0.14	1.5	610	574	6
7	133	0.18	1.5	640	659	3
8	133	0.22	1.5	660	709	7
9	186	0.10	1.5	610	530	13
10	186	0.14	1.5	670	581	13
11	186	0.18	1.5	700	645	8
12	186	0.22	1.5	724	696	4
13	266	0.10	1.5	665	580	13
14	266	0.14	1.5	720	632	12
15	266	0.18	1.5	750	681	9
16	266	0.22	1.5	765	753	2

For the high speed the predicted temperature is smaller than the experimental value and the differnce between them is more than any other cutting condition. The deviation may be attributed mainly to the assumption that the entire cutting energy is converted into heat but in actual case a small fraction of cutting energy remains frozen in the chip as residual strin and its percentage is different for different V_c-S_o-t combinations. As the measured and predicted data of the average chip-tool interface temperature are almost same then it can be concluded that the model is authentic enough to be used for other machining condition for predicting the average chip-tool interface temperature.

By the tool-work thermocouple technique cutting temperature can be measured and from the analytical model cutting temperature can also predicted accurately but these methods are limited to measurement or predict the average cutting temperature. Hence, finite element modeling has been assential for determining the distribution of temperature in the cutting zoneunder HPC condition.

In Fig.6.12 and Fig.6.13 the distribution of the cutting zone temperature is shown. It can be observed that more heat is transferred to the chip and tool areas with the maximum temperatures are localized near the chip and tool. The zone with the highest temperature exists near of the vicinity of the chip-tool contact surface (secondary shear zone). The maximum temperature along the chip-tool contact surface has been seen to occur at about 25% of the contact length from the tool tip. The distribution in the tool shows that a high-temperature gradient is also observed near the tool tip and contact zone.

Fig.6.14 shows that the values of the average chip-tool interface temperature predicted by the model are in adequately close agreenment with their measured value. Concerning the convergence, the accuracy of the finite element technique depends on the

size of the mesh. The smaller meshes produce more accurate result but for that case the computation time is higher.

7.2 Cutting Force

P_z is the major component, which also decides power consumption. For machining conventional materials producing continuous chips the main cutting force is a function of S_o, t, τ_s, ξ and γ. Fig.3.4 and Fig.3.5 clearly show that throughout the present experiment, the value of ξ usually decreases with the increase in V_c under both dry and high-pressure coolant conditions particularly at its lower range due to plasticization and shrinkage of the shear zone for reduction in friction and built-up edge formation at the chip-tool interface due to increase in temperature and sliding velocity. Eq. (4.23) indicates that for the same chip load the magnitude of the cutting forces are governed mainly by the value of ξ. According to Eq. (4.24) and Eq. (4.6), the value of τ_s also decreases, though in lesser degree, with the decrease in ξ. But τ_s may also increases to some extent with the increase in V_c due to softening of the work material by cutting temperature, particularly if it is very high for the work material. From Fig.3.10 and Fig.3.11 shows that the cutting force component, P_z has gradually decreased with the increase in V_c almost in the same way the value of ξ decreased. Therefore, it can be concluded that the main reasons behind decrease in cutting forces with the increase in V_c are that which cause decrease in ξ with increase in V_c.

It is also noted in Fig.3.4 and Fig.3.5 that ξ decreased all along also with the increase in S_o (i.e. uncut chip thickness). It is interesting and important to note that though apparently and according to Eq. (4.23) the magnitude of P_z should increase proportionally with the increase in feed, S_o but actually the rate of increase of P_z with that of S_o has been

much less as can be seen in Fig.3.10 and Fig.3.11. This can be attributed mainly to decrease in ξ with the increase in S_o for increase in average effective rake angle of the tool with the increase in uncut chip thickness. Ultimately, it can be clearly stated that, cutting force is greatly influenced by the behaviour of chip reduction coefficient, cutting speed, feed, depth of cut, effective rake angle, average cutting strain, and percentage elongation due to thermal softening.

Fig.3.10 and Fig.3.11 also show that the cutting force reduces with the application of HPC coolant jet. This can be explained by the fact that HPC coolant deliberately reduce the generation of cutting temperature and the lubrication property of oil used by HPC jet reduce the friction co-efficient that works between the flank surface of the cutting tool and work piece material resulting less cutting force compared to dry machining.

Statistical modeling of the main cutting force has been done by using some experimental data. The predictive model can be used to predict the respose parameter within the range of experimental data cutting parameter. From Fig.5.1 and Fig.5.2, it can be dicided that since there is significant interaction effect of the variables on the response cutting force, first order model is not formulated to predict the cutting force.

The second order model predicted for obtaining the relationship between the cutting force and the machining independent variables has the correlation coefficient of 96.98% which indicates that the equation is able to predict the cutting force values with 96.98% accuracy. The P-values are used to determine which of the effects in the model are statistically significant. The α value is assumed as 0.05. From Table 5.2, it can be clearly stated that, linear, square and the interaction effects of the cutting process variables are statistically significant since their P-values are less than 0.05.

Fort the non-linear mathematical model the regression co-efficient for analysis has been found as 98.2% which indicates that the equation is able to predict the cutting force values with 98.2% accuracy. The α value is assumed as 0.05 and from the Table 5.4 it is clear that the P-value, which is used to determine the model significance, is less than the α value.

The check of the normality assumptions of the data is conducted; it can be seen in Fig.5.3(a) [for second order equation] and Fig.5.4(a) [for non-linear equation] that all the points on the normal plot come to close to forming a straight line. This implies that the data are fairly normal and there is a no deviation from the normality. Notice that the residuals are falling on a straight line, which means that the errors are normally distributed. In addition, Fig.5.3(b) [for second order equation] and Fig.5.4(b) [for non-linear equation] illustrates that there is no noticeable pattern or unusual structure in residual VS fitted value plot. This implies that the proposed second order model and the non-linear equation model are adequate to illustrate the pattern of the cutting force.

Predicted values from two models have been plotted and compared with the measured values in Fig.5.5, Fig.5.6 and Table 7.2. From these figures both the model can predict the trend of the measured value. The second order model cannot predict the cutting force at high speed accurately but for all the cases the non-linear model can predict cutting force accurately with very small error.

Table 7.2 % error for the cutting force prediction

Test No.	V_c (m/min)	S_o (mm/rev)	t (mm)	Measured cutting force (N)	Predicted cutting force (N)		% error	
					second order model	non-linear model	second order model	non-linear model
1	93	0.10	1.0	410	380	406	7	0.8
2	186	0.10	1.0	358	303	361	15	1
3	133	0.14	1.0	468	441	468	6	0
4	266	0.14	1.0	426	321	416	24	2
5	93	0.18	1.0	570	558	579	2	1.6
6	186	0.18	1.0	532	467	515	12	3
7	133	0.22	1.0	605	580	615	4	1.7
8	266	0.22	1.0	560	440	547	21	2
9	93	0.10	1.5	440	434	444	1.5	0.8
10	186	0.10	1.5	387	337	395	13	2
11	133	0.14	1.5	515	490	512	4	0.5
12	266	0.14	1.5	470	341	455	27	3
13	93	0.18	1.5	680	620	633	8	7
14	186	0.18	1.5	558	509	563	8	1
15	133	0.22	1.5	650	638	672	2	3.5
16	266	0.22	1.5	580	469	598	19	3

Chapter-8

Conclusions and Recommendations

8.1 Conclusions

The aim of the present research work is to develop predictive models of cutting temperature and cutting force while turning AISI 1060 steel by uncoated carbide insert (SNMM 120408) under HPC condition. Modeling of the cutting temperature has been done by analytical approach as well as finite element modeling (FEM) by ABAQUS/CAE 6.9. On the other hand, main cutting force has been studied and analyzed to correlate with cutting process variables such as cutting speed, feed rate and depth of cut. Experimental value of chip reduction coefficient, cutting temperature and cutting force is taken for validity test of cutting temperature and cutting force as well as for deriving some input variable for the predictive model.

Based on the research work the following conclusions can be drawn:

i. Chip shape and colour for AISI 1060 steel is studied. When machined under high-pressure coolant condition the color and shape of the chip indicates the amount of reduction of temperature due to high-pressure coolant enabled favourable chip-tool interaction and elimination of even trace of built-up edge formation.

ii. Chip reduction co-efficient ξ has a proportional relation with the cutting force theoretically. So, the lower value of chip reduction co-efficient is better. Controlling coolant pressure and flow rate of HPC jet, effective lubrication can be carried out resulting more reduced friction at the interface zone and thus lower values of ξ can be obtained as desired. The reduction is between 5 and 11% for the ξ for different V_c-S_o-t combinations.

iii. Cutting temperature is found to be proportional with cutting speed, feed rate and depth of cut. High pressure coolant application reduces this high cutting temperature when compared to dry cutting. The reduction is between 9 and 16.5 % for the average chip-tool interface temperature for different V_c-S_o-t combinations. For as the time progresses, due to the development of wear land at the tool flank face, cutting temperature may shift upward, while speed, feed, depth of cut, pressure and flow rate of HPC jet are constant. But this transient character is found to be not significant to a considerable extent. Approximately 7% variation has been observed in cutting temperature values as time progresses.

iv. The trends of cutting forces can be increasing or decreasing with the increase of cutting process parameters. This behaviour solely depends on the range of cutting process variables that are considered as experimental condition of a particular research. In this present research work, main cutting force found to decrease with the increase of speed, and cutting forces increases with the increase of feed and depth of cut. The reduction is between 7 and 17% for the cutting force for different V_c-S_o-t combinations.

v. From the analytical model, the cutting temperature can be predicted accurately within error level of 14%.

vi. From the second order model cutting force can be predicted with maximum error of 27% (at high speed) but from the non-linear equation model cutting force can be predicted within 3.5% error.

vii. The maximum temperature along the contact surface is seen to occur at about 25% of the contact length from the tool tip. The distribution in the tool shows that a high-temperature gradient is also observed near the tool tip and contact zone. The variation between the meausred average chip-tool interface temperature with the value obtained by FEM is from 3 to 11% for some specific cases.

8.2 Recommendations

i. For the experimental part, three variables such cutting velocity, feed rate and the depth of cut are considered for getting the response parameter. This research work can be extended by increasing the variable. The new variable may be the HPC processs parameter such as pressure and flow rate of the jet.

ii. In this research, analytical modelling of cutting temperature has been developed for a particular tool work combination. The model can be strengthened by introducing hardness ratio of tool material and work material, if experimental data can be taken for several tool work combination. Another modification of the analytical model can be the

model with wear out tool. In that method a rubbing heat source (tertiary) need to be considered at the surface of the zone, where the clearance face of the tool rubs the newly machined surface deformation can occur.

iii. The parameter of the HPC jet such flow rate of the cutting oil and the outlet pressure of the jet have significant effect on cutting temperature and cutting force. In the present work these factors are not studied. So, these factors can be studied experimentally in future by doing the experimnt with different pressure and flow rate of the HPC jet. Then the predictive equation for the cutting force and temperature can be derived with the cutting variables and the HPC variables.

iv. In the finite element modelling in ABAQUS/CAE, a fixed metal cutting model is drawn and from the help of some experimental data heat generation and forces is calculated and is applied on the model to determine the temperature distribution in the cutting zone. A chip formation model can be developed where the work piece and tool material property need to be asssigned and the interaction between the tool and work piece need to be defined. Then the chip is automatically formed when a relative velocity between the tool and the workpiece is given. All the response such as cutting temperature, force, stress, strain distribution can be observed after completing the analysis.

References

Al-Ahmari, A.M.A., 2007, "Predictive Machinability Models for a Selected Hard Material in Turning Operations", Journal of Materials Processing Technology, Vol.190(1-3), pp.305-311.

Aly, M.F., Ng, E.-G. and Veldhuis, S.C., 2004, "Cutting Force Prediction Using A Molecular Dynamic Assisted Finite Element Simulation Model", ASPE Proceedings, Orlando, Florida.

Aronson, R.B., 1995, "Why Dry Machining?" Manuf. Eng., pp. 33–36.

Attia M.H. and Kops L., 2004, "A New Approach to Cutting Temperature Prediction Considering the Thermal Constriction Phenomenon in Multi-Layer Coated Tool", CIRP Annals - Manufacturing Technology, Vol. 53(1), pp. 47-52.

Aykut, S., Gölcü, M., Semiz, S. and Ergür, H.S., 2007, "Modeling of Cutting Forces as Function of Cutting Parameters for Face Milling of Satellite 6 Using an Artificial Neural Network", J. of Mat. Processing Technology, Vol. 190(1-3), pp. 199-203.

Bagci, A., 1973, “Prediction of Shear Plane in Machining From Work Material Strain-Hardening Characteristics”, Journal of Eng. For Ind. Trans. ASME, Vol. 105(2), pp.129-131.

Bailey, J.A. and Bhavandia, D.G., 1973, “Correlation of Flow Stress with Strain Rate and Temperature during Machining”, J. of Eng. for Ind. Trans. ASME, pp. 94-98.

Bao, W.Y. and Tansel, I., 2000, “Modeling Micro End Milling Operations, Part I: Analytical Cutting Force Model”, International Journal of machine tool and manufacture, Vol. 40, pp. 2155-2173.

Bareggi, A., O’Donnell, G.E. and Torrance, A., 2007, “Modelling Thermal Effects in Machining by Finite Element Methods”, Proceedings of the 24th International Manufacturing Conference, Vol. 1, pp. 263-272.

Barrow, G., 1973, “A Review of Experimental and Theoretical Techniques for Assessing Cutting Temperatures”, Ann. CIRP, Vol. 22(2), pp. 203–211.

Beaubien S.J. and Cattaneo A.G., 1964, “A Study of the Role of Cutting Fluid in Machining Operating”, Lubrication Engineering, Vol.10, pp. 74-79.

Bennett, E.O. and Bennett, D.L., 1985, “Occupational Air Way Diseases in the Metal-Working industry”, Tribology International, Vol. 18(3), pp. 169-176.

Bever, M.B.,Marshall, E.R. and Ticknor,L.B. , 1953, “ The Energy Stored in Metal Chips During Ortogonal Cutting”, J.Appl. Phys., Vol. 24, pp. 1176-1179.

Black, J.T., 1979, “Flow Stress Model in Metal Cutting”, Journal of Eng. for Ind. Trans. ASME, Vol. 104(4), pp. 403-415.

Blok, H., 1938, “Theoretical Study of Temperature Rise at Surface of Actual Contact under Oiliness Lubricating Conditions”, Proceedings of General Discussion on Lubrication and Lubricants, Institution of Mechanical Engineers, pp. 222–235.

Bono, M. and Ni, J., 2002, “A Model for Predicting the Heat Flow into the Workpiece in Dry Drilling”, Journal of Manufacturing Science and Engineering, Vol. 124(4) pp.773-777.

Boothroyd, G., 1963, “Temperatures in Orthogonal Metal Cutting”, Proceedings of the Institution of Mechanical Engineers, Vol. 177 (29), pp. 789–803.

Boothroyd, G., 1988, “Fundamental of Metal Machining and Machine Tool”, Scripta Book Company, New York.

Bouzid, W., Zghal, A.and Ben Ayed, K., 2004, “Carbide and Ceramic Tool Life in High Speed Turning”, International Journal of Vehicle Design, Vol.39 (1-2), pp.140-153.

Campbell, J.D., 1973, “Dynamic Plasticity: Macroscopic and Microscopic Aspects”, Material science and engineering, Vol. 27(2), pp. 3-21.

Carslaw, H.S. and Jaeger, J.C., 1959, “Conduction of Heat in Solids”, Oxford University Press, Oxford.

Carvalho, S.R., Lima, E., Silva, S.M.M., Machado, A.R., and Guimaraes, G., 2006, “Temperature Determination at the Chip-Tool Interface using an Inverse Thermal Model Considering the Tool and Tool Holder”, Journal of Materials Processing Technology, Vol. 179(1-3), pp. 97-104.

Chao, B.T. and Trigger, K.J., 1953, “The Significance of the Thermal Number in Metal Cutting”, Trans. ASME, Vol. 75, pp. 109–120.

Chao, B.T. and Trigger, K.J., 1955, “Temperature Distribution at The Tool–Chip Interface in Metal Cutting”, Trans. ASME, Vol. 77(2), pp. 1107–1121.

Chao, B.T. and Trigger, K.J., 1958, “Temperature Distribution at Tool–Chip and Tool–Work Interface in Metal Cutting”, Trans. ASME, Vol. 80(1), pp. 311–320.

Chattopadhyay, A.K. and Chattopadhyay, A.B., 1982, “Wear and Performance of Coated Carbides and Ceramic Tools”, Wear, Vol.80, pp.239-253.

Childs, T.H.C., Maekawa, K., Obikawa, T., and Yamane, Y., 2000, “Metal Machining: Theory and Applications”, New York: John Wiley & Sons Inc.

Cozzens, D.A., Olson, W.W., Sutherland, J.W., and Panetta, J.M., 1995, “An Experimental Investigation into the Effect of Cutting Fluid Conditions on the Boring of Aluminum Alloys”, Concurrent Product and Process Engineering, ASME Bound Volume - MED Vol. 1/DE Vol. 85, pp. 251-257.

Crafoord, R., Kaminski, J., Lagerberg, S., Ljungkrona, O. and Wretland, A. , 1999, “Chip Control in Tube Turning using a High-Pressure Water Jet”, Proceedings of the Institution of Mechanical Engineers, Part B, Vol. 213, pp.761–767.

da Silva, M.B. and Wallbank, J., 1999, “Cutting Temperature: Prediction and Measurement Methods-A Review”, Journal of Materials Processing Technology, Vol. 88, pp. 195–202.

Dahlman, P. and Escursell, M., 2004, “High-Pressure Jet-Assisted Cooling: A New Possibility for Near Net Shape Turning of Decarburized Steel”, International Journal of Machine Tools & Manufacture, Vol. 44, pp. 109–115.

Dahlman, P., 2002, “A Comparison of Temperature Reduction in High-Pressure Jet-Assisted Turning using High Pressure Versus High Flowrate”, Proceedings of the Institution of Mechanical Engineers, Part B: Journal of Engineering Manufacture, Volume 216(4), pp. 467-473.

Davies, M.A., Chou, Y. and Evans, C.J., 1996, “On Chip Morphology, Tool wear and Cutting Mechanics in Finish Hard Turning”, Annals of CIRP, Vol. 45(1), pp.77-82.

Davim, J.P., 2003, “Study of Drilling Metal-Matrix Composites Based on the Taguchi Techniques”, J. Materials Processing Technology, Vol. 132, pp. 250-254.

Dawson, P.R. and Malkin, S., 1984, “Inclined Moving Heat Source Model for Calculating Metal Cutting Temperatures”, Trans. ASME, J. Engng for Industry, Vol. 106(3), pp. 179–186.

Dhar, N.R. and Kamruzzaman, M., 2007, “Cutting Temperature, Tool Wear, Surface Roughness and Dimensional Deviation in Turning AISI-4037 Steel under Cryogenic Condition”, International Journal of Machine Tool and Manufacture, Vol. 47, pp. 754-759.

Dhar, N.R., Paul, S., Chattopadhyay, A.B., 2002, “Role of Cryogenic Cooling on Cutting Temperature in Turning Steel”, Journal of Manufacturing Science and Engineering, vol. 124(1), pp. 146-154.

Dhar, N.R., Rashid, M.H. and Siddiqui, A.T., 2006, “Effect of High-Pressure Coolant on Chip, Roundness Deviation and Tool Wear in Drilling AISI-4340 Steel”, ARPN Journal of Engineering and Applied Sciences, vol. 1(3), pp. 53-59.

Dhar, N.R., Siddiqui1, A.T. and Rashid, M.H., 2006, “Effect of High Pressure Coolant Jet on Grinding Temperature, Chip and Surface Roughness in Grinding AISI-1040 Steel”, ARPN Journal of Engineering and Applied Sciences, Vol. 1(4), pp. 22-28.

Elanayar, S.V.T. and Shin, Y.C., 1996, “Modeling of Tool Forces for Worn Tools: Flank Wear Effects”, Transaction of ASME, Journal of Manufacturing Science and Engineering, Vol. 118 (3), pp. 359–366.

Endrino, J.L., Fox-Rabinovich G.S. and Gey C., 2006, “Hard AlTiN, AlCrN pvd Coatings for Machining of Austenitic Stainless Steel”, Surface and Coatings Technology, Vol. 200 (24), pp. 6840-6845.

Ezugwu, E.O. and Bonney, J., 2003, “Effect of High-Pressure Coolant Supply when Machining Nickel-Base, Inconel 718, Alloy with Coated Carbide Tools”, International Conference on Advances in Materials and Processing Technologies (AMPT), Dublin City University, Dublin, Republic of Ireland, pp. 787–790.

Ezugwu, E.O. and Bonney, J., 2004, “Effect of High-Pressure Coolant Supply when Machining Nickel-Base, Inconel 718, Alloy with Coated Carbide Tools”, Journal of Materials Processing Technology, Vol. 153–154, pp. 1045–1050.

Ezugwu, E.O. and Bonney, J., 2004, “Effect of High-Pressure Coolant Supply when Machining Nickel-Base, Inconel 718, Alloy with Coated Carbide Tools”, Journal of Materials Processing Technology, Vol. 153–154, pp. 1045–1050.

Ezugwu, E.O. and Tang, S.H., 1995, “Surface Abuse when Machining Cast Iron (G-17) and Nickel-Base Superalloy (Inconel 718) with Ceramic Tools”, Journal of Materials Processing Technology, Vol. 55, pp. 63–69.

Ezugwu, E.O., Machado, A.R., Pashby, I.R. and Wallbank, J., 1990, “The Effect of High-Pressure Coolant Supply when Machining a Heat-Resistant Nickel-Based Superalloy”, Journal of Tribology and Lubrication Engineering, Vol. 47(9), pp.751–757.

Ezugwua, E.O., Bonney J., Fadare D.A. and Sales, W.F., 2005, “ Machining of Nickel-Base, Inconel 718, Alloy with Ceramic Tools under Finishing Conditions with Various Coolant Supply Pressures”, Journal of Materials Processing Technology, Vol.162–163, pp. 609–614.

Gökkaya, H.,Şeker,U.,and İzciler, M., 2001, “The Review of Experimental Methods to Measure the Generated Heat at the Tool-Workpiece İnterface, and the Evaluation of the Experimental Results Using Different Metods ”, MATIT, pp. 91-105.

Gonzalo O., Jauregi H., Uriarte L.G. and López de Lacalle, L.N., 2009, “Prediction of Specific Force Coefficients from a FEM Cutting Model”, The International Journal of Advanced Manufacturing Technology, Vol. 43(3/4) , pp. 348-356.

Grzesik W. and Nieslony, P., 2003, “A Computational Approach to Evaluate Temperature and Heat Partition in Machining with Multilayer Coated Tools”, International Journal of Machine Tools and Manufacture, Vol. 43(13), pp. 1311-1317.

Grzesik W. and Nieslony, P., 2004, “Physics Based Modelling of Interface Temperatures in Machining with Multilayer Coated Tools at Moderate Cutting Speeds”, International J. of Machine Tools and Manufacture, Vol. 44(9) , pp. 889-901.

Grzesik W., 2006, “Determination of Temperature Distribution in The Cutting Zone using Hybrid Analytical-FEM Technique”, International journal of machine tools & manufacture , Vol. 46(6), pp. 651-658.

Grzesik, W. and Bartoszuk,M., 2009, “Prediction of Temperature Distribution in the Cutting Zone using Finite Difference Approach”, International Journal of Machining and Machinability of Materials (IJMMM),Vol. 6 (1/2), pp .43 – 53.

Grzesik, W., Bartoszuk, M. and Niesłony, P., 2005, “Finite Element Modelling of Temperature Distribution in the Cutting Zone in Turning Processes with Differently Coated Tools”, Proc. of 13th International Scientific Conference on Achievement in Mechanical and Materials Engineering, pp. 259-262.

Hahn, R.S., 1951, “On the Temperature Developed at the Shear Plane in the Metal Cutting Process”, Proc. of First US National Congress of Applied Mechanics, pp.661-666.

Hasçalık A. and Çaydaş U., 2008, “Optimization of Turning Parameters for Surface Roughness and Tool Life Based on the Taguchi Method”, Int. Journal of Advanced Manufacturing Technology, Vol. 38, pp. 896–903.

Hu, J., Song, H. and Chou, Y.K., 2008, “3D Cutting Force Analysis in Worn-Tool Finish Hard Turning”, International Journal of Machining and Machinability of Materials, Vol. 4(1), pp. 3-13.

Huang, Y. and Liang, S.Y., 2003, “Cutting Forces Modeling Considering the Effect of Tool Thermal Property—Application to CBN Hard Turning”, International Journal of Machine Tools & Manufacture, Vol. 43(3), pp. 307–315.

Huang, Y. and Liang, S.Y., 2003, “Modelling of the Cutting Temperature Distribution under the Tool Flank Wear Effect”, Journal of mechanical engineering science, Vol. 217(11), pp. 1195-1208

Huang, Y. and Liang, S.Y., 2004, “Modeling of CBN Tool Flank Wear Progression in Finish Hard Turning”, ASME Journal of Manufacturing Science and Engineering, Vol. 126 (1), pp. 98–106.

Huang, Y. and Liang, S.Y., 2005, “Cutting Temperature Modeling Based on Non-Uniform Heat Intensity and Partition Ratio”, Machining Science and Technology. Vol. 9(3), pp. 301-323.

Ibraheem, A.F., Shather, S.K. and Khalaf, K.A., 2008, “Prediction of Cutting Forces by using Machine Parameters in end Milling Process”, Eng.&Tech., Vol.26(11).

Jaeger, J.C., 1942, “Moving Sources of Heat and the Temperatures at Sliding Contacts”, Proc. R. Soc. NSW, Vol. 76, pp. 203–224.

Jen, T.C. and Lavine, A.S., 1994, “Prediction of Tool Temperatures in Cutting”, Proceedings of the Seventh International Symposium on Transport Phenomena in Manufacturing, pp. 211–216.

Jian, L. and Hongxing, L., 2003, “Modeling System Error in Batch Machining Based on Genetic Algorithms”, International Journal of Machine Tools & manufacture, Vol. 43(6), pp. 599-604.

Jiao, Y., Lei, S., Pei Z.J. and Lee, E.S., 2004, “Fuzzy Adaptive Networks in Machining Process Modeling: Surface Roughness Prediction for Turning Operations”, International Journal of Machine Tools & Manufacture, Vol. 44, pp. 1643-1651.

Junz Wang, J.-J. and Zheng, C.M., 2002, “An Analytical Force Model with Shearing and Ploughing Mechanisms for End Milling”, International Journal of Machine Tools and Manufacture, Vol. 42, pp. 761-771.

Kaminski J., Alvelid B., 2000, “Temperature Reduction in The Cutting Zone in Water-Jet Assisted Turning”, J. of Mat. Processing Technology, Volume 106(1), pp. 68-73.

Kato, T. and Fujii, H., 1996, “PVD Film Method for Measuring the Temperature Distribution in Cutting Tools”, Trans. ASME, J. Engng for Industry, Vol. 118, pp. 117–122.

Khan A. A. and Ahmed M. I., 2008, “Imporving Tool Life using Cryogenic Cooling”, Journal of Materials Processing Technology, Vol. 196, pp. 149-154.

Khidhir, B.A., Mohamed B. and Younis, M.A.A., 2010, “Modification Approach of Fuzzy Logic Model for Predicting of Cutting Force When Machining Nickel Based Hastelloy C-276”, American J. of Engineering and Applied Sciences, Vol. 3 (1), pp.207-213.

Kienzle, O. and Victor, H., 1957, “Spezifische Shnittkraefte Bei Der Metall-Bearbeitung”, Werkstattstehnik und Maschinenbau, Bd. 47, H.5.

Kim, K.W., Lee, W.Y. and Sin, H., 1999, “A Finite Element Analysis for the Characteristics of Temperature and Stress in Micro-Machining Considering the Size Effect”, International Journal of Machine Tools & Manufacture, Vol. 39 (9), pp. 1507–1524.

Kitagawa, T., Kubo, A. and Maekawa, K., 1997, “Temperature and Wear of Cutting Tools in High Speed Machining of Inconel 718 and Ti-6V-2Sn”, Wear, Vol. 202, pp.142.

Kline, W.A., and DeVor, R.E., 1983, “The Effect of Run-Out on Cutting Geometry and Forces”, IJMTDR, Vol. 23(l), pp. 123-140.

Kline, W.A., DeVor, R.E., and Lindberg, J.R., 1982, “The Prediction of Cutting Forces in End Milling with Application to Concerning Cuts”, IJMTDR, Vol. .22(l), pp. 7-22.

Klocke, F., Konig, W. and Gerschwiler, K., 1996, “Advanced Machining of Titanium and Nickel-Based Alloys”, Proceedings of the fourth international conference on Advanced manufacturing systems and technology, pp. 7-21.

Klocke. F., 1997, “Dry Machining”, Annanls of CIRP, Vol. 46 (2), pp. 519–526.

Komanduri, R. and Hou, Z.B., 2000, “Thermal Modeling of the Metal Cutting Process, Part 1: Temperature Rise Distribution due to Shear Plane Heat Source”, Int. J. Mech. Sci., Vol. 42, pp. 1715–1752.

Komanduri, R. and Hou, Z.B., 2001, “Thermal Modeling of the Metal Cutting Process, Part 2: Temperature Rise Distribution due to Frictional Heat Source at the Tool–Chip Interface”, Int. J. Mech. Sci., Vol. 43, pp. 57–88.

Komanduri, R. and Hou, Z.B., 2001, “Thermal Modeling of the Metal Cutting Process, Part 3: Temperature Rise Distribution due to the Combined Effects of Shear Plane Heat Source and the Tool–Chip Interface Frictional Heat Source”, Int. J. Mech. Sci., Vol. 43, pp. 89–107.

Kovacevic, R., Cherukuthota, C. and Mazurkiewicz, M., 1995, “High-Pressure Water Jet Cooling/Lubrication to Improve Machining Efficiency in Milling”, International Journal of Machine Tools and Manufacture, Vol.35 (10), pp.1459–1473.

Kumar, A.S., Rahman, M. and Ng, S.L., 2002, “Effect of High-Pressure Coolant on Machining Performance”, The International Journal of Advanced Manufacturing Technology, Vol. 20(2), pp. 83-91.

Lazoglu , I. and Altintas, Y., 2002, “Prediction of Tool and Chip Temperature in Continuous and Interrupted Machining”, International Journal of Machine Tools & Manufacture, Vol. 42, pp. 1011–1022.

Lee, E.H. and Shaffer, B.H., 1951, “The Theory of Plasticity Applied to a Problem of Machining”, Journal of applied mechanics, Vol. 18, pp. 405–413.

Lee, E.H. and Shaffer, B.W., 1951, “Theory of Plasticity Applied to Problems of Machining”, ASME J. Appl. Mech, Vol. 18 (4), pp. 104–113.

Leonardo, R.S. and Davim, J.P., 2009, “The Effect of Tool Geometry on the Machinability of Polyamide During Precision Turning”, Journal of Composite Materials, Vol. 43(23), 2793-2803.

Li, H.Z. and Li, X.P., 2002, “Milling Force Prediction using a Dynamic Shear Length Model”, Int. Journal of Machine Tools and Manufacture, Vol. 42(2), pp. 277-286.

Li, K.-M. and Liang, S.Y., 2007, “Modeling of Cutting Forces in Near Dry Machining under Tool Wear Effect”, International Journal of Machine Tools and Manufacture, Vol. 47, pp. 1292-1301.

Li, X.P., Nee, A.Y.C., Wong, Y.S. and Zheng, H.Q., 1999, “Theoretical Modeling a Simulation of Milling Force”, J. Mater. Proc. Technol., Vol. 89-90, pp. 266-272.

List, G., Nouari, M., G´ehin, D., Gomez, S., Manaud, J.P., Le Petitcorps, Y. and Girot, F., 2005, “Wear Behavior of Cemented Carbide Tools in Dry Machining of Aluminum Alloy”, Wear, Vol. 259, pp. 1177–1189.

Liu, X.L., Wen, D.H., Li, Z.J., Xiao, L. and Yan, F.G., 2002, “Experimental Study on Hard Turning Hardened GCr15 Steel with PCBN Tool”, Journal of Materials Processing Technology, Vol. 129, pp.217-221.

Lo´pez de Lacalle, L.N., Pe´rez-Bilbatua, J., Sa´nchez, J.A., Llorente, J.I., Gutie´rrez, A. and Albo´niga, J., 2000, “Using High Pressure Coolant in the Drilling and Turning of Low Machinability Alloys”, The International Journal of Advanced Manufacturing, Vol. 16(2), pp. 85–91.

Loewen, E.G. and Shaw, M.C., 1954, “On the Analysis of Cutting Tool Temperatures”, Trans. ASME, Vol. 76, pp. 217–231.

Luo, T., Lu, W., Krishnamurthy, K. and McMillin, B., 1998, “A Neural Network Approach for Force and Contour Error Control in Multi-Dimensional End Milling Operations”, Int. J. Machine Tools and Manufacture, Vol. 38, pp. 1343-1359.

Luttervelt, C.A.van, Childs, T. H.C., Jawahir; I.S., Klocke, F. and Venuvinod, P.K., 1998, “Present Situation and Future Trends in Modelling of Machining Operations”, Annals of the ClRP, Vol. 47(2), pp. 587–626.

Mamalis, A.G., Kundrák, J., Markopoulos, A. and Manolakos, D.E., 2008, “On the Finite Element Modelling of High Speed Hard Turning”, Int J Adv Manuf Technol, Vol. 38, pp. 441–446.

Marusich, T.D. and Ortiz, M., 1995, “Modeling and Simulation of High-Speed Machining”, Int. J. Num. Meth. Eng., Vol. 38, pp. 3675-3694.

Marusich, T.D., 2001, “Effects of Friction and Cutting Speed on Cutting Force”, Proceedings of ASME Congress, New York, pp. 197–204.

Mazurkiewicz, M., Kubula, Z. and Chow, J., 1989, “Metal Machining with High Pressure Water Jet Cooling Assistance-A New Possibility”, J. Eng. Ind., Vol.111, pp. 7-12.

McFeron, D.E., and Chao, B.T., 1958, “Transient Interface Temperatures in Plain Peripheral Milling”, Transactions of ASME, Journal of Engineering for Industry, Vol. 80, pp. 321–329.

Merchant, M.E., 1945, “Mechanics of the Metal Cutting Process, Part 2: Plasticity Conditions in Orthogonal Cutting”, J. Appl. Phys, Vol. 16, pp. 318–324.

Merchant, M.E., 1945, “Mechanics of the Metal Cutting Process”, Journal of applied physics, Vol. 16(5), pp. 267-275.

Montgomery, Douglas C, 2005, “Design and Analysis of Experiments: Response surface method and designs”, New Jersey: John Wiley and Sons, Inc.

Mukherjee, I. and Ray, P.K., 2006, “A Review of Optimization Techniques in Metal Cutting Processes”, Computers & Industrial Engineering, Vol. 50, pp. 15–34.

Muller, C. and Blumke, R., 2001, “Influence of Heat Treatment and Cutting Speed on Chip Segmentation of Age Hardenable Aluminum Alloy”, Material Science and Technology, Vol.17, pp. 651-654.

Nabhani, F., 2001, “Machining of Aerospace Titanium Alloys”, Robotics and Computer Integrated Manufacturing, Vol. 17, pp. 99–106.

Narutaki, N. and Yamane, Y., 1979, “Tool Wear and Cutting Temperatures of CBN Tools in Machining Hardened Steels”, Annals of CIRP, Vol. 28(1), pp.23-27

Ng, E.G., Aspinwall, D.K., Brazil, D., and Monaghan, J., 1999, “Modeling of Temperature and Forces when Orthogonally Machining Hardened Steel”, International Journal of Machine Tools and Manufacture, Vol. 39, pp. 885–903.

Nigm, M.M., Sadek, M.M., and Tobias, S.A., 1977, “Dimensional Analysis of the Steady State Orthogonal Cutting Process”, IJMTDR, Vol. l7(l), pp.l-18.

Obikawa, T. and Usui, E., 1996, "Computational Machining of Titanium Alloy-Finite Element Modeling and a Few Results", Journal of Manufacturing Science and Engineering, Vol. 118(2), pp. 208-215.

Obikawa, T., Sasahara, H., Shirakashi, T. and Usui, E., 1997, "Application of Computational Machining Method to Discontinuous Chip Formation", Journal of Manufacturing Science and Engineering, Vol. 119(4), pp. 667-674.

Otieno, A. and Mirman, C., 2008, "Finite Element Analysis of Cutting Forces and Temperatures on Microtools in the Micromachining of Aluminum Alloys", Proc. of the 2008 IAJC-IJME International Conference, Paper 191, ENG 103.

Oxley, P.L.B., 1989, "Mechanics of Machining, an Analytical Approach to Assessing Machinability", Ellis Horwood, Ellis Horwood, Chichester, pp. 223-227.

Oxley, P.L.B., 1989, "Mechanics of Machining: An Analytical Approach to Assessing Machinability", John Wiley & Sons, New York, USA.

Özel, T. and Altan, T., 2000, "Process Simulation using Finite Element Method—Prediction of Cutting Forces, Tool Stresses and Temperatures in High speed Flat End Milling", International Journal of Machine Tools & Manufacture, Vol. 40, pp. 713–738.

Özel, T., Lucchi, M., Rodríguez, C.A. and Altan, T., 1998, "Prediction of Chip Formation and Cutting Forces in Flat End Milling: Comparison of Process Simulations with Experiments", Transactions of NAMRI/SME, Vol. XXVI, pp. 231-237.

Patrascu, G. and Carutasu, G., 2007, “Using Virtual Anufacturing Simulation in 3d Cutting Forces Prediction”, Annals of the Oradea University, Fascicle of Management and Technological Engineering, Vol. VI (XVI), pp1423-1426.

Paul, S., Dhar, N. and Chattopadhyay, A.B, 2001, “Beneficial Effects of Cryogenic Cooling over Dry and Wet Machining on Tool Wear and Surface Finish in Turning AISI 1060 Stee”, Journal of Materials Processing Technology, Vol. 116, pp. 44-48.

Paul, S., Dhar, N.R. and Chattopadhyay, A.B., 2000, “Beneficial Effects of Cryogenic Cooling over Dry and Wet Machining on Tool Wear and Surface Finish in Turning AISI 1060 Steel”, Proc. of the ICAMT-2000, Malaysia, pp. 209-214.

Petropoulos, G., Ntziantzias, I. and Anghel, C., 2005, “A Predictive Model of Cutting Force in Turning Using Taguchi and Response Surface Techniques”, 1st International Conference on Experiments/Process/System Modelling/ Simulaton/ Optimization, Athens.

Popke, H., Emmer, Th. And Steffenhagen, J., 1999, “Environmentally Clean Metal Cutting Process-Machining on The Way to Dry Machining”, Proceedings of the Institution of Mechanical Engineers, Part B: Journal of Engineering Manufacture, pp. 329-332.

Radulescu, R. and Kapoor, S.G., 1994, “An Analytical Model for Prediction of Tool Temperature Fields during Continuous and Interrupted Cutting”, Transactions of ASME, Journal of Engineering for Industry, Vol. 116, pp. 135–140.

Rahman M. and Ng, S.L., 2002, “Effect of High-Pressure Coolant on Machining Performance”, Int J Adv Manuf Technol, Vol. 20, pp. 83–91.

Rahman, M., Seah, W.K.H. and Teo, T.T., 1997, “The Machinability of Inconel 718”, Journal of Materials Processing Technology, Vol. 63(1-3), pp. 199–204.

Reed, R.P. and Clark, A.F., 1983, “Materials at Low Temperatures”, American Society for Metals, Carnes Publication, Metal Park, OH.

Ren, H. and Altintas, Y., 2000, “Mechanics of Machining with Chamfered Tools”, Trans. ASME, Journal of Manufacturing and Engineering and Science, Vol. 122, pp. 650–659.

Rosenberg, A.M., Rosenberg, O.A., 1987, “Calculation of Cutting Forces in Cutting Ductile Metals”, Sverkhtcerdyne materially, Vol. 14, pp.48-54.

Ross, P., 1988, “Taguchi Techniques for Quality Engineering”, McGraw-Hill, New York.

Sarma, P.M.M.S., Karunamoorthy, L. and Palanikumar, K., 2008, “Modeling and Analysis of Cutting Force in Turning of GFRP Composites by CBN Tools”, Journal of Reinforced Plastics and Composites, Vol. 27(7), pp. 711-723.

Satoshi, I., Teiji, Y., Shinichi, M. and Kazuo, M., 1997, “Machinability of Ni_3Al Based Intermetallic Compounds”, Journal of Materials Processing Technology, Vol. 63 (1-3), pp. 181-186.

Seah, K.H.W., Li, X. and Lee, K.S., 1995, “The Effect of Applying Coolant on Tool Wear in Metal Machining”, Journal of Materials Processing Technology, Vol. 48, pp. 495-501.

Sekhon, G.S. and Chenot, J.L., 1993, "Numerical Simulation of Continuous Chip Formation during Non- Steady Orthogonal Cutting", Engineering Computations, Vol. 10(1), pp. 31-48.

Sharma, V.S., Dhiman, S., Sehgal, R. and Sharma, S.K., 2008, "Estimation of Cutting Forces and Surface Roughness for Hard Turning using Neural Networks", Journal of Intelligent Manufacturing, Vol. 19, pp. 473–483.

Shatla, M., Yen, Y. C., Castellanos, O., Menegardo, L. and Altan, T., 1999, "Prediction of Cutting Forces, Temperatures and Stresses from Flow Stress Data and Cutting Conditions—Research in Progress", Proceedings of the Second CIRP International Workshop on Modeling of Machining Operations, Ecole Centrale De Nantes, Nantes, France, January 25-26.

Shaw, M., 1989, "Metal Cutting Principles", Oxford University Press, Oxford, United Kingdom.

Shaw, M.C., 1984, "Metal Cutting Mechanics", Oxford: Oxford series on advance manufacturing. Clarendon Press.

Shaw, M.C., Cook, N.H. and Smith, P.A., 1952, "The Mechanics of Three Dimensional Cutting Operations", Transaction of ASME, Vol. 74(3), pp. 1055-1064.

Singh, S.B., Chakraborty, A.K. and Chattopadhyay, A.B., 1997, "A Study of the Effects of Inclusion Contact on the Machinability and Wear Characteristics of 0.24% Carbon Steel", Journal of Materials Processing Technology, Vol.66, pp. 90-96.

Smith, A.J.R. and Armarego, J.A., 1981, “Temperature Prediction in Orthogonal Cutting with a Finite Difference Approach”, Annals of CIRP.

Smithey, D.W., Kapoor, S.G. and DeVor, R.E., 2000, “A Worn Tool Cutting Force Model for Three-Dimensional Cutting Operations”, International Journal of Machine Tools and Manufacture, Vol. 40, pp. 1929–1950.

Smithey, D.W., Kapoor, S.G. and DeVor, R.E., 2000, “A Worn Tool Cutting Force Model for Three-Dimensional Cutting Operations”, International Journal of Machine Tools and Manufacture, Vol. 40, pp. 1929–1950.

Smithey, D.W., Kapoor, S.G. and DeVor, R.E., 2001, “A New Mechanistic Model for Predicting Worn Tool Cutting Forces”, Machining Science and Technology, Vol. 5(1), pp. 23–42.

Soo, S.L. and Aspinwall, D.K., 2007, “Developments iIn Modelling of Metal Cutting Processes”, Journal of Materials: Design and Applications, Vol. 221(4), pp.197-211.

Sreejith, P.S. and Ngoi, B.K.A., 2000, “Dry Machining: Machining of the Future”, Journal of Materials Processing Technology, Vol. 101, pp. 287-291.

Stephenson, D.A. and Ali, A., 1992, “Tool Temperatures in Interrupted Metal Cutting”, Transactions of ASME, Journal of Engineering for Industry, Vol. 114, pp. 127–136.

Stephenson, D.A., Jen, T.C. and Lavine, A.S., 1997, "Cutting Tool Temperatures in Contour Turning: Transient Analysis and Experimental Verification", ASME, Journal of Manufacturing Science and Engineering, Vol. 119, pp. 494–501.

Strafford, K.N. and Audy, J., 1997, "Indirect Monitoring of Machinability in Carbon Steels by Measurement of Cutting Forces", Journal of Materials Processing Technology, Vol. 67, pp. 150–156.

Strenkowski, J.S. and Athavale, S.M., 1997, "A Partially Constrained Eulerian Orthogonal Cutting Model for Chip Control Tools", Journal of Manufacturing Science and Engineering, Vol. 119(4), pp. 681-688.

Strenkowski, J.S., Moon, K.J., 1990, "Finite Element Prediction of Chip Geometry and Tool/Workpiece Temperature Distributions in Orthogonal Metal Cutting", Transactions of ASME, Journal of Engineering for Industry, Vol. 112, pp. 313–318.

Sultana, S., Zaman, P.B. and Dhar, N.R., 2009, "Performance Evaluation of Different Types of Cutting Fluid in MQL Machining of Alloy Steel by Coated Carbide Insert", Proceedings of the International Conference on Mechanical Engineering (ICME2009).

Sun, W.P., Pei, Z.J. Lee, E.S. and Fisher, G.R., "Optimization of Process Parameters in Manufacturing: An Approach of Multiple Attribute Decision Making", Thirty-third Annual North American Manufacturing Research Conference (NAMRC 33) May 24-27, 2005 · Columbia University · New York, NY, USA

Sundaram. S., Anantharaman. N., Ravikumar. K., and Vijay Anand. S., 2003, "Analysis of Temperature Distribution in Grinding of Composites Using Finite Element Method", Proceedings of the International Conference on Mechanical Engineering 2003 (ICME2003).

Suresh, P.V.S., Rao, P.V. and Deshmukh, S.G., 2002, "A Genetic Algorithm Approach for Optimisation of Sueface Roughness Prediction Model", Int. J. Machine Tools and Manufacture, Vol. 42, pp. 675-680.

Tay, A.A.O., 1993, "A Review of Methods of Calculating Machining Temperature", Journal of Materials Processing Technology, Vol. 36, pp. 225–257.

Tay, A.O., Stevenson, M.G. and de Vahl Davis, G., 1974, "Using the Finite Element Method to Determine Temperature Distributions in Orthogonal Machining", Proc. Instn Mech. Engrs, Vol. 188, pp. 627–638.

Taylor, F.W., 1907, "On the Art of Cutting Metals", Trans. ASME, Vol. 29, pp. 231–248.

Thiele, J.D. and Melkote, S.N. , 1999, "Effect of Cutting Edge Geometry and Work-piece Hardness on Surface Generation in the Finish Hard Turning of AISI 52100 Steel", Journal of Materials Processing Technology, Vol. 94, pp. 216–226.

Thornberg, J. and Leith, D., 2000, "Mist Generation during Metal Machining", Journal of Tribology, Transaction of ASME, Vol. 122(3), pp. 544-549.

Tlusty, J. and Orady, E., 1981, "Effect of Thermal Cycling on Tool Wear in Milling", Proceedings of the Ninth NAMRC Conference**,** May 1981**,** pp. 250-255.

Tlusty. J, and Macneil. P., 1975, “Dynamics of Cutting Forces in End Milling”, Annals of CIRP, 24(1), pp. 21-25.

Tönshoff, H.K., Bussmann, W., and Stanske, C., 1986, “Requirements on Tools and Machines when Machining Hard Materials”, Proc. of the 26th Int. Mach. Tool and Res. Conf. pp.349-357.

Trigger, K.J. and Chao, B.T., 1951, “An Analytical Evaluation of Metal Cutting Temperatures”, Transactions of the ASME, Vol. 73, pp. 57–68.

Tsai, Y.H., Chen, J. C. and Lou, S.J., 1999, “An In-Process Surface Recognition System Based on Neural Networks in End Milling Cutting Operations”, International Journal of Machine Tools & Manufacture, Vol. 39, pp. 583–605.

Ueda, N., Hoshi, T. and Matsuo, T., 1986, “An Investigation of Some Shear Angle Theories”, Annals of CIRP, Vol. 35(1), pp. 27-30.

Usui, E., Shirakashi, T. and Kitagawa, T., 1978, “Analytical Prediction of Three Dimensional Cutting Process, Part 3: Cutting Temperature and Crater Wear Of Carbide Tool”, Transactions of ASME, Journal of Engineering for Industry, Vol.100, pp. 236–243.

Usui, E., Shirakashi, T. and Kitagawa, T., 1984, “Analytical Prediction of Cutting Tool Wear”, Wear, Vol.100, pp.129-151.

Vleugels, J., 1995, “Machining of Steel with Sialon Ceramics: Influence of Ceramic and Workpiece Composition on Tool Wear”, Wear, Vol.189, pp. 32-44.

Waldorf, D.J., DeVor, R.E. and Kapoor, S.G., 1998, "A Slip-Line Field for Ploughing during Orthogonal Cutting", Transaction of ASME, Journal of Manufacturing Science and Engineering, Vol. 120(4), pp. 693–699.

Wang, J.Y. and Liu, C.R., 1998, "A New Concept for Decoupling the Cutting Forces Due to Tool Flank Wear and Chip Formation in Hard Turning", Machining Science and Technology, Vol. 2(1), pp. 77–90.

Wang, J.Y. and Liu, C.R., 1999, "The Effect of Tool Flank Wear on the Heat Transfer, Thermal Damage and Cutting Mechanics in Finish Hard Turning", Annals of the CIRP, Vol. 48(1), pp. 53–58.

Weinert, K., Inasaki, I., Sutherland, J.W. and Wakabayashi, T., 2004, "Dry Machining and Minimum Quantity Lubrication", Annals of the CIRP, Vol. 53(2), pp. 511-537.

Wenge, S., 2006, "Development of Predictive Force Models for Classical Orthogonal and Oblique Cutting and Turning Operations Incorporating Tool Flank Wear Effects", PhD thesis, Queensland University of Technology.

Wright, P.K. and Trent, E.M., 1973, "Metallographic Methods of Determining Temperature Gradients in Cutting Tools", J. Iron and Steel Inst., pp.364–368.

Wright, P.K., 1982, "Predicting Shear Plane Angle in Machining from Work Material Strain Hardening Characteristics", Journal of Eng. for Ind. Trans. ASME, Vol. 104(3), pp.285-292.

Wright, P.K., McCormick, S.P., and Miller, T.R., 1980, “Effect of Rake Face Design on Cutting Tool Temperature Distributions”, ASME Journal of Engineering for Industry, Vol. 102(2), pp.123–128.

Wu, D.W. and Matsumoto, Y., 1990, “The Effect of Hardness on Residual Stresses in Orthogonal Machining of AISI 4340 Steel”, Journal of Engineering for Industry, Vol. 112, pp. 245-252.

Xie, Q., Bayoumi, A.E., and Kendall, L.A., 1990, “On Tool Wear and its Effect on Machined Surface Integrity”, Journal of Materials Shaping Technology, Vol. 8(4), pp. 255-265.

Yellowley, I., 1985, “Observations on the Mean Values of the Forces, Torque and Specific Power in the Peripheral Milling Process”, International Journal of machine tool manufacture design and research, Vol. 25(4), pp. 337-346.

Yen, D.W. and Wright, P.K., 1986, “Remote Temperature Sensing Technique for Estimating the Cutting Interface Temperature Distribution”, Trans. ASME, J. Engng for Industry, Vol. 108(4), pp. 252–263.

Zhang, S. and Liu, Z., 2008, “An Analytical Model for Transient Temperature Distributions in Coated Carbide Cutting Tools”, Journal of International Communications in Heat and Mass Transfer, Vol. 35, pp. 1311–1315.

Zorev, N.N., 1966, “Metal Cutting Mechanics”, Oxford: Pergamon Press.